December 2013

# Life After Adhesion: L-Selectin Throughout the T Cell Lifespan

Abner Garcia Fernandez
*University of Wisconsin-Milwaukee*

# LIFE AFTER ADHESION: L-SELECTIN THROUGHOUT THE T CELL LIFESPAN

by

Abner Fernandez

A Thesis Submitted in

Partial Fulfillment of the

Requirements for the Degree of

Master of Science

in Biological Sciences

at

The University of Wisconsin-Milwaukee

December 2013

ABSTRACT
LIFE AFTER ADHESION: L-SELECTIN THROUGHOUT THE T CELL LIFESPAN

by

Abner Fernandez

The University of Wisconsin-Milwaukee, 2013
Under the Supervision of Dr. Douglas Steeber, Ph.D.

Lymphocytes require antigenic encounter to activate and proliferate, eventually clearing the source of antigenic challenge. The peripheral lymph nodes (PLN) are the primary sites of antigenic encounter and thus the ability of lymphocytes to migrate to this tissue is a requirement for mounting effective immune responses. The process of lymphocyte migration to the PLN is known as the “adhesion cascade”. Specifically, lymphocytes are captured from the blood through the adhesion molecule, L-selectin, followed by CC chemokine receptor 7 (CCR7)-mediated integrin activation, which ultimately results in cell transmigration into the PLN. Because the PLN is the site where antigenic encounter is most likely, we hypothesized that migration may induce pro-proliferative signaling, mediated by L-selectin and conducted through CCR7. To study the potential “priming” effects of adhesion to antigen-mediated lymphocyte proliferation, spleen and PLN lymphocytes were subjected to *in vitro* transmigration and proliferation assays. Subsequently, multi-color flow cytometry analysis was used to examine treatment effects on the T cell population. Results showed that lymphocyte proliferation was significantly increased when L-selectin and CCR7 were activated simultaneously, compared to CCR7 activation alone.

Specifically, bulk tissue populations, as well as the $CD4^+$ and $CD8^+$ T cell subsets showed enhanced proliferation from both spleen and PLN sources at early and late time points. Additionally, to discern whether this enhanced proliferation may be a by-product of decreased apoptosis, an apoptosis assay was also performed at the same time points. Interestingly, L-selectin engagement resulted in protection from apoptosis for all T cell populations 72 hour following activation. However, this protective effect was not observed at the 36 hour time point. Taken together, these results suggest a role for L-selectin in enhancing T cell proliferation, at least in part, through an anti-apoptotic effect. This research will add to a better understanding of the regulation of lymphocyte proliferation and increase our knowledge of L-selectin signaling function.

TABLE OF CONTENTS

LIST OF FIGURES

LIST OF TABLES

## Chapter 1: General Introduction

Migration and recirculation of lymphocytes are important prerequisites for generating an effective immune response. These processes are accomplished through the adhesion cascade in conjunction with chemoattractive factors. The role of L-selectin in lymphocyte migration and recirculation is well documented (1-4). However, its subsequent role late in the adhesion cascade remains unclear. In the peripheral lymph nodes (PLN), circulation of lymphocytes that have not encountered antigen (naïve cells) is primarily mediated by L-selectin and CCR7 (5). The PLN is where lymphocytes encounter their cognate antigen leading to activation and cell proliferation. The manipulation of CCR7 and L-selectin is therefore an attractive avenue for either augmenting or attenuating the lymphocyte response. Limiting the responding cell population in states of pathological hyperactive immune response, as seen in autoimmune disorders, may alleviate the negative manifestations of such disorders. In contrast, a robust response may be desired in other cases such as infections and vaccinations.

Recent results from our lab suggest that L-selectin engagement along with subsequent ligand (secondary lymphoid tissue chemokine, SLC, CCL21) binding of CCR7 enhances chemotaxis (6), and decreases apoptosis (7) L-selectin also contributes to the effectiveness of $\beta_2$-integrin- mediated lymphocytic arrest (8-10). In neutrophils, L-selectin engagement also causes increased secretion of products that degrade pathogens, thus contributing to the effectiveness of the responses (11). Therefore, mounting evidence suggests that the initial step in

leukocyte migration involving L-selectin, contributes to the effectiveness of other subsequent steps such as transmigration and terminal effector response.

**1. T cells**

T cells are white blood cells that arise from hematopoietic stem cells from red bone marrow (Figure 1). They are named T lymphocytes due to their maturation in the thymus (12). They are a subset of lymphocytes that express the T cell receptor (TCR, Figure 2)-a multi-molecular complex that recognizes specific peptide antigens normally presented by a self-cell expressing a marker known as the major histocompatibility complex (MHC, 13). Thus, T cells require a cognate antigen with a corresponding MHC to mount an effective or any response. T cells are divided into $CD8^+$ or $CD4^+$ T cells. T cells that express the CD4 co-receptor on their membrane are classified as helper T cells ($T_h$ cells). Their primary role is to coordinate the immune response, thus helping other immune cells in antigenic clearance and the maintenance of homeostasis (14). $CD4^+$ T cells recognize antigens on antigen presenting cells (APC) which express the MHC-class II molecule. $CD4^+$ T cells are primarily responsible for the clearance of pathogens of extracellular origin. The TCR of $CD4^+$ T cells can recognize longer peptide antigens compared to the TCR of $CD8^+$ T cells (15).

$CD8^+$ T cells on the other hand recognize peptide antigen along with the MHC-class I molecule which is a self-marker expressed by virtually all nucleated cells. $CD8^+$ T cells are called cytotoxic T cells ($T_c$ cells) due to their ability to secrete factors that result in cell death. $CD8^+$ T cells are primarily responsible for the destruction of virally-infected or defective self-cells (tumors) and therefore

respond to intracellular challenges. $CD8^+$ T cells are also responsive to $CD4^+$ T cell-mediated co-stimulation. The biggest driver of $CD8^+$ T cell proliferation is interleukin-2 (IL-2) secreted primarily by $CD4^+$ T cells (16).

The TCR expressed by the majority of T cells is a dimer of $\alpha$ and $\beta$ chains that have arisen independently from each other through genetic rearrangement of their membrane distal variable regions. This provides for high variability and accounts for the unimaginable repertoire of variable regions specific for a multitude of peptide antigens. The TCR dimer is surrounded by 5 invariant chains of the CD3 complex: 2 $\varepsilon$, 1 $\gamma$, 1 $\delta$ and 2 $\zeta$ chains. The CD3 molecules contain conserved cytoplasmic regions called Immunoreceptor-Tyrosine-based-Activation-Motifs (ITAM) which are rich in potential phosphorylation residues. Interestingly, due to its short cytoplasmic tail, the TCR cannot generate intracellular signaling on its own and must therefore signal by coopting neighboring molecules such as the CD3 molecule. The co-receptor CD4 or CD8 is also expressed, dependent on the T cell subset ,and interacts with MHC-class II or MHC-class I molecules, respectively. Finally, a CD28/CTLA-4 (Cytotoxic T-Lymphocyte Antigen-4) dimer is also considered part of the TCR complex. CTLA-4 is up-regulated in activated cells. CD28 stimulation results in an “on” signal while CTLA-4 stimulation results in an “off” signal (17).

T cells react to antigens presented by other cells called APCs in a stepwise fashion. A cognate peptide for the TCR must be detected along with two other signals for proper T cell activation to occur. First, the TCR+peptide/MHC contact must be accompanied by a CD4+MHC-class II or

CD8+MHC-class I interaction; second, a co-stimulatory molecule, specifically the CTLA-4/CD28 dimer must also be stimulated by their respective ligands on the APC. Failure for any of these interactions to happen almost simultaneously results in T cells that are anergic and thus unable to activate (18). This anergy can still be overcome if the incoming signal is of high duration and quality (19). Once a T cell is stimulated properly, a kinase normally associated with the cytoplasmic tail of CD4 or CD8, light chain kinase (Lck), phosphorylates the ITAM's of the $\zeta$ chains of CD3. The phosphorylated $\zeta$ chains in turn recruit zeta associated protein of 70 kDa (ZAP-70), which due to its close proximity to the inner leaflet of the cell membrane can now interact with scaffolding proteins such as linker of activated T cells (LAT) and the SH2 domain-containing leukocyte protein of 76 kDa (SLP-76). The final products of TCR signaling are the transcriptional up-regulation of proteins required for cell activation and proliferation and down-regulation of genes that are in opposition. Additionally, effector molecules to clear the immunogenic challenge are also transcribed, which include but are not limited to: IL-2 (20) and interferon-$\gamma$ (21) for $CD4^+$ T cells, or granzyme and perforin for $CD8^+$ T cells (22). The signaling pathways that are normally utilized involve the Ras (rat sarcoma family of proteins, 23), PLC (phospholipase-C, 24), and NF$\kappa$B (nuclear factor kappa B proteins, 25).

The result of TCR activation is the clonal expansion of that specific T cell lineage. In the best case scenario, the cause of antigenic challenge is eventually eliminated and the response of other T cell populations eventually down-regulates the effector response (26). T cells that are products of antigen-induced

proliferation and have survived the initial response are called memory T cells ($T_m$ cells). This memory pool is yet divided into at least two other subsets: effector memory T cells ($T_{em}$) which are sequestered in the tissue in which they are activated in, and central memory T cells ($T_{cm}$) which can still recirculate between the blood and the periphery (27). Their interaction with antigen in subsequent encounters creates a rapid and heightened response, resulting in the faster elimination of the immune challenge.

**2. T cell migration**

Lymphocytes require antigenic encounter to respond effectively, and antigenic encounter requires that these cells circulate throughout the whole organism. In the blood, the hemodynamic flow provides for maximal interaction between circulating lymphocytes and possible antigens. However, in areas of the body where flow dynamics is not dominant, such as in the PLN or cutaneous tissue, discrete and overlapping steps that capture lymphocytes from the blood must be established (28). Lymphocyte recirculation into the parenchyma is mediated by several overlapping steps with corresponding receptor engagements, intracellular responses, and ultimately a cellular physical response. In a homeostatic state, immune cell circulation in the PLN is mediated sequentially (Figure 3). First, the adhesion molecule L-selectin interacts with its ligands expressed on the endothelium (collectively called peripheral node adressins, PNADs) to arrest high velocity immune cells in the bloodstream. The cells, now decreased in their velocity, have the opportunity for the CCR7 receptor to interact with its ligand, CCL21. CCL21 is a soluble chemokine generated by local lymphoid tissue, thus its other name, secondary lymphoid tissue chemokine

(SLC). CCL21, although soluble, is sequestered on the vascular endothelium by glycosylaminoglycans (GAG's, 29). The CCR7+CCL21 interaction triggers the change in conformation of $\beta_2$-integrins (lymphocyte function associated antigen-1, LFA-1), another class of adhesion molecule expressed on the lymphocyte (30). The change in conformation from a low affinity to a high affinity conformation of the integrin allows it to interact with its ligand, intercellular adhesion molecule-1 (ICAM-1), expressed on the endothelium to firmly arrest the cells. Finally, the lymphocytes transmigrate through the blood vessels into the PLN through processes such as cystoskeletal remodeling and basement membrane degradation (31). Once in the lymph node, lymphocytes may encounter their cognate antigen (activation). This interaction along with co-stimulatory signals, results in clonal expansion (proliferation) and terminal differentiation, into either effector cells that mediate antigenic clearance ($CD8^+$ T cells) or response-coordinating cells ($CD4^+$ T cells).

**3. L-selectin**

L-selectin belongs to the selectin family of adhesion molecules and is expressed by all leukocytes (32). The E/P/L-selectins are multi-domain transmembrane proteins that have a ligand binding lectin domain, an epidermal growth factor-like domain, and short consensus repeat (SCR) domains (Figure 4). The differences between the 3 selectin molecules rest on two factors, cell expression patterns and the number of SCR domains. E-selectin is expressed by inflamed endothelium and P-selectin is expressed by activated platelets and inflamed endothelium. Both E-and P-selectin have a varied SCR number

between species, normally ranging from 4-9, whereas L-selectin's SCR is conserved between species at 2. Interestingly, all selectins seems to share ligands perhaps due to the common post-translational modifications required of their respective ligands. Naïve or circulating T cells have been shown to express higher levels of L-selectin compared to B cells (4). Because of migration differences in the spleen's open circulation, and the PLN (separated from the blood by high endothelial venules (HEV)), the majority of cells in the PLN express high levels of L-selectin (33). Furthermore, naïve T cells express the highest levels of L-selectin, because activated T cells are normally sequestered in their activation sites to create an environment conducive to antigenic clearance, and thus are not required to recirculate (34) .

L-selectin can be cleaved upon engagement at a membrane proximal region by a metalloproteinase, tumor necrosis factor $\alpha$-converting enzyme (TACE or ADAM17, 35). This cleavage results in a soluble form of the molecule, sL-selectin, that can be detected in the plasma. It has also been shown that sL-selectin can still bind to its ligands and perhaps serve to saturate L-selectin ligands on the endothelium not actively participating in cell-to-cell interactions (36). Interestingly, L-selectin-mediated tethering which normally happens between lymphocytes and the endothelium can also occur between leukocytes. This phenomenon of "secondary tethering" may help recruit more leukocytes to the endothelium, especially when the endothelium is inflamed (37).

The ligands specific to L-selectin are varied and widespread among a variety of tissues and cells, especially in HEV of lymph nodes (31). The conserved

ligand structure is rich in posttranslational addition of modified carbohydrates, and so far 9 ligands that bind to L-selectin with varying affinities have been identified. There is a consensus that the molecule sialyl Lewis x (sLex), a tetrasaccharide, can bind to all 3 selectins (38). However, this seems to stem from a sulfated modification in sLex. Thus, structures that are sulfated, fucosylated and sialylated seem to be preferred L-selectin ligands.

The intracellular domain of L-selectin is normally associated with ezrin-radixin-moesin (ERM) and calmodulin (CaM) molecules that serve as a scaffold for spanning adjacent L-selectin molecules (39). The tail is also associated with $\alpha$-actinin which binds L-selectin to the actin cytoskeleton. This putative binding is proposed to orient L-selectin into a conformation that restricts access of TACE to the membrane proximal cleavage region. Once L-selectin binds to ligand, the ERM scaffold dissociates, leading to L-selectin cleavage and clustering of the cytoplasmic tail. Clustering of L-selectin upon engagement promotes downstream signaling effects such as oxidative burst, and an increase in kinase activity (10, 40-41). This suggests that L-selectin although a canonical adhesion molecule, may play a role in other pathways not restricted to adhesion.

**4. CCR7 and Secondary Lymphoid Tissue Chemokine (SLC)**

Chemokines and their receptors are classified based on the position of the N terminus conserved cysteine residues (42). Chemokine receptors are serpentine transmembrane receptors that are often called G-protein coupled receptors due to their putative signaling mechanism (43). These receptors are normally

associated intracellullarly with a heterotrimeric G protein that dissociates upon ligand binding and results in subsequent activation of downstream signals.

CCR7 (Figure 5) is a chemokine receptor that is involved in homeostatic recirculation of naïve lymphocytes and is highly specific for two ligands, CCL19 (ELC) and CCL21 (SLC) (44). The former is primarily produced in secondary lymphoid tissues, and serves as a chemoattractive factor for recirculating lymphocytes (45-46). The CCR7 and SLC/ELC interaction is known to involve GAGs. GAGs serve as a scaffold upon which soluble SLC can bind (47). The downstream signaling invoked upon ligand binding has been shown to involve $Ca^{+2}$ release mediated by CaM and tyrosine kinase activity (48). These signals converge downstream to facilitate nuclear translocation of NFκB, among many other factors, resulting in enhanced transcription of a multitude of factors that enhance chemotaxis through cytoskeletal remodeling and cell polarization (49). Interestingly, the current body of knowledge also points to chemokine-driven enhanced effector effects. Chemokines and their receptors have been shown to serve a role in T cell development (50-51). Specifically for CCR7, it has been shown that intrathymic development of T cells is impaired in the absence of CCR7 (52). Furthermore, effector phenotypes such as the ability to lyse cells and to effectively proliferate can also be enhanced in the presence of CCR7 (53). Thus, CCR7 has been shown to have post-adhesive effects, which are more established than for L-selectin.

**5. Lymphocyte surface receptor architecture and relationships**

The cell membranes are very crowded places. It must be understood that membrane receptors are in close proximity with each other and impact the fluidity of the membrane ultrastructure (54). This is more so in cells that specialize in signaling such as a T cell. If we consider the number of clusters of differentiation (CD) antigens alone, one can only imagine the number of receptors on the T cell surface (55). Additionally, most of these receptors are present in high copy numbers, thus, creating a higher density of membrane proteins. The effect of receptors in close proximity to each other implies that they exert pressures and influences on each other. The crowding effect alone implies that a group of receptors must be down-regulated in order for another to be overexpressed. This may be the reason why cells constantly change their receptor repertoire, dependent on temporal and spatial contexts (56-58).

In the context of the TCR, CCR7 and L-selectin molecules, a direct association between the three of them is yet un-established. However, in regards to L-selectin and CCR7, we already alluded to their proposed close association. Previous studies have suggested that L-selectin activation enhances SLC induced chemotaxis (6). However, the Subramanian paper is the first paper to show such a relationship between L-selectin and CCR7 (6). Additionally, L-selectin has also been shown to decrease apoptotic rates in transmigrating cells when the L-selectin molecule is previously activated (7). Additionally, the same report indicates an upregulation of the active monomer of NF$\kappa$B, p65, when cells that are transmigrated in the presence of SLC are previously exposed to an L-

selectin activating antibody (7). Taken together, L-selectin activation prior to transmigration to SLC, may increase levels of signaling molecules that serve a role in proliferation and apoptosis.

In regards to receptor relationships in our context, association between the TCR and CCR7 is much more established. In a paper by Schaueble (59), it was shown that TCR-induced activation enhanced short term migration of peripheral blood mononuclear cells (PBMC). Another paper by Gollmer (60) also showed that SLC, a ligand for CCR7, can also contribute to CD4 co-receptor stimulation. Taken together, one can surmise that a relationship between these three molecules may exist.

**6. Hypothesis**

Based on the background information presented above, we propose that a relationship between L-selectin, CCR7 and TCR exists. We hypothesize that L-selectin due to its increasing contributions to events far removed from initial tethering can also affect TCR-mediated proliferation, transduced through CCR7. Because of the role of L-selectin in moving lymphocytes from the sterile blood environment to the antigen rich parenchyma, we propose that L-selectin “primes” cells before antigenic encounter and thus hypothesize:

1. That L-selectin can increase TCR-induced proliferation.
2. That L-selectin exerts an anti-apoptotic effect on T cells

3. That L-selectin-mediated effects will be more pronounced in $CD8^+$ T cells, due to a higher density of L-selectin in this subset, and in the PLN, due to the higher number of L-selectin positive cells in this tissue.

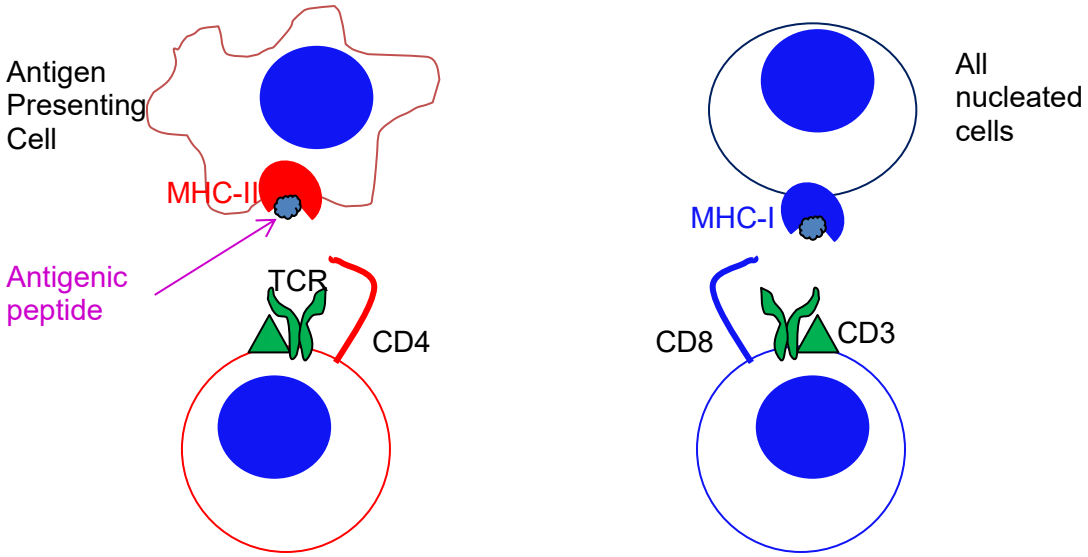


**Figure 1.** T lymphocytes. T (matures in the Thymus) lymphocytes consist of two major subsets: $CD4^+$ and $CD8^+$ cells. Both types have a common CD3 marker but possess the distinct co-receptors: CD4 or CD8. The TCR itself has variable regions specific to distinct antigenic peptide arrangements. Thus, T cells do not react to the same antigen. $CD4^+$ T cells respond to peptides presented by antigen presenting cells (APC): dendritic cells primarily and phagocytic cells to a lesser extent. APCs display MHC-class II molecules which must be recognized by the $CD4^+$ T cell for a response. $CD8^+$ T cells respond to all nucleated cells (including APCs) but requires MHC-class I on the presenting cell for a response. $CD4^+$ T cells are coordinating cells of the immune system, signaling other immune cells to increase or decrease their respective responses relative to the challenge, thus they are called helper T cells. $CD8^+$ T cells act by directly killing cells presenting the proper antigen and MHC molecule, thus they are called cytotoxic T cells.

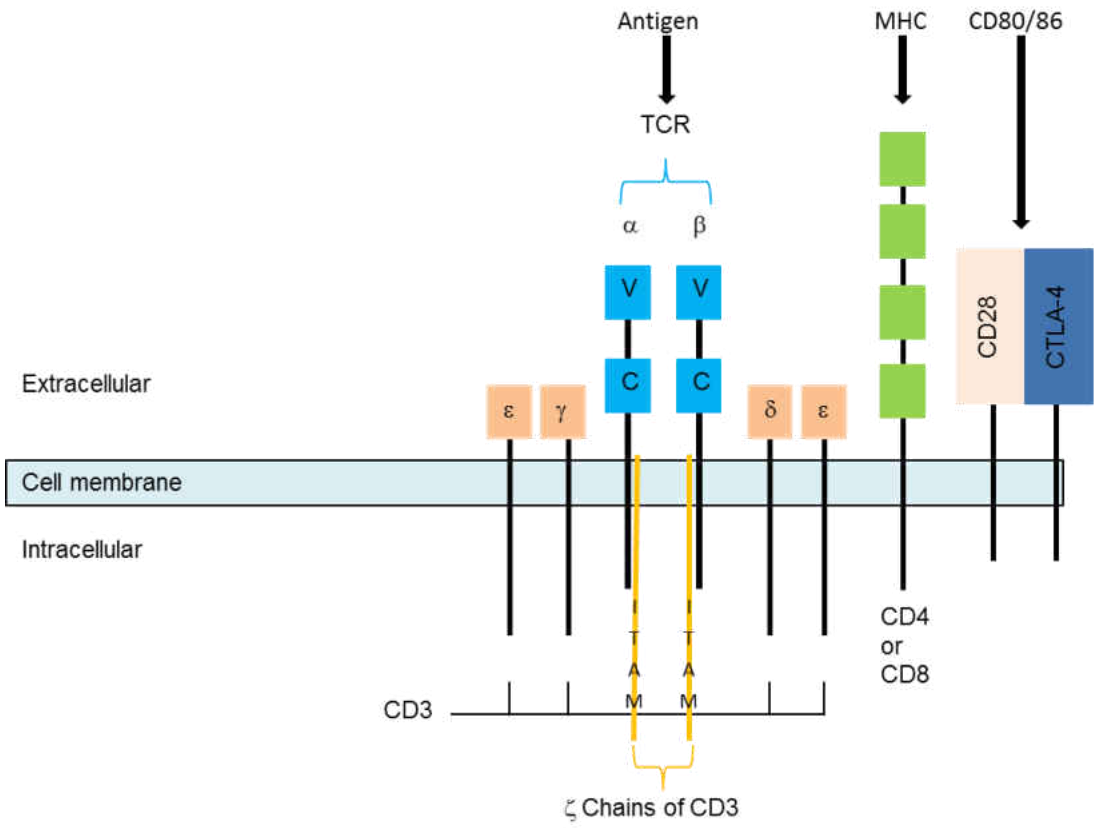


**Figure 2.** T cell receptor complex. The T cell receptor complex consists of multiple molecules. It utilizes the TCR dimer (most commonly an α and β chain) and the CD4/8 co-receptor to respond to antigen. The TCR dimer consists of two independent variable region (V) and two constant regions (C). The V region is responsible for antigen specificity. Once an antigen complementary to the V region is encountered and presented by a self-cell displaying the proper MHC, a response is initiated by the CD4/8 molecule's light chain kinase (Lck) which induces phosphorylation of the ζ chains of CD3. This in turn recruits other signaling proteins to perpetuate kinase cascades: NFAT, NFκB, MAPK, as the 3 most important kinase pathways. The antigen presentation to the TCR must be accompanied by a co-stimulatory signal which is transduced through the CD28+CTLA-4 dimer. Co-stimulatory failure results in cells that are anergic.

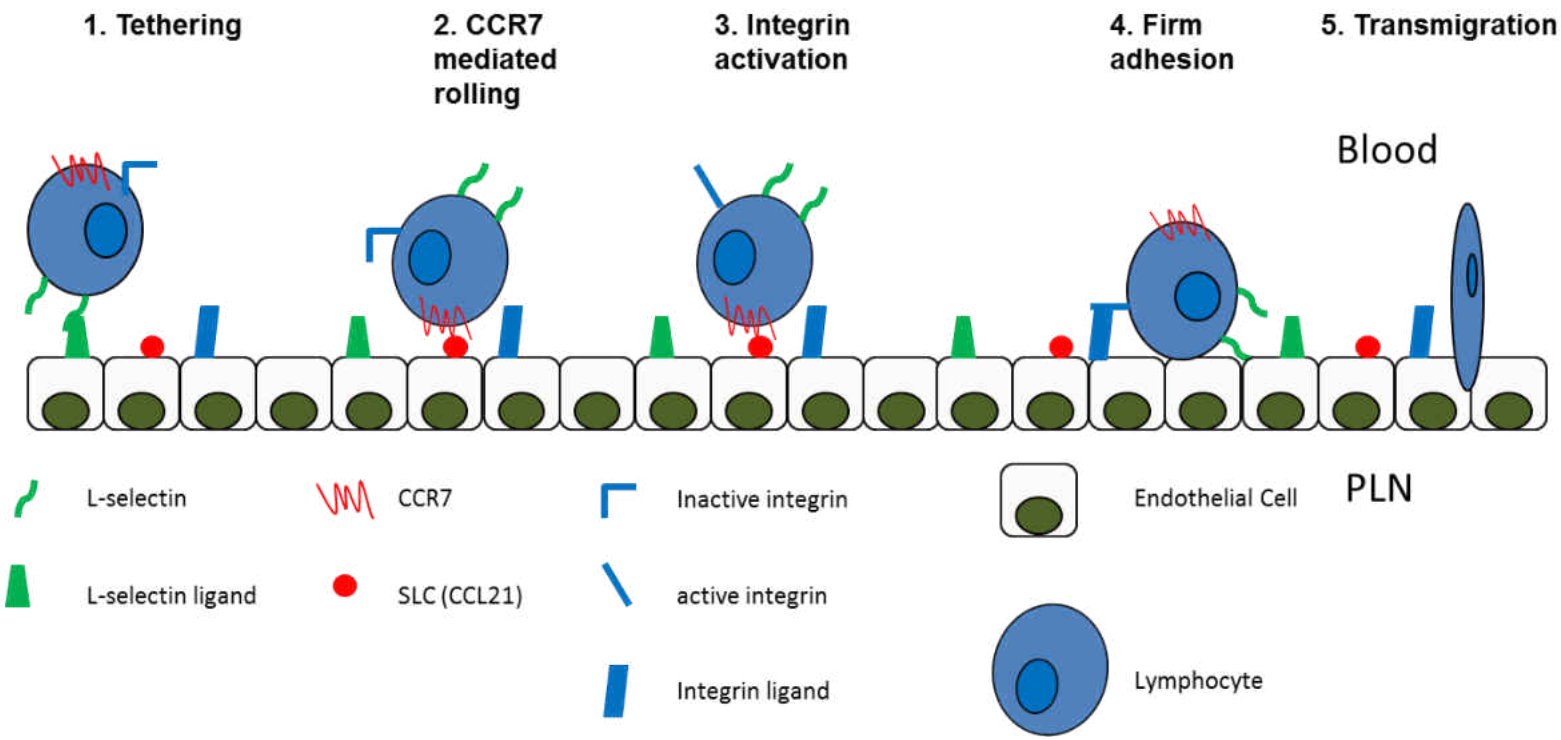


**Figure 3.** Adhesion Cascade. Events that follow are typical at the interface between the blood and the vascular endothelium of the PLN. A lymphocyte is slowed down by L-selectin interacting with its ligand expressed on the vascular endothelium, resulting in lymphocyte rolling (1). The rolling cell's chemokine receptor can now interact with its ligand that is sequestered on the endothelium by glycosylaminoglycans (2). This result in activation and a conformation change in the integrin receptor into an active form (3), which results in integrin-mediated firm arrest (4). Cells can then transmigrate into the underlying tissue (5).

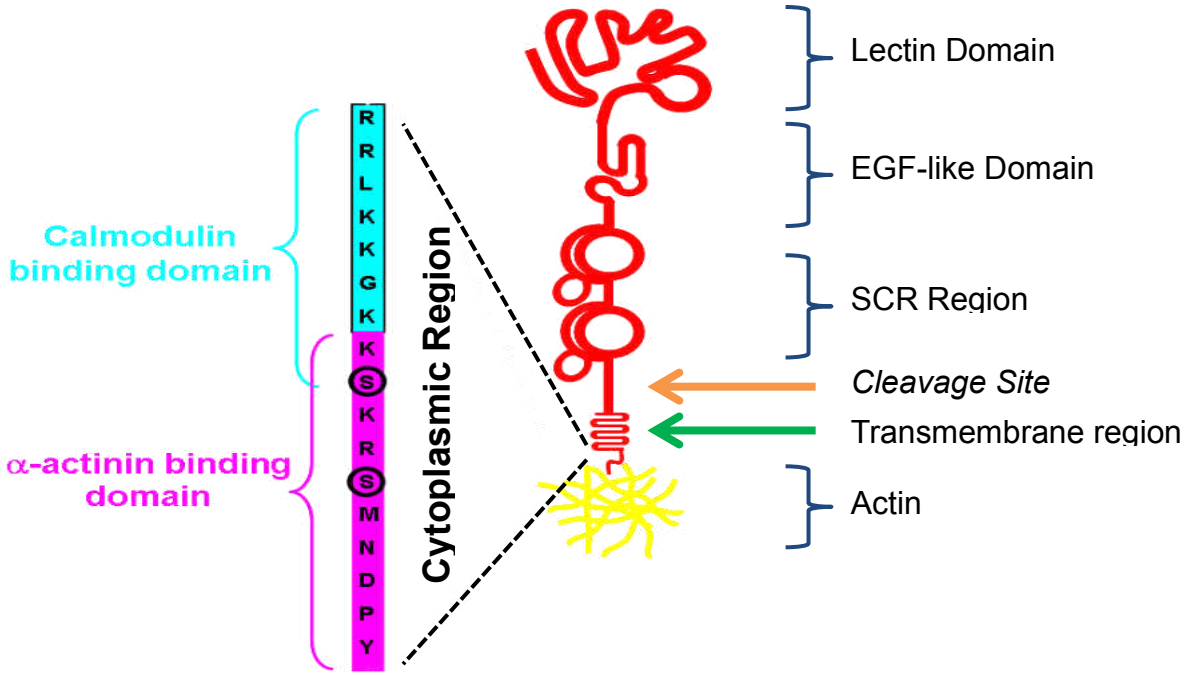


**Figure 4.** Structure of human L-selectin. L-selectin consists of 4 extracellular regions along with a short (17 amino acids) cytoplasmic tail. The activation domain which is farthest from the cell is the lectin domain, followed by an epidermal growth factor (EGF)-like domain. It has 2 short consensus repeats (SCR), which is numerically conserved among species. A cleavage site that becomes accessible for a metalloproteinase during activation is present in the membrane proximal region. The short cytoplasmic domain which anchors the molecule to the actin cytoskeleton has putative binding sites for calmodulin and α-actinin. Protein Kinase C is known to phosphorylate the two serine residues (circled). Figure courtesy of Steeber et al., 2007 (31).

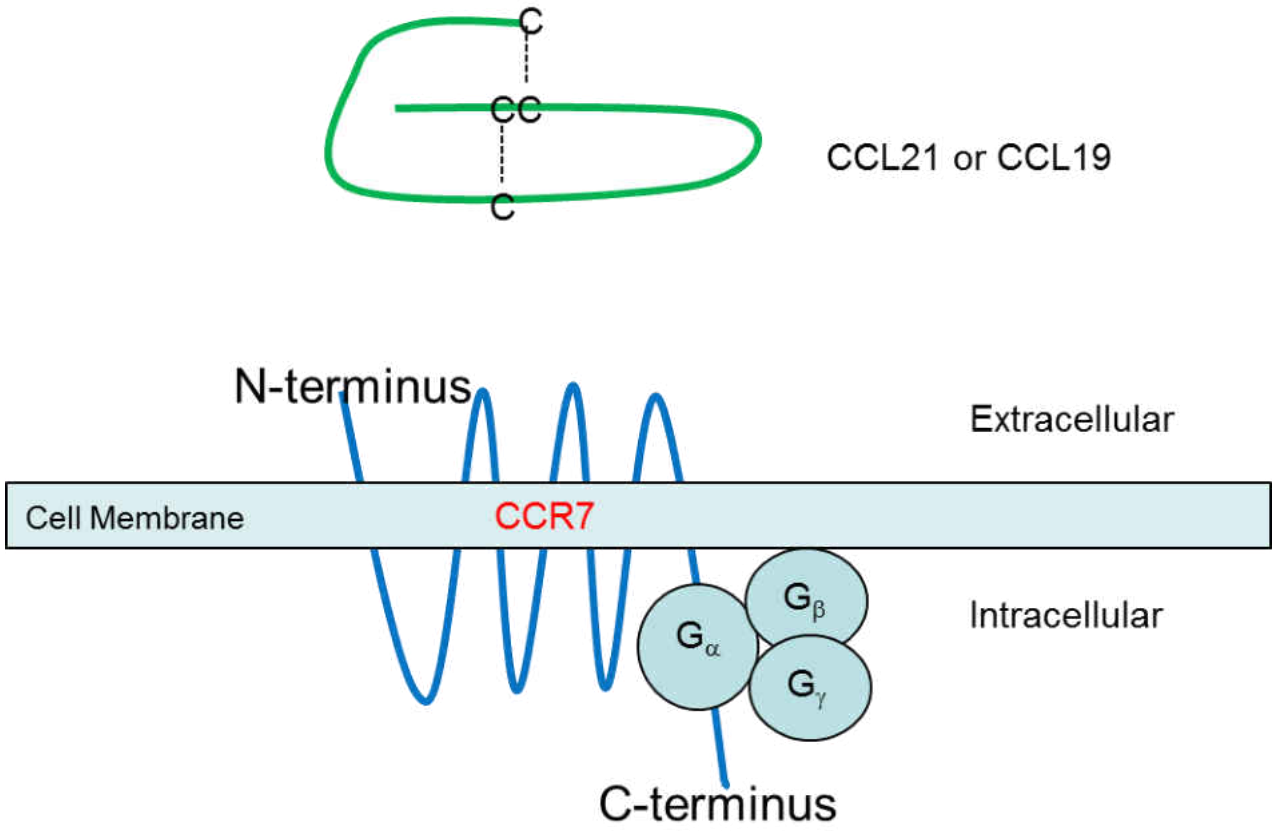


**Figure 5.** CC chemokine receptor 7 (CCR7) and its ligands. CCR7 is a chemokine receptor expressed by dendritic cells and T and B cells. The two known ligands are CCL19 (also known as ELC) and CCL21 (also known as SLC). The CCR7/SLC combination induces chemotaxis of lymphocytes into the parenchyma of the PLN, in cooperation with selectins and integrins. CCR7, as are all other chemokine receptors, is a G-protein coupled receptor. Thus signaling involving G$\alpha$ and G$\beta\gamma$ molecules is activated during receptor-ligand interaction.

## Chapter 2: Characterization of T cell proliferation with L-selectin and CCR7 activation

### 1. Research design

As previously covered in the introduction, lymphocytes need to be able to recirculate between the blood and lymphoid tissues to maximize the surveillance capacity of these cells and thus optimize conditions for mounting the adaptive immune response. L-selectin plays a crucial step in minimizing cell velocity in the blood-lymph node boundary. This “speed bump” effect increases cell contact with the vascular endothelium which polarizes the cell and induces its transmigration. As evident in the above description and from the adhesion cascade review in the introduction, L-selectin is not a stand-alone molecule, as compared to the TCR complex. Its effects towards the succeeding events after transmigration of the cell requires transduction via other molecules involved in the same pathway. Although direct studies of L-selectin contributions to vast arrays of T cell processes have been performed (61-62), most have centered on migratory capacity and none have dissected its contribution to TCR-induced proliferation; an event far removed from the initial L-selectin-mediated tethering and rolling steps.

The direct activation of L-selectin and subsequent measurements of TCR-independent proliferation is possible. However, we surmised that the signaling effects of L-selectin may be weak and transitory (63-64) and thus may not truly mirror its signaling effects *in vivo*. Furthermore, direct measurement of proliferation after L-selectin activation is not physiologically relevant, because most T cell activation occurs after the cell has migrated from the blood into the

lymph nodes, where the vast array of antigen presenting cells can directly interact with the transmigrated T cell (65-66). It is important to note that this mechanism of T cell activation is also possible in the spleen (67-68). However, the spleen is a predominantly B cell organ (69), where humoral immunity is more involved. Because T cell activation may come from both spleen and lymph nodes, regardless of the T cell proportion, both tissue T cell residents were isolated and analyzed for L-selectin-induced proliferative effects. To correct for the possible weak effect of L-selectin-mediated signaling which may be masked by “all or none” events such as TCR-induced proliferation; we coopted a molecule that serves with L-selectin *in vivo*. To this end we selected another molecule that has been shown to act with L-selectin in the adhesion pathway; CCR7 (70-71). *In vivo*, SLC is present on the surface of HEV in lymph nodes and thus its receptor, CCR7, is immediately activated after L-selectin-induced rolling (72). It has also been shown that activation of chemokine receptors on leukocytes can result in phosphorylation of serine residues in the cytoplasmic tail of L-selectin (73). A connection between L-selectin and CCR7 was recently shown by our lab with the demonstration of increased lymphocyte chemotaxis to SLC following L-selectin activation (6). CCR7 in this regard may serve as a molecular bridge between the initial L-selectin step and the terminal step of TCR-induced proliferation. To test this idea, a *in vitro* assay was developed that mimics T cell transmigration and eventual TCR-induced activation and proliferation. This assay was performed by activating L-selectin via a specific

antibody, followed by chemotaxis in a transwell system in the presence of SLC and finally a terminal assay of anti-TCR-induced activation and proliferation.

To measure levels of activation and proliferation empirically, resulting cell populations may be assessed with an activity assay such as the 3-(4,5-dimethylthiazol-2-yl)-2,5-diphenyltetrazolium bromide (MTT) assay. The shortcoming of such an assay is that MTT reduction into the colored formazan product requires an active NADH dehydrogenase (74). NADH dehydrogenase is a mitochondrion-restricted enzyme (75-77). Mitochondrial enzymatic activity may be down regulated in cells that have been exposed to sustained proliferative signals and cell-to-cell inhibition due to volume restrictions and hypoxic conditions (78-79). Furthermore, the use of an organic hydrophobic substance such as dimethyl sulfoxide (DMSO) to solubilize the crystals is problematic, because hydrophobic substances, especially DMSO readily diffuses into the vapor phase. The MTT assay also requires a response/cell standard. Because this assay is based on enzymatic activity, cell populations from the same conditions must be used for analysis and as standards. Analyzing subset effects also requires homogenous cell purification prior to the assay, which is time and resource intensive. Carboxyfluorescein diacetate succinimidyl ester (CFDA-SE) is an intracellular fluorescent stain (80). In the CFDA-SE form it is non-fluorescent and readily passes through the hydrophobic cell membrane (81). Once it is in the cytoplasm, intracellular esterases cleave it into the carboxyfluorescein succinimidyl ester (CFSE) form. CFSE is fluorescent with an excitation/emission signature of 492nm/517nm. Furthermore, CFSE is not readily

permeable and can be covalently linked to protein residues in the inner leaflet of the cell membrane. Thus in its CFSE form it is restricted to the intracellular compartment. Another advantage of CFSE is that only viable cells can convert and retain it. The intracellular esterases responsible for its conversion are also not mitochondrion restricted. Furthermore, cell division results in a stoichiometric halving of the CFSE signal (82). Thus, each progeny population will have a CFSE fluorescence intensity signature of approximately half of the previous generation. However, optimal concentrations of CFSE must be empirically determined because excessive amounts, although non-toxic, will render the cells anergic (83).

The monoclonal antibody (mAb) against the lectin domain of L-selectin, LAM1-116, was generated previously and has been shown to induce homotypic adhesion between lymphocytes *in vitro* (10). Interestingly another L-selectin antibody generated from the same fusion, LAM1-101, recognizes the EGF/SCR region of the molecule and has been shown to induce no phenotypic effects on cells. In relation to this thesis, we utilized LAM1-116 as an activating anti-L-selectin antibody and LAM1-101 as a negative control antibody. The superiority of using two antibodies generated against the same molecule, but specific to two different domains with corresponding phenotypic effects, has huge advantages. Using isotypic antibodies that can bind to the same molecule with approximately equal affinity is superior to assays utilizing non-specific mouse antibodies, most notably in cases where non-specific mouse IgG is used. Alternatively activation of L-selectin with phorbol myristate acetate (PMA) could have been used but its

relevance *in vivo* would have been lost, since the mechanism of PMA activation is via an inside-out signaling mechanism utilizing protein kinase C (PKC, 84), which is atypical of L-selectin function in the context of migration. A different approach for activating L-selectin would have been to utilize its natural ligands. However, a preferred or dominant L-selectin ligand has still not been identified (32). Instead, L-selectin is known to bind to a vast array of ligands, including ligands that have been shown to bind to other adhesion molecules, such as P-selectin glycoprotein ligand-1 (PSGL-1), a ligand that can bind to all selectin molecules (85). Some reports have also shown that L-selectin can be activated by binding molecules known to have been incorporated post-translationally, such as sulfatides or glycoproteins. However, these modifications are not unique to L-selectin ligands and their activaty may require other molecules besides L-selectin such as sulfatide receptors.

A transwell or transmigration system mimics the interface between blood and the parenchymal tissues such as the PLN (86). The system that we used has an upper and lower chamber, corresponding to the blood and parenchyma respectively. The bottom chamber can be loaded with chemokines or any other putative chemoattractive substance, which can be separated from the lower chamber with polycarbonate membranes with varying pore sizes. The pore size is important because transmigration into the periphery requires T cell polarization and cytoskeletal rearrangement (87). If a smaller pore size compared to the cellular diameter of the population of interest is used, only cells that actively transmigrate through cellular polarization and rearrangement can be found in the

lower chamber after a pre-determined amount of time. The time utilized for this transmigration/chemotaxis assay must be determined empirically because the chemokine or any chemoattractive substance will readily diffuse between chambers, ultimately resulting in equilibrium where no chemical gradient is present and thus resulting in cell inertia or worse, reverse transmigration, which may happen in cases where the chemical has partial solubility and less density than the media. The limitation of the transmigration assay is that the number of cells that transmigrate dictates any subsequent assays. In our case, the volume of the chambers is quite small and thus the numbers of cells available for the subsequent proliferation assay is limited. Another possible challenge is that the transmigrated cell population may have a preponderance to favor a specific T cell subset. If this is the case, the proliferation analysis will already have an established bias towards the dominant transmigrating subset. To correct for this population issue and still maintain research integrity of paired tests, the assays were performed one tissue at a time and multiple wells were utilized per treatment. Briefly, there were 4 transmigration treatments: 1) untreated cells, 2) cells transmigrated in the presence of SLC, 3) cells previously treated with activating LAM1-116 mAb and transmigrated in the presence of SLC, and 4) cells previously treated with control LAM1-101 mAb and transmigrated to SLC. Wells coinciding with the same treatment were pooled to generate enough cells for the next assay. Subset analysis by flow cytometry was also performed after pooling to guard against any subset bias.

The cells from the transmigration assay were subsequently exposed to a TCR-induced proliferation assay using monoclonal antibodies against two trans-membrane proteins, the TCR-associated epsilon subunit of the CD3 complex and the co-stimulatory molecule, CD28. Cross linking of surface proteins, especially those with signaling capabilities such as CD3 and CD28, provokes downstream signaling that induces proliferation (88-89). Both antibodies were needed because ligation of CD3 alone only invokes the initial activation of T cells (90-91) whereas co-ligation of CD28 is needed for sustained cell proliferation (92). Because TCR signaling puts T cells under extreme duress, time points were empirically determined to assess the peak levels of proliferation.

Cell analysis was performed using a flow cytometer. A flow cytometer has a distinct advantage of analyzing high numbers of cells in multiple populations in minimal amounts of time. Antibodies with conjugated fluorescence molecules or fluorescent dyes specific to the cell of interest can be detected via a flow cytometer. An important property of flow cytometry that allows for detection of labeled cells one at a time is called hydrodynamic focusing. Hydrodynamic focusing is similar to liquid chromatography albeit without a stationary phase. Two layers of fluid diameters are aligned; the outer layer called the sheath volume pushes the inner fluid diameter layer which makes up the sample. Cell suspensions are pushed through the flow cytometer system via differing velocities of a buffering liquid, hence the word “flow”. The sheath diameter of fluid pushing the cells is a product of its velocity. Slower flow is a product of a smaller sheath fluid diameter, hence a larger sample fluid diameter. When the sheath

diameter increases, the sample fluid diameter decreases resulting in greater force and greater sample velocity. Due to the small sheath diameter, the inner cell suspension can be optimized to a diameter slightly larger than the cell of interest. This results in one cell per unit volume. The fluorescently labeled cells, one at a time are then passed through an excitation source and their resulting emission, which is of a low magnitude is amplified via a series of photomultiplier tubes. This system does not just detect cell surface proteins but with a cell permeabilization step can also detect intracellular molecules.

## 2. Materials and Methods

### i. Animals and Tissues

C57BL/6 mice (Jackson Labs, Bar Harbor, ME) were raised in pathogen-free conditions with unrestricted access to food and water. Mice were used at 2-4 months of age. Cells isolated from the spleen, and inguinal and axillary lymph nodes were exclusively used for all experiments. All tissues were dissected under aseptic conditions. Mice were sacrificed via $CO_2$ inhalation. All animal procedures were approved by the Institutional Animal Care and Use Committee of the University of Wisconsin-Milwaukee.

### ii. Lymphocyte Isolation

Single-cell suspensions of mouse splenocytes were prepared by mechanical homogenization of the spleen while in suspension with 0.1 M phosphate buffered saline (PBS), and filtration of debris through a 120 μm pore sized nylon mesh (Elko Filtering, Miami FL). Red blood cells were lysed in a $KHCO_3$-buffered 0.15 M $NH_4Cl$ solution. The resulting red blood cell-free cell solution was filtered,

washed and centrifuged twice in PBS. All cells were re-suspended in Dulbecco's PBS (DPBS, Life Technologies, Carlsbad CA) unless otherwise stated. Lymphocytes from bilateral inguinal and axillary lymph nodes were similarly prepared with the exception of the red blood cell lysis step. Cell counts were determined using a 0.04% trypan blue exclusion assay with a hemacytometer. Dead cells have permeable membranes and thus will present with a blue cytoplasm which can be excluded from the resulting cell count.

iii. CFSE Staining

Lymphocytes (10 x $10^6$ cells/mL) from the spleen and lymph nodes that were isolated as previously described, were incubated for 15 minutes at 37°C in 0.25 μM of CFDA-SE (Molecular Probes, Carlsbad CA) in pre-warmed DPBS, with regular mixing. The required cell and CFSE concentrations were previously determined empirically. The concentrations used gave high CFSE Mean Fluorescence Intensity (MFI) of equal to or greater than $10^3$, yet still provided responsive reporter cells. Resulting suspensions were washed twice with DPBS supplemented with 10% Heat-Inactivated Fetal Bovine Serum (HI-FBS, Life Technologies). HI-FBS was needed to quench excess CFSE, minimizing its anti-proliferative effects. The cells were then re-suspended in RPMI-1640 medium (Life Technologies) supplemented with 10% HI-FBS, and allowed to equilibrate at a 37°C water bath for 30 minutes. The previous 30 minute step at that temperature allows the cells to cleave the diacetate moiety of CFDA-SE and covalently link CFSE intracellularly, allowing for staining stability and reproducibility. All antibodies used in the subsequent experiments were

purchased from BD Pharmingen (San Jose, CA) unless otherwise stated. Flow cytometric subset analysis for L-selectin expression was then undertaken, using anti-mouse CD4 (Clone:RM4-5) conjugated to Phycoerythrin (PE), anti-mouse CD8 (Clone:53-6.7) conjugated to AlexaFluor 647, and biotin conjugated LAM1-116 monoclonal antibody against L-selectin, which was revealed with a PE-Cy5.5 fluorophore conjugated to avidin. Briefly, LAM1-116 mAb and LAM1-101 mAb were isolated from the ascites fluid of RAG-1-knockout mice injected in the peritoneum with the hybridomas for each antibody. The antibodies were isolated and concentrated from ascites by $NH_4SO_4$ precipitation, followed by extensive dialysis with column buffer (0.1 M $NaC_2H_3O_2$, pH 5). The antibodies were then purified by protein G affinity chromatography and released with elution buffer (0.1 M glycine-HCl, pH 2.8). The eluted antibody fractions were neutralized by 1M Tris, pH 9.0. The neutralized chromatography fractions were pooled and after extensive 0.1 M PBS dialysis, the antibody purity was confirmed by reducing Sodium Dodecyl Sulfate Polyacrylamide Gel Electrophoresis (SDS-PAGE). Aliquots of the purified mAbs were divided into fractions and stored at -20°C until use. Biotinylated LAM1-116 was prepared by mixing 0.15 mg of EZ-Link®-NHS-LC-Biotin (Thermo Scientific, Waltham MA) per 1 mg of purified antibody, for one hour at room temperature. Free biotin was removed from antibodies by extensive dialysis with 0.1 M PBS. The antibody concentrations of the pooled fractions were determined using a NanoDrop® scanning spectrophotometer (Thermo Scientific) at $OD_{280}$. The resulting solutions were re-suspended in 0.1 M PBS and stored at 4°C until use.

L-selectin staining of CFSE-treated cells was done 12 hours post CFSE staining. L-selectin staining was undertaken at the 12 hour time point because initial CFSE fluorescence interfered with any flow cytometric analysis by bleeding into multiple fluorescent channels that was not correctable by instrument compensation. To ensure that L-selectin was not prematurely shed by CFSE-labeled cells during the 12 hour waiting period, all samples were stored at 4°C until L-selectin staining was performed. Optimum antibody concentrations were determined empirically through fluorescence titration studies. All working antibody solutions were diluted in PBS+ 2% NHS. All antibody staining was carried out on ice for 30 minutes. Non-specific mouse IgG mAbs conjugated to the same fluorophores (Southern Biotech, Birmingham, AL) were utilized as non-specific isotypic controls in all cases. Unbound antibodies were removed prior to flow analysis with a terminal wash step using PBS supplemented with 2% normal horse serum (Thermo Scientific). All flow cytometric acquisitions were performed using a BD FACSCalibur instrument (BD Biosciences, San Jose, CA). Cells were gated on the population that showed forward and side light scatter properties of mononuclear cells. At least 5000 events were collected for each sample. All subsequent data were analyzed with CellQuest$^{TM}$ Pro (BD Biosciences) software.

iv. Chemotaxis Assay

CFSE-labeled lymphocytes (1 x $10^6$ cells/mL), re-suspended in RPMI-1640 supplemented with 0.1% bovine serum albumin (DNAse/RNAse/Protease free BSA (Fraction V), Fisher Scientific, Waltham MA) were then subjected to a chemotaxis assay, using the 48 well Neuroprobe System (Neuroprobe Inc.,

Gaithersburg, MD). The lower chamber was loaded with 50 μL of RPMI-1640+0.1% BSA, with or without 500 ng/mL of SLC (Peprotech, Rocky Hill, NJ). The SLC concentration used has been shown to induce chemotaxis of at least 50% of input T cells (6). The whole apparatus was then assembled with a 5 μm pore size polycarbonate membrane separating the upper and lower chambers. The upper chamber was then loaded with 3 treatment groups of cells ($5 \times 10^4$ cells/50 μL/well). The different treatments were: cells in media alone, cells treated with 10 μg/mL of LAM1-116 mAb, and cells treated with 10 μg/mL of LAM1-101 mAb. The appropriate antibodies were added to the cells prior to chemotaxis. Cells were then allowed to chemotax in a humidified, 37°C, 5% $CO_2$ incubator (Thermo Scientific) for one hour. The chemotaxed cells from the same treatment were pooled and adjusted to a final cell concentration of $2.5 \times 10^5$ cells/mL, in RPMI-1640 medium supplemented with: 0.1% BSA, 100 U/mL penicillin, 100 μg/mL streptomycin, 2 mM L-glutamine and 55 μM β-mercaptoethanol (all supplements were from Life Technologies). β-mercaptoethanol was not initially used due to the possibility of disulfide bond reduction in the presence of this chemical. SLC and L-selectin have multiple disulfide linkages that may be reduced and thus may result in the loss of functional secondary structure of these two molecules. However, β-mercaptoethanol was ultimately used after LAM1-116 mAb and SLC treatment to prevent the cellular aggregation inherent in long-term subculturing of primary cells. Prior to incubation in the presence of anti-TCR antibodies, lymphocyte subset analysis via flow cytometry was then performed using PE-conjugated anti-

mouse CD4 and AlexaFluor 647-conjugated anti-mouse CD8 mAbs. This analysis was performed prior to the cells being used for the subsequent assays.

v. Proliferation Assay

The previously pooled chemotaxed cells were then subjected to a TCR-induced proliferation assay. A sterile 96 well round-bottom assay plate (Thermo Scientific) was coated with low endotoxin/$NaN_3$-free grade anti-mouse CD3 (Clone:145-2C11) and anti-mouse CD28 (Clone:37.51) mAbs, both used at 2 μg/30 μL diluted in 37°C DPBS. The maximum amount of antibody that can bind to round-bottom wells has been shown to be approximately 3 μg/well (93). After 90 minutes in a 37°C, 5% $CO_2$ incubator, unbound antibodies were removed by washing the wells with 4°C DPBS. Cells from the previous assay were then added to each well at a density of 5 x $10^4$ cells/200 μL, and were allowed to proliferate in a 37°C, 5% $CO_2$ incubator. Cells were collected at the 36 and 72 hour time points and were subsequently analyzed for proliferation and apoptosis. Proliferation effects per subset were analyzed singly using anti-mouse CD4 and anti-mouse CD8 mAbs both conjugated to AlexaFluor 647 and in some cases, double staining with the same Alexa Fluor conjugated anti-mouse CD8 but with an anti-mouse CD4 conjugated to PE. Cells that displayed increasing side and forward light scatter, a property of proliferating lymphoblasts, were included in the live cell gating. Histograms of proliferating cells were compared to a corresponding CFSE-stained cell sample without TCR-induced proliferation. A similarly prepared CFSE sample must be utilized because the fluorescence intensity of CFSE exhibits some time-dependent decay. Autofluorescence

correction for negative cells was done using corresponding samples not labeled with CFSE. Thus, the area of the histogram flanked by the non-proliferated sample and the unlabeled cell sample were considered to be the proliferating population. The percentages of the proliferating population of the SLC-treated samples were compared to the sample exposed to media alone.

vi. Data Analysis

After analyzing the raw data for homogeneity of variance with the Bartlett test and normality with a Q-Q line plot, deviations were detected that proved the raw data unusable. To correct for these departures from normality and variance all data were normalized as follow:

%Proliferation Enhancement = (frequency of cells proliferating in the treated sample/frequency of proliferating cells in the untreated sample) *100

In some cases the frequency of each cell division was also determined. Manual gates were drawn to peaks corresponding to the area flanked by the negative and positive CFSE sample. Each subsequent peak had to display relative fluorescence intensity approximately half of its parent population to be considered for analysis.

Transformed data were subjected to normality and variance tests, through Q-Q line plot and Bartlett tests, respectively. No significant departures were noted or the residuals of the outliers did not impact the outcome of the factors. Data were then analyzed with one-way ANOVA. If data sets showed significant variance ($p < 0.05$), further analysis between groups was performed using the Tukey Honestly Significant Difference (HSD) test. A *P* value of less than 0.05

was considered significant. Pearson correlation was also performed between Proliferation versus % L-selectin positive cells. All summary data are displayed with standard error from the mean (SEM) bars. All data analysis was performed using R 2.15.2 (R Foundation for Statistical Computing, Vienna, Austria).

**3. Results**

i. Data transformation to correct for statistical bias in raw data from proliferation studies.

Cells labeled with CFSE and subjected to the transmigration and proliferation assays were analyzed by flow cytometry. Raw data that was collected provided a spread that affected data analysis. In the bulk lymphocytic proliferation assays at the 36 hour time point for the spleen, the numbers that corresponded to TCR-induced proliferating cells for the CFSE-labeled sample untreated with SLC or mAb, ranged from 38.7% to 94.36%. This was an important data spread because the most responsive population treated with SLC and LAM1-116 simultaneously, also had a big data spread of 48.3% to 98%. Using a Q-Q plot to determine normality, outliers that impacted the outcome of the dependent factors were detected. Furthermore, the Bartlett test for homoscedasticity also yielded departures from variances that were not a product of normal distribution. In other instances, where data were normally distributed and homogenous variances were established, the results yielded a *P* value of less than 0.05. However, upon closer examination using the *post hoc* Tukey HSD test, the significant finding was the result of the negative sample exhibiting lower proliferation than the treated samples, with no variances between SLC-treated samples, which rendered our data set differences statistically insignificant. To

eliminate the departures from normality and homoscedasticity, we transformed the data sets by comparing all effects to the proliferated but untreated control. As such, for proliferation, the equation Treatment (SLC, SLC+LAM1-116, and SLC+LAM1-101)/Control * 100, was used to generate a proliferation index. Numbers lower than 100% indicate a lower proliferative effect than the control and numbers greater than 100% indicate effects higher than the control. The added benefit of this transformation is that the comparisons between samples are now restricted to 3 samples treated with SLC, narrowing the dependent variable to L-selectin activation alone. This comparison is utilized for the remainder of these studies, unless otherwise stated.

ii. Spleen and PLN lymphocytes treated with SLC and LAM1-116 mAb have increased proliferation at 36 and 72 hours post-TCR stimulation

To mimic *in vivo* conditions, we utilized mAbs to CD3 and CD28 to create a condition, parallel to that encountered by T cells during MHC-restricted antigenic challenge. As expected, all samples showed enhanced proliferation over the control, likely as a product of SLC treatment (Figure 6). In all cases, SLC treated samples pre-treated with the L-selectin activating LAM1-116 mAb showed the greatest enhancement in proliferation (Figure 6 C and G). In the 36 hour spleen sample, the variance between the 3 treatment group samples compared to the control was significant at $P$=0.04 (n=10). Interestingly, Tukey's HSD test tended towards a significant difference between the SLC+LAM1-116 mAb treated sample versus the SLC treated sample with a $P$=0.06 (n=10). This was the same in comparing the LAM1-116 mAb treated sample to the LAM1-101 mAb treated sample with a $P$=0.09 (n=10). In the PLN sample at the same period

of 36 hours, the variance was significant at *P*=0.01 (n=9) with Tukey's HSD test showing *P*=0.01 (n=9) and *P*=0.04 (n=9) for the LAM1-116 mAb treated sample compared to SLC alone and the LAM1-101 mAb treated sample, respectively. Visually analyzing the histograms also showed a discernible increase in the late cell division population ( by the number of peaks, and the height of the terminal peak) of the LAM1-116 mAb-treated samples as compared to other samples, in both the spleen and PLN. We expected proliferation effects to be higher in the PLN, because this secondary lymphoid organ is T cell rich compared to the spleen, and T cells as a population have higher frequencies of L-selectin positive cells. During the early post-stimulation period of 36 hours, this was the case with proliferation enhancement in the PLN ranging from 115%-134% as compared to the range in the spleen of 105%-116% (Figure 7).

Interestingly, at 72 hours post-TCR stimulation, treatment groups showed a general decrease in proliferation enhancement (Figure 8). The decrease in proliferation of the 72 hour samples does not seem to be a product of time sensitization but rather a by-product of samples reaching or approaching asymptotic growth at the later times post-TCR stimulation, indicating all cell populations have reached close to maximal divisions (Figure 8). This seems to be a shortcoming of our data transformation which we will address later.

At the 72 hours post-TCR stimulation time point, both the spleen and the PLN showed an almost equal level of enhanced proliferation with ranges of 108%-117% and 107%-120%, respectively. The ANOVA test showed significant variances for both spleen and PLN at *P*=0.015 (n=7) and *P*=0.016 (n=6),

respectively (Figure 9). However, regardless of the decreased proliferative enhancement effect of SLC and LAM1-116 mAb treatment at 72 hours post-stimulation, in comparison to the similarly treated 36 hour sample, Tukey's HSD test show significant increases for the LAM1-116 mAb treated splenic sample, with a *P*=0.02 (n=7) compared to SLC treatment alone, and a *P*=0.04 (n=7) compared to LAM1-101 mAb treatment.

iii. Transmigrating cell subsets show homogeneity regardless of treatment

The significant levels of proliferation in bulk populations at the 36 and 72 hour mark gave us an impetus to determine if these enhanced proliferation levels were present in both the $CD4^+$ and $CD8^+$ T cell subsets. We initially chose to focus on T cells due to the higher density of L-selectin and CCR7 expression in these cells in comparison to B cells. Furthermore, activation in B cells seems to result in CCR7 up-regulation which is in opposition to the T cell-specific effect (94).

The transmigration step before the proliferation assay was a potential pitfall because it was possible that there would be a transmigration bias towards a particular subset and thus affect subset proliferation results. Fortunately, there were no statistical variances between treatment groups as to the proportion of transmigrated $CD4^+$ and $CD8^+$ T cell subsets as shown in representative dot plots (Figure10, upper left and lower right quadrant numbers) or as shown in summary data (Figure 11). Specifically, the frequency of transmigrated splenic $CD4^+$ T cells regardless of treatment was not varied (n=7, *P*=0.91) at a range of 21±1.2%. The results were similar for splenic $CD8^+$ T cells at a range of 17±2%

with a variance of *P*=0.98 (n=7). PLN $CD4^+$ T cells also showed no variance between treatments at *P*=0.99 (n=7). $CD8^+$ T cells from the PLN also were not statistically varied at a *P*=0.97 (n=7).

The homogenous proportions of both T cell subsets in all treatments allowed us to undertake the subsequent experiments with ease and without bias

iv. Spleen and PLN $CD4^+$ T cells treated with SLC and LAM1-116 mAb have increased proliferation at 36 and 72 hours post-TCR stimulation

To determine the effects of L-selectin activation among the $CD4^+$ T cell subset, we labeled samples for CD4 and determined the frequency of proliferating cells in the treatment groups as discussed in the previous experiments. After gating for cells that exhibited the side and forward light scatter properties of mononuclear cells, $CD4^+$ T cells as distinguished by PE-conjugated antibody staining, were analyzed for CFSE intensity, to examine proliferation using the same strategy as outlined in the previous experiments. A representative experiment illustrating an increase in $CD4^+$ T cell proliferation as compared to the negative control is shown in Figure 12. Comparing the SLC-treated sample to the negative control, an increase from 61% to 66% was found in the spleen sample (Figures 12 A and B), and an increase from 44% to 48% was found in PLN samples (Figures 12 E and F). The SLC+LAM1-101 mAb-treated samples showed similar increases in comparison to the negative control for both splenic and PLN samples but show an equal increase in proliferation when compared to the SLC-treated sample alone (Figures 12 A and D, and Figures 12 E and H, respectively). Interestingly, the SLC+LAM1-116 mAb-treated samples showed the highest increases in proliferation (12 C and G).

The increases outlined above were statistically significant, as shown in the summary data (Figure 13), with variance in the spleen sample, after data transformation, at $P$=0.01 (n=7) and for the PLN sample with $P$=9x10$^{-4}$ (n=7). In the spleen, the increase in the SLC+LAM1-116 mAb-treated sample compared to the SLC-treated cells was significant at $P$=0.01 (n=7), or with the SLC+LAM1-101 mAb-treated sample $P$=0.03 (n=7). In the PLN, the same levels of significance were noted with $P$=0.01 (n=7) between LAM1-116 mAb treated SLC transmigrated cells versus SLC-treated alone transmigrated cells. The increase in proliferation for the LAM1-116 mAb treatment as compared to the LAM1-101 mAb treatment was also statistically significant with a $P$=0.02 (n=7).

In the samples analyzed 72 hours post stimulation, all samples showed increased proliferation over the 36 hour sample. In the representative histograms shown in Figure 14, all SLC-treated samples showed appreciable increases in proliferation when compared with the untreated negative control. As expected, the LAM1-116 mAb-treated samples showed the highest increase in proliferation.

The summary data (Figure 15) reflects the above described enhancements with the splenic and PLN samples showing significant variance at $P$=0.01 (n=5) and $P$=0.03 (n=5), respectively. In the spleen, the Tukey's HSD test showed statistical difference between the SLC- vs. SLC+LAM1-116 mAb-treated samples with a $P$= 0.01 (n=5). A similar difference in the same tissue was found between the SLC+LAM1-101 mAb- vs. SLC+LAM1-116 mAb-treated samples with a $P$=0.03 (n=5). In the PLN, the Tukey's HSD test showed significant differences between the LAM1-116 mAb-treated sample vs. SLC alone with a

*P*=0.05 (n=5), and with the LAM1-101 mAb-treated sample with a *P*=0.04 (n=5). Taken together, these results strongly support the idea that L-selectin activation prior to SLC-induced chemotaxis significantly enhances $CD4^+$ T cell proliferation through the TCR, regardless of tissue origin.

iv. Spleen and PLN $CD8^+$ T cells treated with SLC and LAM1-116 mAb have increased proliferation at 36 and 72 hour post-TCR stimulation

Analysis of $CD8^+$ T cells showed enhancements that mirrored the effects seen in $CD4^+$ T cells. Representative data (Figure 16) showed increased proliferation for all SLC-treated samples compared to the negative control. As expected, the SLC+LAM1-116 mAb-treated sample showed the highest enhancement in proliferation. The summary data (Figure 17) demonstrates statistical significance in the 36 hour samples with the spleen and PLN showing significant variances of *P*=0.003 (n=8) and $P=4.9 \times 10^{-5}$ (n=9), respectively. In the splenic sample, Tukey's HSD test for the SLC+LAM1-116 mAb treated sample vs. the SLC alone treatment or SLC+LAM1-101 mAb treated was significant with *P*=0.007 (n=8) and *P*=0.009 (n=8), respectively. The same trend was seen in the PLN with comparison between the SLC and SLC+LAM1-116 mAb groups showing a $P=6.2 \times 10^{-5}$ (n=9), and the SLC+LAM1-116 to SLC+LAM1-101 mAb treated groups showing a $P=9.2 \times 10^{-4}$ (n=9).

For the $CD8^+$ T cell analysis for 72 hour proliferation, all proliferation levels increased, similar to the 72 hour $CD4^+$ proliferation. Representative data shown in Figure 18 demonstrates similar increases for all SLC-treated samples, with the LAM1-116 mAb-treated sample showing the highest enhancement in proliferation. Variance between treatments after data transformation was

significant for both the spleen and PLN, with *P*=0.0004 (n=5) and *P*=0.002 (n=5), respectively (Figure 19). In the PLN, *post hoc* tests showed HSD values to be significant between the SLC+LAM1-116 mAb-treated sample vs. SLC alone or SLC+LAM1-101 mAb treatment (n= 5, *P*=0.002; n=5, *P*=0.02, respectively). In the spleen, Tukey's HSD test also showed significant differences between the SLC+LAM1-116 mAb treated samples vs. the SLC-treated alone sample (n=5, *P*=0.0005) or the SLC+LAM1-101 mAb-treated sample (n=5, *P*=0.002). Thus, these findings of L-selectin-mediated increases in $CD8^+$ T cell proliferation are in good agreement to the results seen in $CD4^+$ T cells.

v. Samples treated with SLC and LAM1-116 mAb showed higher frequencies of $CD4^+$ and $CD8^+$ T cells at the terminal divisions for samples reaching asymptotic growth.

To address the limitations of samples reaching asymptotic growth at the 72 hour time point, and thereby providing no distinguishable differences between samples, we decided to analyze dividing subpopulations (Figure 20). To this end, we isolated 3 samples from both the spleen and PLN that showed at least 3 discernible division peaks. These peaks had to show a MFI of at least half of the preceding peak to be considered for analysis. Without exception, SLC+LAM1-116 mAb-treated samples showed a higher frequency of both $CD4^+$ and $CD8^+$ T cells in the terminal division ($P_5$, Table 1). In splenic $CD4^+$ T cells, the LAM1-116 mAb-treated sample showed a doubling of cells in the $G_5$ subpopulation vs. all other treatments. A similar result was also observed for the splenic $CD8^+$ T cells.

In the PLN, $CD4^+$ T cells treated with LAM1-116 mAb showed the highest means compared to all other treatments. $CD8^+$ T cells in the same tissue also

showed similar increases in cell frequency at the terminal division, when compared to SLC treatment alone or the SLC+LAM1-101 mAb treatment group. Unfortunately, the variability between experiments along with the small n, did not allow us to find any significant differences. Transforming the data set similar to the steps outlined in the previous experiments provided no relief from the large variances or did not eliminate normality outliers. Using power analysis (power=0.80) an n=44.5 would be required to overcome this statistical quandary.

vi. Frequency of L-selectin$^+$ cells and enhanced proliferation do not show a correlation.

While virtually all naïve T cells express high levels of L-selectin, subsets of effector and memory T cells express low to negative levels (95). Using Pearson's correlation, we then embarked on determining whether the frequency of L-selectin positive cells effected proliferation. All transformed proliferation numbers were compared to the frequency of L-selectin positive cells in each sample, corresponding to all cell populations regardless of tissue origin and subset. Pearson's *r* for L-selectin frequency vs. 36 hour proliferation showed an $r$=0.01, indicating no relationship between the two variables whatsoever. The same was detected in the 72 hour time point with $r$=0.00. However, visualizing the data set (Figure 21), one can see a minor positive r value for L-selectin frequency vs. the 72 hour proliferation levels. The presence of outliers may have negated this effect, with a steep decline of correlation at the highest levels of proliferation. Interestingly, there is significant positive correlation between the 36 and 72 hour proliferation time points with an $r$=0.37, $P$=0.0085. An alternative approach to discern whether the frequency of L-selectin$^+$ cells affect proliferation would be to

subject the samples to multi-variate analysis, perhaps by using MANOVA or using a general linear model (GLM). However, because the frequency L-selectin$^+$ cells between tissues and subsets do not have an appreciable difference, analysis of L-selectin$^+$ cell effects may prove unattainable.

**4. Discussion**

The bulk of the results from the current studies point to a general contribution of L-selectin activation to T cell proliferation. This effect is most likely directly related to L-selectin activation since the antibody used was a monoclonal antibody that has previously been shown to bind to the activation (i. e., lectin) domain of L-selectin (10). This is in comparison to the lack of response of cells treated with the control antibody that also binds L-selectin but at a region distinctly distant from the activating site. The current results also show that activation through CCR7 via SLC contributes to increases in TCR-mediated proliferation. However, while SLC activation alone did induce a modest increase in T cell proliferation, the highest level of proliferation was exclusively found in the L-selectin-activated samples. In regards to subset analysis, because of the transmigration step prior to TCR-induced proliferation, it was possible that subsets could show a distinct preference for chemotaxis based on mAb treatment or chemokine used. This would have a dire consequence on subset bias. If the SLC+LAM1-116 mAb treatment induced higher levels of CD4$^+$ or CD8$^+$ T cell migration in comparison to the SLC- or SLC+LAM1-101 mAb-treated samples, the sheer difference in cell proportion between treatments could be the simple explanation for any observed proliferative effects. However, subset

analysis of treatment populations indicated homogenous populations negating any population effects that may have rendered our analysis invalid (Figure 11).

In the 36 hour post-TCR stimulation analysis, proliferation levels were significantly higher in the LAM1-116 mAb-treated, SLC transmigrated samples. The PLN bulk sample showed a distinct higher increase in proliferation compared to the spleen bulk sample (Figure 7). This is reasonable because of the higher proportion of T cells in this tissue, which in turn have higher expression levels of L-selectin (4). Similarly, $CD4^+$ T cells from the PLN also showed a better response to LAM1-116 mAb treatment compared to the corresponding splenic sample. This most likely reflects the finding that 88±3% of PLN $CD4^+$ cells expressed high levels of L-selectin in comparison to 80±2% for splenic $CD4^+$ T cells (data not shown). In regards to $CD8^+$ T cells, the increase in proliferation was opposite of that observed for $CD4^+$ T cells. Specifically proliferation of splenic $CD8^+$ T cells treated with LAM1-116 mAb surpassed that similarly treated PLN $CD8^+$ T cells by at least 10% (131±6% vs 120±2%, respectively). This was unexpected due to higher levels of L-$selectin^+$ $CD8^+$ T cells in the PLN. However, the nature of the $CD8^+$ T cells in each tissue also has to be taken into account. $CD8^+$ T cells of the central memory phenotype may be present in higher numbers in the spleen and therefore may exhibit a more responsive proliferative effect compared to naïve cells that have just recently transmigrated to the PLN. Central memory cells are products of clonal expansion during antigenic encounter which possess the ability to migrate between the blood and parenchyma. This population has been known to be more reactive and more efficient in clearing

antigenic challenges (96). Furthermore, the difference in L-selectin$^+$ CD8$^+$ T cells that are between compartments were negligible at less than 2%, with the PLN residents at the high end (data not shown). Another possible explanation for this difference is the nature of the microenvironment from where the cells originated. T lymphocytes and therefore CD8$^+$ T cells are not the dominant cell type in the spleen. In the transmigrated population analyzed via flow cytometry, less than 50% of splenic cells were T cells as compared to almost 80% of PLN cells (Figure 11). A possible population that may create an environment in which CD8$^+$ T cells from the spleen proliferate better may be the CD56$^{dim}$ natural killer cells. This NK subset is more abundant in the spleen and has been shown to be more prolific in responding to antigen and produces high levels of pro-inflammatory cytokines at early stages of antigenic encounter (97-98). Another interesting finding came from comparing CD4$^+$ versus CD8$^+$ T cells in the same tissue. Although, the CD8$^+$ T cells in the spleen showed a better response to L-selectin-mediated signaling compared to splenic CD4$^+$ T cells, this was not the case in the PLN. In the PLN, CD4$^+$ T cells proliferated better than CD8$^+$ T cells following L-selectin engagement (Figure 13 and 14). We expected CD8$^+$ T cells to have a more robust response to LAM1-116 mAb treatment because of the frequency of L-selectin positive cells for this subset (93.5±0.5%) in comparison to the CD4$^+$ T cells (87±1%) (data not shown). Additionally, experiments using bulk populations also showed a better predisposition of PLN lymphocytes to proliferate compared to the spleen (Figure 7). A possible explanation for this difference is the larger proportion of CD4$^+$ T cells in the PLN transmigrating population (Figure 11). This

PLN $CD4^+$ T cell population is distinct from that of the spleen due to the higher frequency of L-selectin positive cells. Another contributing factor to the enhancement in $CD4^+$ T cell proliferation in this tissue may be the higher density of dendritic cells (99). Dendritic cells are extremely efficient at presenting antigen and activating $CD4^+$ T cells and thus their increased presence in the PLN samples may contribute to the observed enhanced proliferation.

In the 72 hour samples, the results were much clearer. As expected, all LAM1-116 mAb-treated samples produced the greatest proliferative responses (Figures 9, 15 and 19). In the bulk populations, both tissue samples were almost identical in proliferation enhancement. As discussed before, we expected a more robust response in the PLN proportional to the increased frequency of L-selectin$^+$ cells. It must be noted that at the 72 hour time point, most of the samples regardless of treatment had reached 90% or higher levels of proliferation (Figures 8, 14 and 18). Therefore, the differences between tissues were less distinct. Regardless of this convergence on asymptotic growth for the bulk populations, our expectations were supported for cell subsets in all tissues. In the spleen and PLN, the $CD8^+$ T cell subset exhibited a higher degree of proliferation enhancement over the $CD4^+$ T cell subset, consistent with the frequency of L-selectin$^+$ cells (Figures 15 and 19). PLN residents also showed a higher level of proliferation enhancement over their splenic counterparts, again consistent with L-selectin$^+$ cell frequency (Figures 15 and 19).

To determine the preference of subsets reaching a terminal division, we utilized samples reaching asymptotic growth and compared the frequency of

each T cell subset per terminal division (Figure 21, Table 1). This particular experiment was only performed with samples reaching asymptotic growth because samples reaching submaximal growth do not exhibit the same number of cell divisions and thus a true comparison between samples cannot be made. In all tissue subsets, L-selectin activation resulted in more cells reaching terminal division (Table 1). Furthermore, $CD4^+$ spleen T cells, which contained the lowest frequency of L-$selectin^+$ cells, also displayed the lowest rates of terminal division. As expected, $CD8^+$ T cells and PLN residents displayed the highest rates of terminal division with the PLN $CD8^+$ T cells exhibiting the highest rate. However, the variance between samples made the data set inconclusive but with trends following our predictions. The variance problem can be easily solved by increasing the sample size. However, at the 72 hour time point post-stimulation, finding treatments that have reached asymptotic growth is not definite. This problem could be easily solved by moving time points farther forward, possibly to 4 or 5 days post stimulation. Another problem that arose from this study was the non-linear relationship between the frequency of L-$selectin^+$ cells and proliferation as outlined in Figure 21. Just by visual inspection, no correlation between L-selectin frequency and the two time points could be detected. In the 36 hour proliferation time point, no correlation could be ascertained statistically or visually (Figure 21A and 21C). In the 72 hour data set, a positive correlation between L-selectin frequency and proliferation was apparent at the lower levels that increased proportionally as L-selectin frequency increased (Figure 21E). However, there was a decline in the relationship in the latter parts of the figure,

thus, negating the initial positive correlation. Interestingly, there was a clear positive correlation between the 36 hour and 72 hour time points of proliferation, indicating that cells that have proliferated better at 36 hours also proliferated better at the 72 hour time point.

Aside from the minor issues outlined previously, our data shows that L-selectin activation contributes to the ability of T cells to proliferate in response to signaling. Because this study is singularly based on phenotypic analysis *in vitro*, we are hampered by our inability to pinpoint a mechanism for such proliferative effects. To this end, we propose the following mechanistic model.

It has been shown that the cytoplasmic tail of L-selectin associates with CaM (100-102). The cytoplasmic tail is also known to associate with ezrin radixin moesin (ERM) proteins (101, 39). Based on these observations, a model of L-selectin multimerization involving CaM and ERM binding adjacent L-selectin molecules was proposed (101). It is known that L-selectin activation oftentimes involves ectodomain shedding (103-104), which in turn disrupts cytoplasmic tail associations. Subsequently, CaM and ERM proteins are released exposing the two serine residues in the cytoplasmic tail that in turn has been shown to be phosphorylated (84). What happens after? This phosphorylation step most likely mediates a response because it is difficult to understand why a molecule would be phosphorylated and not used.

It has previously been shown that L-selectin can bind growth factor receptor-bound protein 2/son of sevenless (Grb2/SOS), and activate the Ras pathway (105). However, Grb2/SOS binding requires a Src homology 2 (SH2)

binding domain which is not present in the L-selectin cytoplasmic tail. It should be noted that SH2 domains bind to phosphorylated tyrosine residues and L-selectin does possess a terminal tyrosine residue in the cytoplasmic domain that can potentially be phosphorylated. However, this is unlikely because of its terminal position and the absence of an SH2 domain. A likely candidate that could bridge L-selectin and Grb2/SOS binding is the 14-3-3 protein. The cytoplasmic terminal amino acid sequence of mouse L-selectin (RRLKKGKKSQERMDDPY), and human L-selectin (RRLKKGKKSKRSMNDPY), both show a potential homologous sequence to the putative 14-3-3 binding mode 1 sequence of RS*X*p**S***X*P (106, the bold serine residue indicates required phosphorylation). Although the sequence of the L-selectin tail is not 100% complementary to the putative binding domain, it must be noted that 14-3-3 can bind to some proteins displaying a dissimilar sequence as in the case of insulin-like growth factor-1 (107), or insulin receptor substrate-1 (108). The ability of 14-3-3 to bind to regions without complete complementarity seems to rest on its ability to utilize a 14-3-3 dimer as well as dual phosphoserine residues for partner binding (109). It is then possible that 14-3-3 binding to the L-selectin tail can recruit Grb2/SOS. It must be noted that Grb2 and 14-3-3 possess SH2 and Src homology 3 (SH3) domains, respectively. It has been shown that SH2 and SH3 domains can interact with each other (110-112).

In light of the possibility of L-selectin+14-3-3 binding and the eventual recruitment of the Grb2/SOS dimer, one can now see that the potential of Ras sarcoma protein (Ras) involvement is quite likely. The Grb2/SOS and Ras

relationship has been firmly established. SOS serves as a guanine exchange factor (GEF), and its primary role is in the transition for Ras to exchange its bound GDP to GTP (113-115). The GDP to GTP transition activates Ras (116). Importantly, it must be noted that the same paper by Brenner in 1996, also showed Ras involvement. The involvement of Ras is expected with the diversity of signaling molecules that are activated during L-selectin activation. Specifically, reports have shown that L-selectin activation involves Rac protein (117), p38 mitogen activated protein kinase (MAPK) (118), urokinase receptors (119), light chain kinase (Lck) (120), in addition to others. The Ras pathway is logical because most of the signaling molecules outlined above are downstream events of Ras activation. Furthermore, Ras is an oncogenic protein responsible for proliferation signals in tumorigenic cells, in parallel to our proliferation assays.

The proposed mechanism of phosphorylated L-selectin+14-3-3+Grb/SOS+Ras is a very plausible one in relation to enhancement that has been reported in other cell mechanisms. In the Subramanian paper (6), an L-selectin signaling contribution to CCR7-mediated chemotaxis was described. SOS is a guanine exchange factor, responsible for the GDP-GTP transition, in its function, as well as the function of other molecules. The G$\alpha$ subunit of G-protein coupled receptors (GPCR) requires a transition from GDP to GTP, which is normally catalyzed by a GPCR ligand docking to the receptor. It is foreseeable that SOS can also induce this GDP-GTP exchange in GPCR's, activating them in the absence of ligand, and in our case enhancing the activity of CCR7 in the presence of its ligand, SLC. This indirect relationship between L-selectin and

proliferation by way of Ras also explains the absence of significant correlation in our study (Figure 21). The TCR-induced proliferation may have masked any contributions to proliferation by L-selectin, with TCR-induced proliferation being much stronger than L-selectin-induced proliferation. This could also explain the small amounts of LAM-116 mAb-induced proliferation observed relative to the control.

The proposed mechanism outlined above directly supports the L-selectin-induced enhancement in TCR-mediated proliferation outlined in this thesis as well as the chemotactic enhancement reported previously (6). Further work to clarify the molecular mechanisms must be undertaken to provide a better understanding of the underlying mechanism and lend additional support for our proposed model.

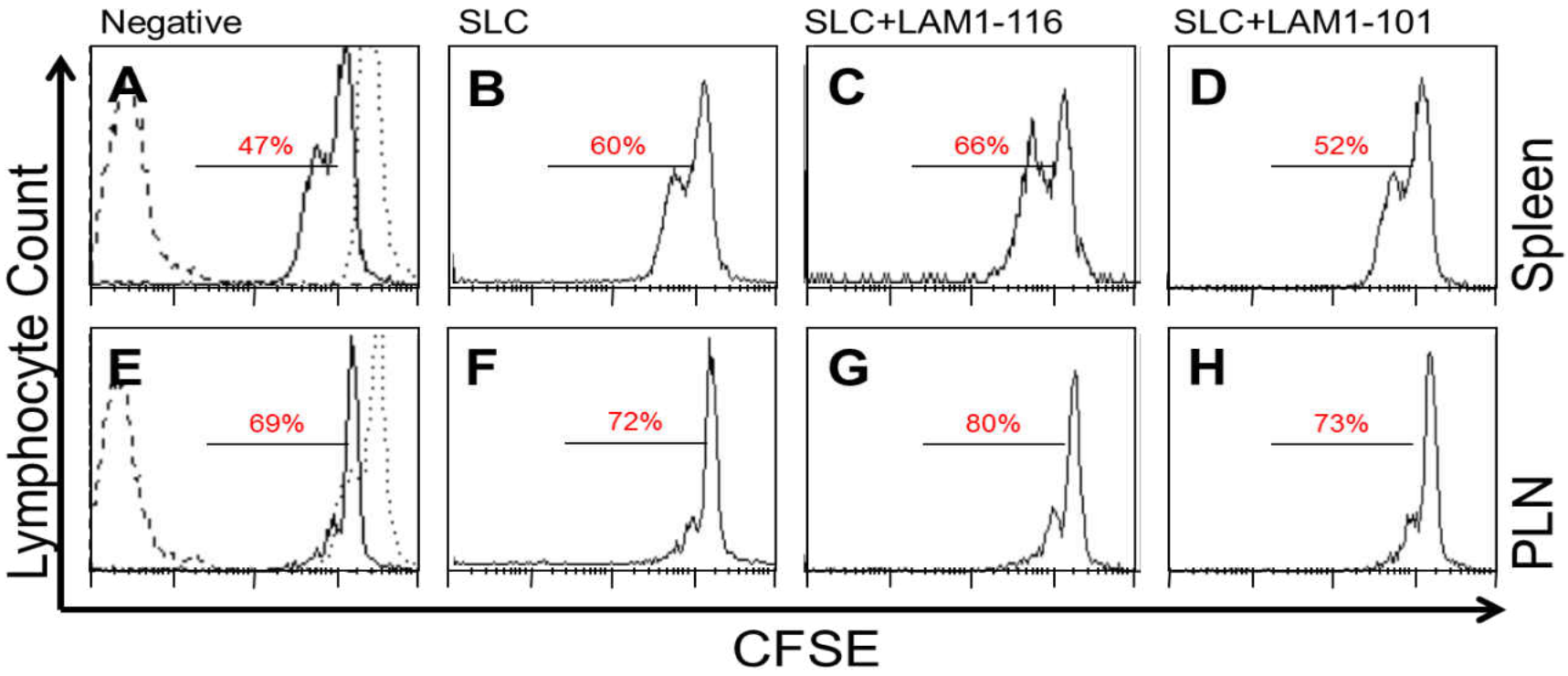


**Figure 6**. Representative proliferation histograms of spleen and PLN lymphocytes at 36 hours post-TCR stimulation. Cells were isolated from Spleen (A-D) and PLN (E-H), and stained with 0.25 μM of CFSE (intensity shown on the X axis). Some samples were treated with 10 μg/mL of the L-selectin activating mAb, LAM1-116, before transmigration in the presence of 500 ng/mL of SLC (SLC+LAM1-116, C and G). Other samples were transmigrated to the same concentration of SLC with no mAb treatment (SLC, B and F) or treated with 10 μg/mL of a control mAb, LAM1-101 (SLC+LAM1-101, Figures D and H). Cells that transmigrated to media alone without mAb treatment are considered negative (Figures A and E). All 4 treatment subsets were subsequently induced to proliferate in the presence of anti-CD3 and anti-CD28 mAbs in a 96 well plate. Numbers in red indicate the frequency of actively proliferating cells. Proliferating cells were identified as the population flanked by a non-CFSE stained sample (dashed line) and a non-proliferated CFSE stained sample (dotted line). Both controls were from the same population as the treated samples and were analyzed at the same time point. Results are representative of 10 and 9 experiments for spleen and PLN, respectively.

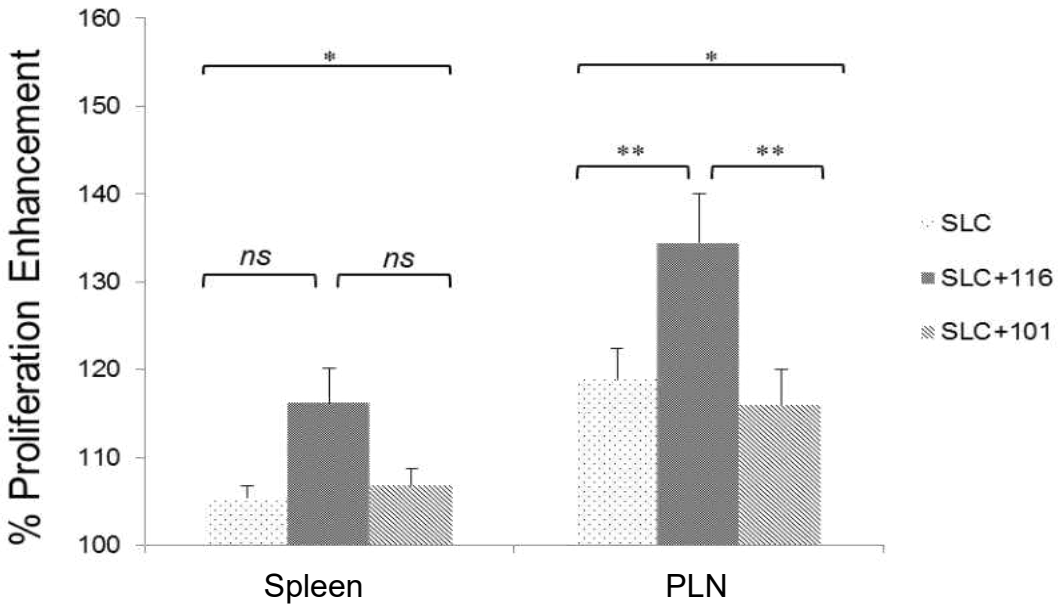


**Figure 7**. Summary data of spleen and PLN lymphocyte proliferation at 36 hours post-TCR stimulation. Results are from experiments shown in Figure 6. All numbers (mean±SEM) are in comparison to a proliferated and CFSE-stained control sample exposed to media alone (Treatment/Control*100). In both the spleen and PLN, variances (one-way ANOVA) between treatments were significant, n=10, *P*=0.04; n=9, *P*=0.01; respectively. In the spleen, ***post hoc*** Tukey HSD tests showed no significant difference between the LAM1-116 treated sample compared to the sample treated with SLC alone, n=10, *P*=0.06, or the sample treated with SLC along with the control mAb, LAM1-101, n=10, *P*=0.09. In the PLN, the differences between groups were significant in both cases: n=9, *P*=0.01; n=9, *P*=0.04; respectively. Statistical analysis was performed using R version 2.15.2. * indicates $_{P}$Anova<0.05. ** indicates $_{P}$Tukey HSD<0.05. *ns* indicates not significant.

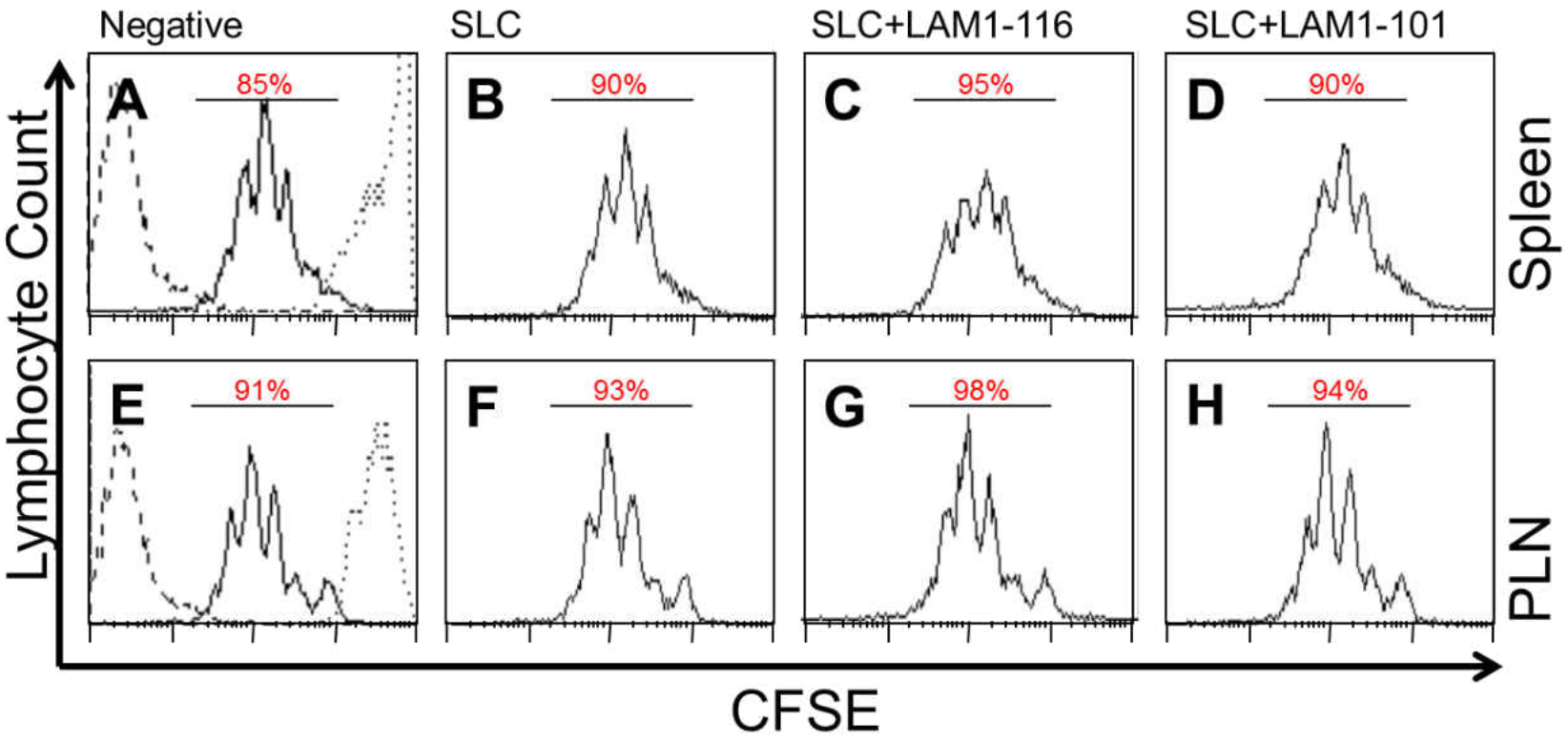


**Figure 8**. Representative proliferation histograms of spleen and PLN lymphocytes at 72 hours post-TCR stimulation. Cells were isolated from Spleen (A-D) and PLN (E-H), and stained with 0.25 μM of CFSE (intensity shown in the X axis). Samples were treated as described in Figure 6 and analyzed 72 hours following TCR stimulation. Numbers in red indicate the frequency of actively proliferating cells. Proliferating cells were identified as the population flanked by a non-CFSE stained sample (dashed line) and a non-proliferated CFSE stained sample (dotted line). Both controls were from the same population as the treated samples and were analyzed at the same time point. Results are representative of 6 and 7 experiments for spleen and PLN, respectively.

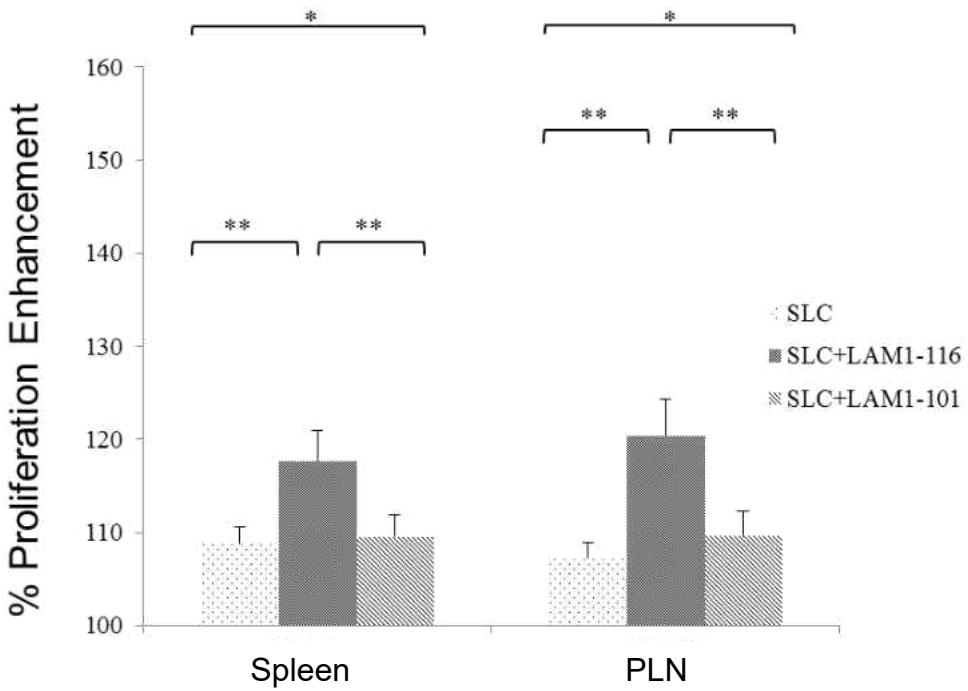


**Figure 9.** Summary data of spleen and PLN lymphocyte proliferation at 72 hours post-TCR stimulation. Results are from experiments shown in Figure 8. All numbers (with SEM bars) are in comparison to a proliferated and CFSE-stained control sample exposed to media alone (Treatment/Control*100). In both the spleen and PLN, variances (one-way ANOVA) between treatments were significant, n=7, *P*=0.015; n=6, *P*=0.016; respectively. In the spleen, *post hoc* Tukey HSD tests showed significant difference between the LAM1-116 treated sample compared to the sample treated with SLC alone, n=7, *P*=0.02, or the sample treated with SLC along with the control mAb, LAM1-101, n=7, *P*=0.04. In the PLN, the differences between groups were significant in both cases: n=6, *P*=0.05; n=6, *P*=0.02; respectively. Statistical analysis was performed using R version 2.15.2. * indicates $_{P}$Anova<0.05. ** indicates $_{P}$Tukey HSD<0.05.

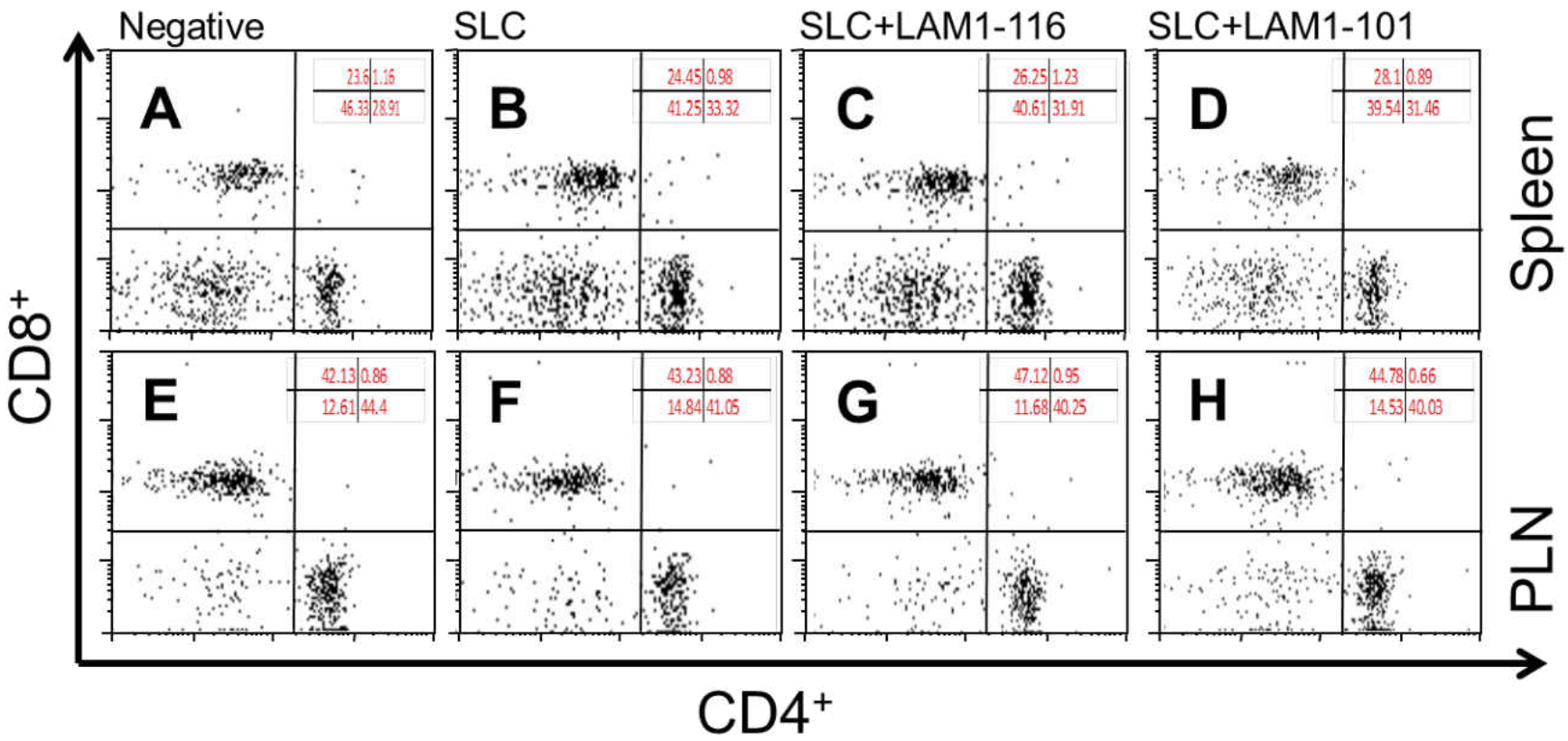


**Figure 10.** Representative subset dot plots of transmigrated cells. Cells were isolated from spleen (A-D) and PLN (E-H), and treated as described in Figure 6. After chemotaxis, wells for the same treatment were pooled and subset frequencies for $CD4^+$ T cells (x axis) and $CD8^+$ T cells (y axis) in the transmigrated population were determined using flow cytometry. Numbers in red indicate the frequency of cells in each quadrant. No significant variations between treatment groups were detected. Results are representative of 7 experiments.

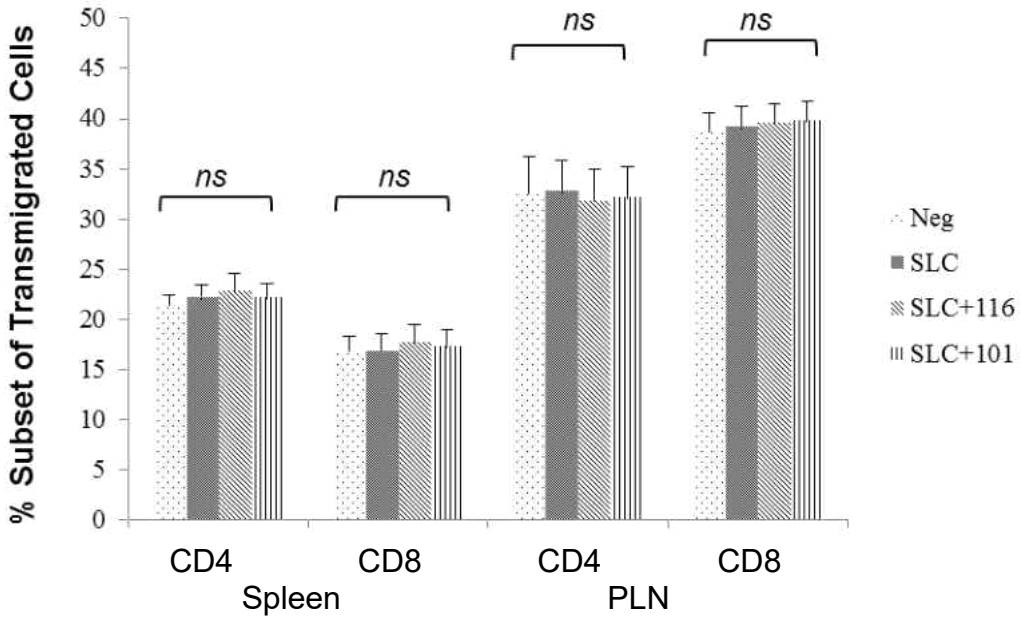


**Figure 11**. Summary data of transmigrated cell subset analysis. Data was obtained from the experiments shown in Figure 10 (n=7 independent experiments). *ns* indicates not significant.

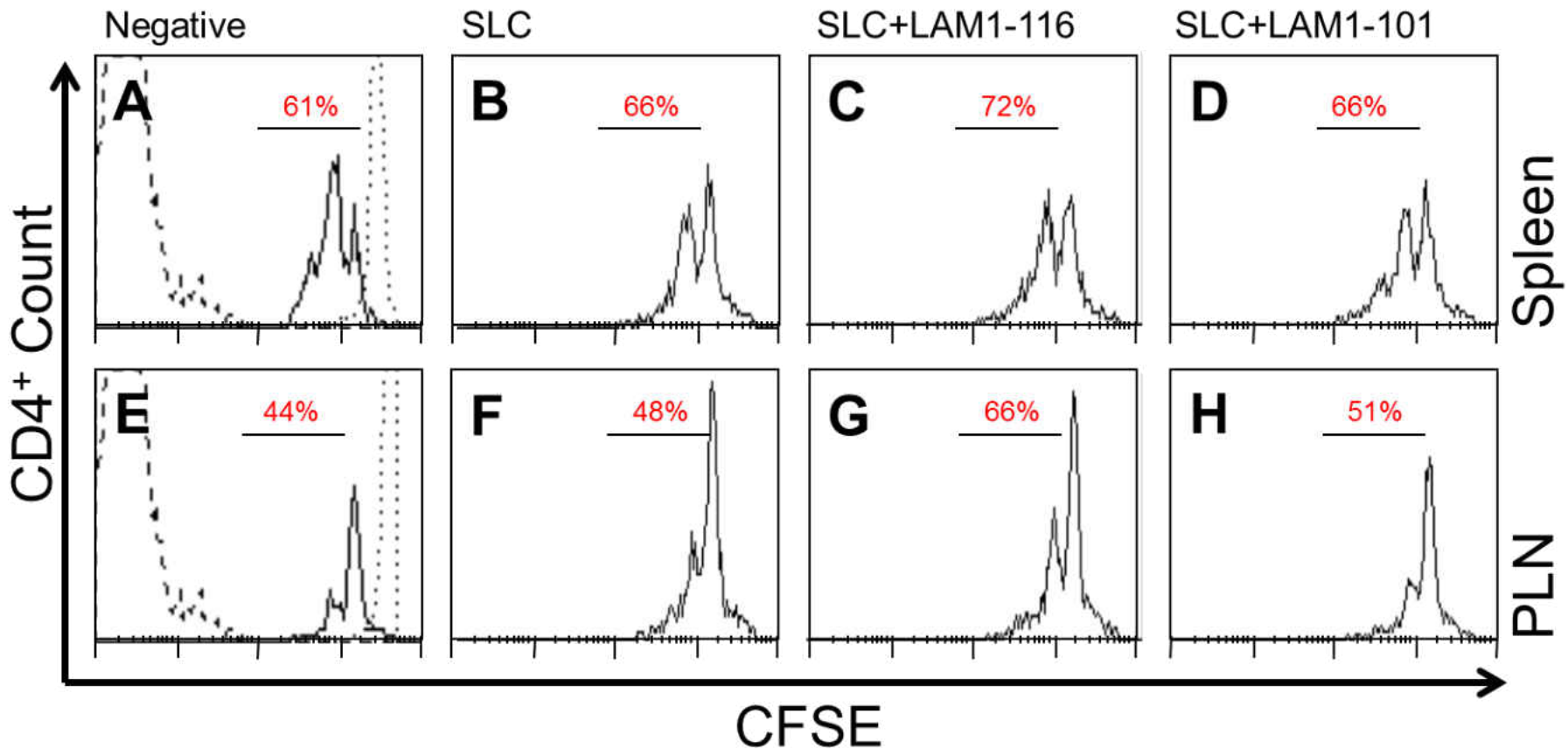


**Figure 12**. Representative histograms of proliferating $CD4^+$ T cells at 36 hours post-TCR stimulation. Cells were isolated from spleen (A-D) and PLN (E-H), and treated as described in Figure 6 except that the samples were labeled for CD4 expression. Numbers in red indicate the frequency of actively proliferating $CD4^+$ T cells. Proliferating cells were identified as the population flanked by a non-CFSE stained sample (dashed line) and a non-proliferated CFSE stained sample (dotted line). Both controls were from the same population as the treated samples and were analyzed at the same time point. Results are representative of 7 independent experiments per tissue.

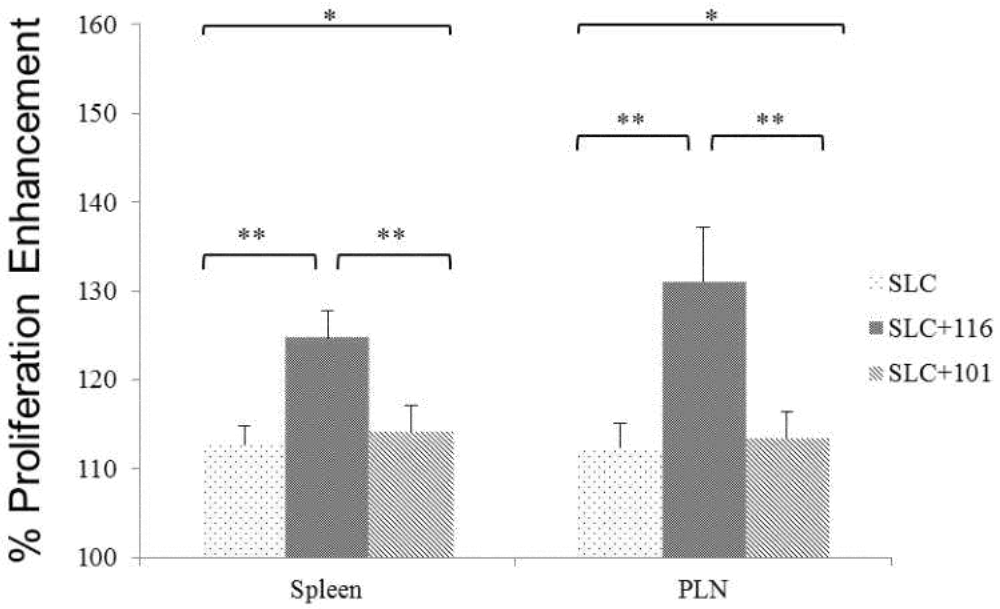


**Figure 13**. Summary data of $CD4^+$ T cell proliferation at 36 hours post-TCR stimulation. Results are from experiments shown in Figure 12. All numbers (with SEM bars) are in comparison to a proliferated and CFSE stained control sample exposed to media alone (Treatment/Control*100). In both the spleen and PLN, variances (one-way ANOVA) between treatments was significant, n=7, *P*=0.01; n=7, *P*=0.0009; respectively. In the spleen, *post hoc* Tukey HSD tests showed significant difference between the LAM1-116 mAb treated sample compared to the sample treated with SLC alone, n=7, *P*=0.01, or the sample treated with SLC along with the control mAb, LAM1-101, n=7, *P*=0.03. In the PLN, the differences between groups were significant in both cases: n=7, *P*=0.01; n=7, *P*=0.02; respectively. Statistical analysis was performed using R version 2.15.2. * indicates $_P$Anova<0.05. ** indicates $_P$Tukey HSD<0.05.

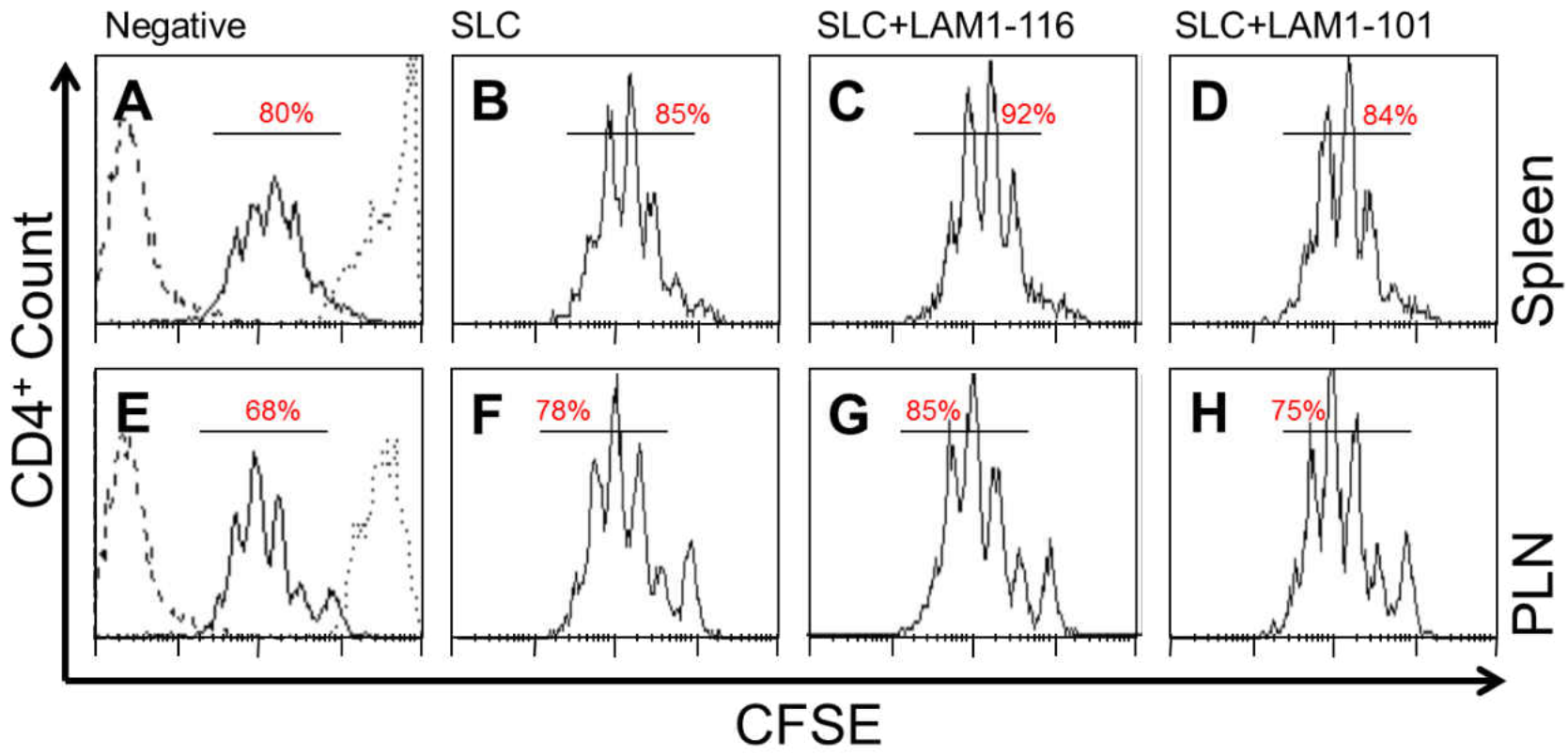


**Figure 14**. Representative histograms of proliferating $CD4^+$ T cells at 72 hours post-TCR stimulation. Cells were isolated from Spleen (A-D) and PLN (E-H), and treated as described in Figure 12. Numbers in red indicate the frequency of actively proliferating cells. Proliferating cells were identified as the population flanked by a non-CFSE stained sample (dashed line) and a non-proliferated CFSE stained sample (dotted line). Both controls were from the same population as the treated samples and were analyzed at the same time point. Results are representative of 5 independent experiments.

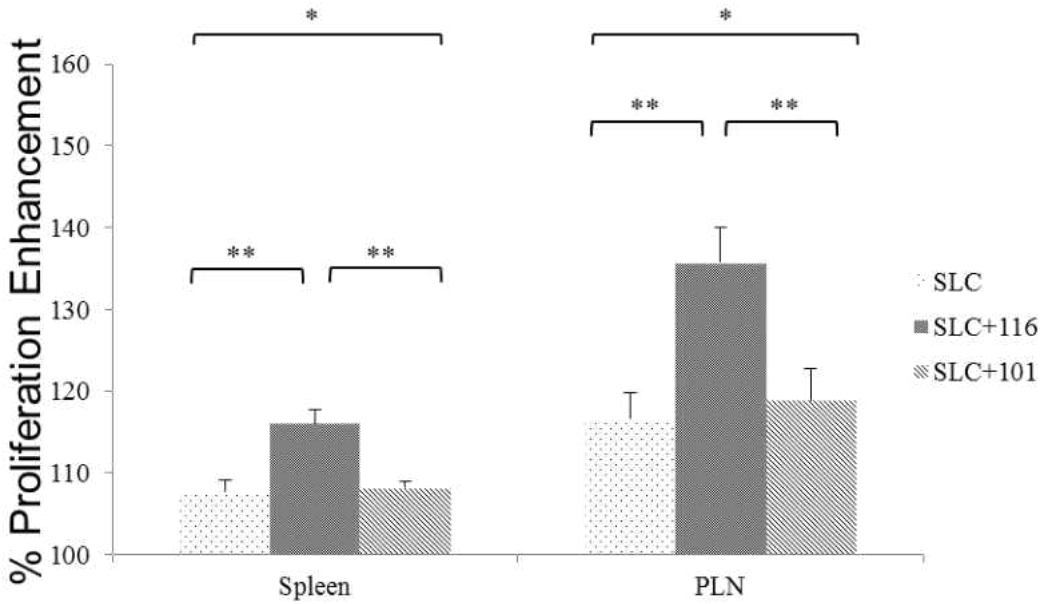


**Figure 15.** Summary data of proliferating $CD4^+$ T cells at 72 hours post-TCR stimulation. Results are from experiments shown in Figure 14. All numbers (with SEM bars) are in comparison to a proliferated and CFSE stained control sample exposed to media alone (Treatment/Control*100). In both the spleen and PLN, variances (one-way ANOVA) between treatments were significant, n=5, *P*=0.01; n=5, *P*=0.03; respectively. In the spleen, *post hoc* Tukey HSD tests showed significant difference between the LAM1-116 treated sample compared to the sample treated with SLC alone, n=5, *P*=0.01, or the sample treated with SLC along with the control mAb, LAM1-101, n=5, *P*=0.03. In the PLN, the differences between groups were significant in both cases: n=5, *P*=0.05; n=5, *P*=0.04; respectively. Statistical analysis was performed using R version 2.15.2. * indicates $_P$Anova<0.05. ** indicates $_P$Tukey HSD<0.05.

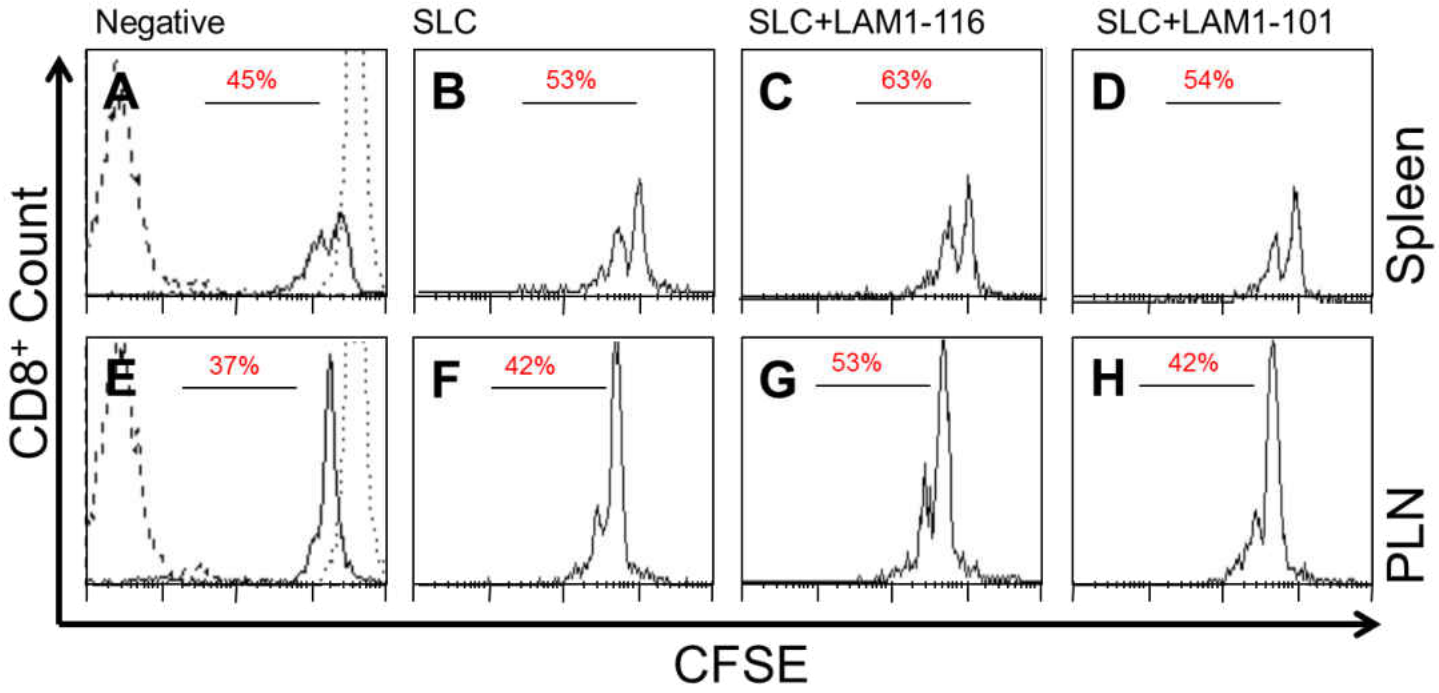


**Figure 16**. Representative histograms of proliferating $CD8^+$ T cells at 36 hours post-TCR stimulation. Cells were isolated from spleen (A-D) and PLN (E-H), and treated as described in Figure 6 except that the samples were labeled for CD8 expression. Numbers in red indicate the frequency of actively proliferating cells. Numbers show increased proliferation in all SLC treated cells, with the LAM1-116 mAb treated sample displaying the highest proliferation. Proliferating cells were identified as the population flanked by a non-CFSE stained sample (dashed line) and a non-proliferated CFSE stained sample (dotted line). Both controls were from the same population as the treated samples and were analyzed at the same time point. Results are representative of 8 and 9 independent experiments for the spleen and PLN, respectively.

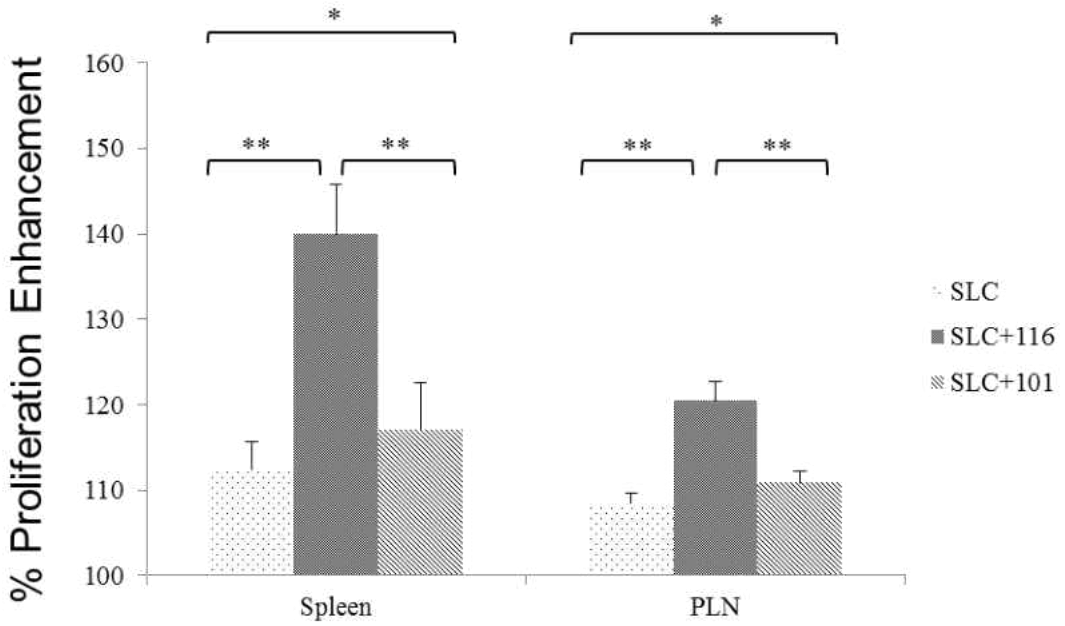


**Figure 17**. Summary data of $CD8^+$ T cell proliferation at 36 hours post-TCR stimulation. Results are from experiments shown in Figure 16. All numbers (with SEM bars) are in comparison to a proliferated and CFSE stained control sample exposed to media alone (Treatment/Control*100). In both the spleen and PLN, variances (one-way ANOVA) between treatments were significant, n=8, $P$=0.003; n=9, $P$=$4.9 \times 10^{-5}$; respectively. In the spleen, *post hoc* Tukey HSD tests showed significant difference between the LAM1-116 treated sample compared to the sample treated with SLC alone, n=8, $P$=0.007, or the sample treated with SLC along with the control mAb, LAM1-101, n=8, $P$=0.009. In the PLN, the differences between groups were significant in both cases: n=9, $P$=$6.2 \times 10^{-5}$; n=9, $P$=$9.2 \times 10^{-4}$; respectively. Statistical analysis was performed using R version 2.15.2. * indicates ${}_P$Anova<0.05. ** indicates ${}_P$Tukey HSD<0.05.

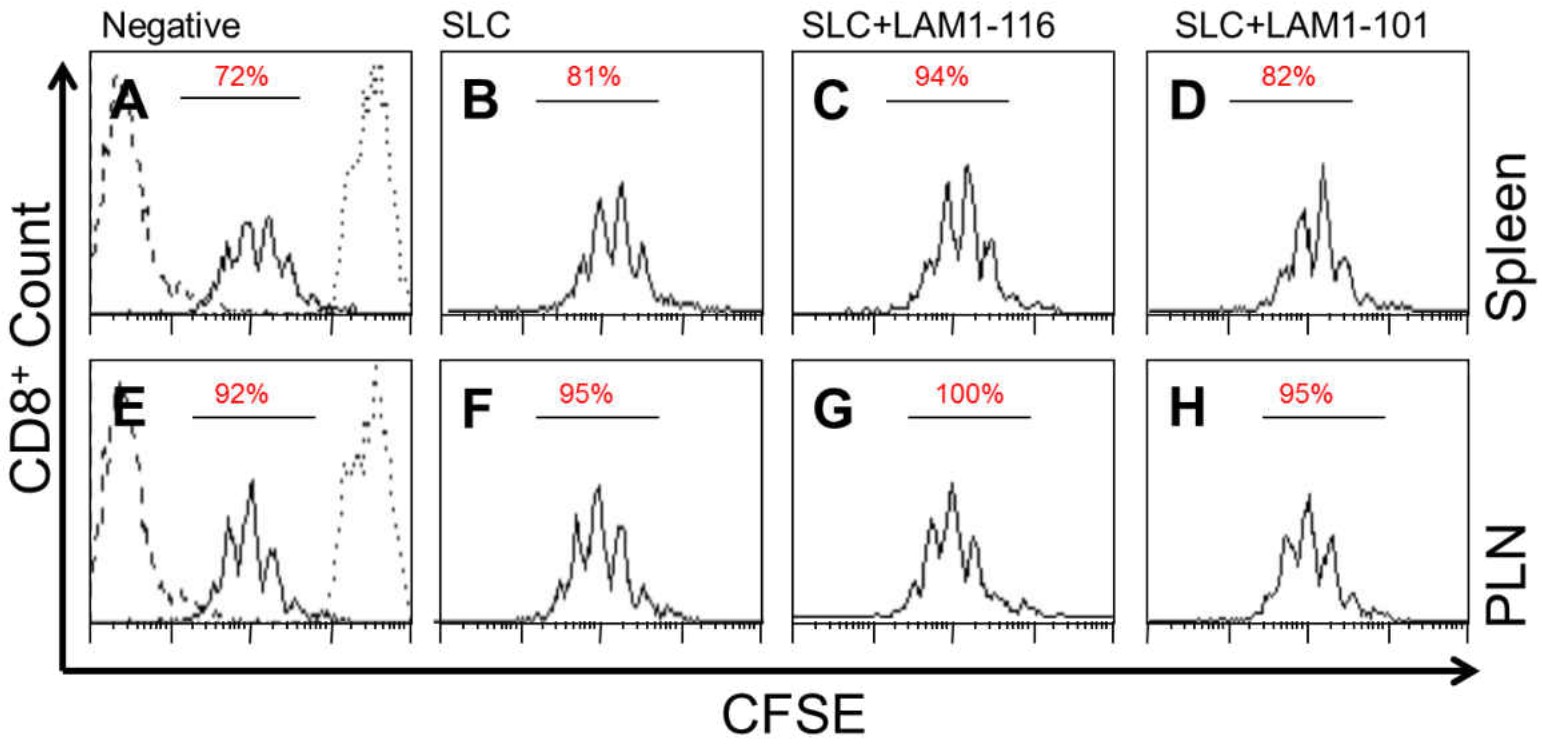


**Figure 18.** Representative histograms of proliferating $CD8^+$ T cells at 72 hours post-TCR stimulation. Cells were isolated from spleen (A-D) and PLN (E-H), and treated as described in Figure 16. Numbers in red indicate the frequency of actively proliferating cells. Proliferating cells were identified as the population flanked by a non-CFSE stained sample (dashed line) and a non-proliferated CFSE stained sample (dotted line). Both controls were from the same population as the treated samples and were analyzed at the same time point. Results are representative of 5 independent experiments per tissue.

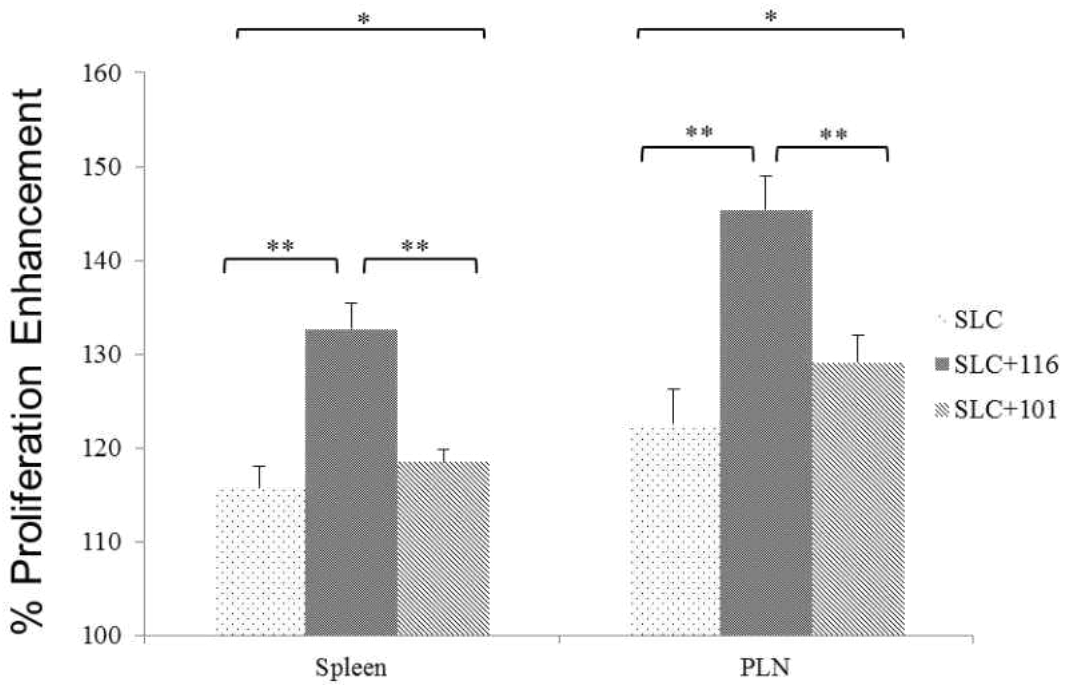


**Figure 19**. Summary data of proliferating $CD8^+$ T cells at 72 hours post-TCR stimulation. Results are from experiments shown in Figure 18. All numbers (with SEM bars) are in comparison to a proliferated and CFSE stained control sample exposed to media alone (Treatment/Control*100). In both the spleen and PLN, variances (one-way ANOVA) between treatments were significant, n=5, *P*=0.0004; n=5, *P*=0.002; respectively. In the spleen, *post hoc* Tukey HSD tests showed significant difference between the LAM1-116 treated sample compared to the sample treated with SLC alone, n=5, *P*=0.0005, or the sample treated with SLC along with the control mAb, LAM1-101, n=5, *P*=0.002. In the PLN, the differences between groups were significant in both cases: n=5, *P*=0.002; n=5, *P*=0.02; respectively. Statistical analysis was performed using R version 2.15.2. * indicates $_P$Anova<0.05. ** indicates $_P$Tukey HSD<0.05.

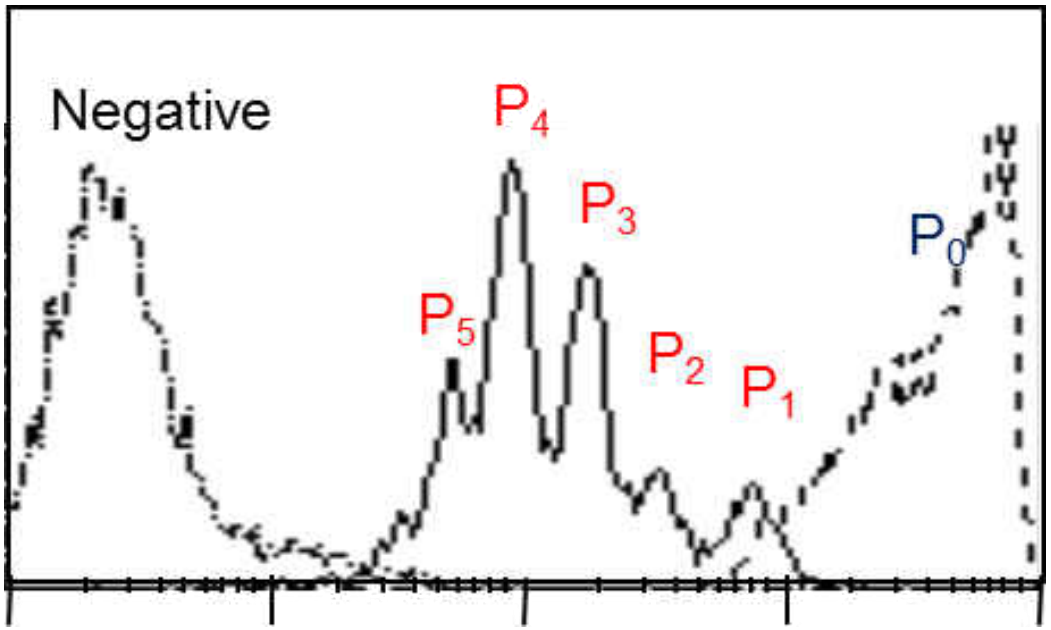


**Figure 20.** Representative histogram of a 72 hour sample post-TCR stimulation that had reached asymptotic growth. Samples were treated as described in Figure 6. The area bound by the negative control (dotted and dashed line) and positive control (dashed line) was analyzed for divisions (Progeny:$P_0$-$P_5$).Divisions must exhibit mean fluorescence intensity of approximately half of the preceding peak to be considered for analysis. The frequency of $CD4^+$ and $CD8^+$ T cells in each division were then analyzed. Result is representative of 3 independent experiments per tissue.

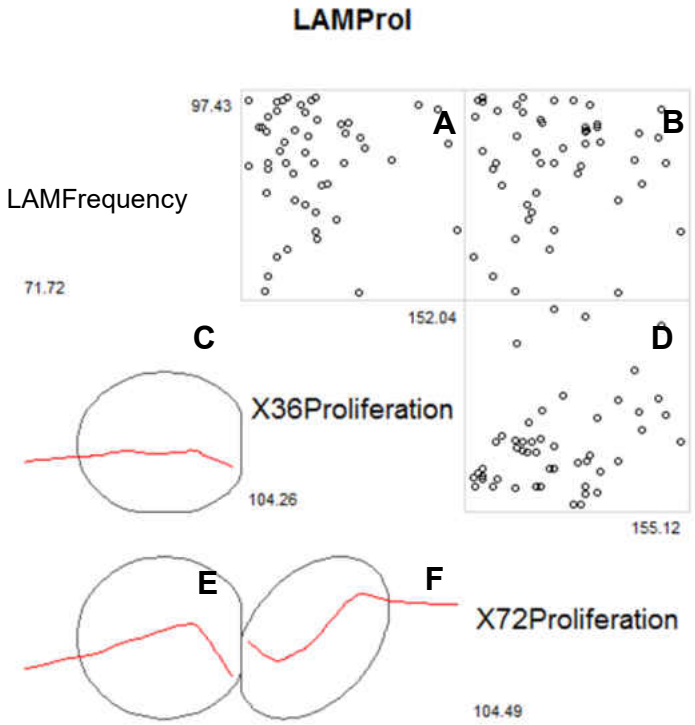


**Figure 21**. Correlogram of L-selectin positive cell frequency versus 36 and 72 hour proliferation. Data is from experiments shown in Figures 6-19. L-selectin (LAMFrequency) from both $CD4^+$ and $CD8^+$ T cells were then compared to proliferation levels using Pearson's correlation. Dot plots illustrates proliferation levels (x axis) versus L-$selectin^+$ cells (y axis) at both 36 (A) and 72 (B) hours. Results were statistically not significant with r values of 0.00 and 0.01 (n=50), respectively. Interestingly high proliferation levels at the 36 hour time point positively correlates with proliferation levels at 72 hours (n=50, *r*=0.37, *P*=0.0087), shown in figures D and F. Figures C and E are best fit lines for the dot plots for the 36 and 72 hour time points respectively. Statistical analysis was performed using R version 2.15.

| Tissue | Treatment | $G_1$ | $G_2$ | $G_3$ | $G_4$ | $G_5$ |
|---|---|---|---|---|---|---|
| SpleenCD4 | Negative | 5.88± 3.33 | 23.41±5.53 | 37.38±4.50 | 20.69±3.61 | 3.27±1.58 |
| | SLC | 4.65±3.11 | 21.97±3.68 | 37.40±3.07 | 17.66±0.85 | 3.38±0.21 |
| | SLC+LAM1-116 | 4.91±2.35 | 18.84±1.33 | 42.16±1.91 | 24.03±0.51 | 6.17±0.78 |
| | SLC+LAM1-101 | 5.15±1.68 | 17.38±1.57 | 38.76±3.93 | 20.96±0.51 | 2.845±0.33 |
| | | | | | | |
| SpleenCD8 | | G1 | G2 | G3 | G4 | G5 |
| | Negative | 3.46±0.14 | 24.89±7.32 | 32.36±3.70 | 22.71±5.89 | 6.52±4.39 |
| | SLC | 5.42±0.93 | 23.53±5.32 | 36.48±2.78 | 20.15±5.74 | 6.44±4.81 |
| | SLC+LAM1-116 | 4.21±0.56 | 20.75±4.93 | 35.07±1.42 | 26.81±5.19 | 10.5±3.89 |
| | SLC+LAM1-101 | 3.90±0.11 | 17.37±3.74 | 34.98±1.20 | 26.57±5.67 | 7.32±2.31 |
| | | | | | | |
| PLNCD4 | | G1 | G2 | G3 | G4 | G5 |
| | Negative | 2.27±0.61 | 6.80±2.05 | 17.21±6.20 | 35.72±2.96 | 20.87±8.26 |
| | SLC | 1.97±0.55 | 6.17±1.62 | 17.66±5.31 | 31.95±5.05 | 30.35±8.35 |
| | SLC+LAM1-116 | 1.74±0.38 | 5.16±0.95 | 20.11±4.92 | 39.54±2.55 | 35.87±8.87 |
| | SLC+LAM1-101 | 2.17±0.78 | 5.98±2.05 | 17.98±6.55 | 42.13±0.35 | 26.93±8.69 |
| | | | | | | |
| PLNCD8 | | G1 | G2 | G3 | G4 | G5 |
| | Negative | 3.21±2.56 | 5.39±1.66 | 12.72±3.89 | 28.96±4.61 | 28.39±8.75 |
| | SLC | 2.51±1.89 | 5.66±2.01 | 13.35±3.94 | 24.84±4.01 | 37.00±7.92 |
| | SLC+LAM1-116 | 2.19±1.69 | 5.27±1.58 | 15.19±4.03 | 30.96±2.90 | 43.20±8.96 |
| | SLC+LAM1-101 | 2.96±2.47 | 5.11±1.60 | 13.48±4.19 | 35.18±2.68 | 33.97±7.91 |

**Table 1.** Population analysis of cell division population at 72 hour post-TCR stimulation. Results are from experiments shown in Figure 20 (n=3). Results between treatments in the $G_4$ and $G_5$ populations, although showing greater frequencies of $CD4^+$ and $CD8^+$ T cell subsets in the SLC+LAM1-116 treated samples, were not significant.

## Chapter 3: Characterization of T cell apoptosis during simultaneous activation of L-selectin and CCR7

### 1. Research design

The effects outlined in Chapter 2 of L-selectin-mediated enhanced TCR-induced proliferation could be a product of two effects separately or in synchrony. Specifically, these effects could be a result of: 1) populations that truly respond by increasing cell proliferation, 2) cell samples showing a decrease in the rate of cell death (apoptosis) and finally, 3) a contribution by both phenomena. In relation to the effects listed above, signaling through several adhesion molecules has been implicated in lowering rates of apoptosis (121-122). Interestingly, in some reports, apoptosis and proliferation were inversely related following activation of adhesion molecules (123-124). Transmigration as a cellular process has also been shown to inhibit apoptosis. This is true for neutrophils exposed to stimulation by bacterial lipopolysaccharide (125). However, in the previously mentioned paper, L-selectin engagement was positively associated with apoptosis. By contrast, others studies have shown that the apoptotic rate of peripheral mononuclear cells was inversely related to L-selectin expression levels (126). To ascertain whether our observed increased proliferative effect of L-selectin engagement was from either a combination of enhanced proliferation and lower apoptosis or a stand-alone effect; a corresponding assay for apoptosis was utilized using propidium iodide (PI). PI staining can be used as a fluorescence method for determining cell viability. PI can intercalate double stranded nucleic acids if the cell membrane is permeable. Thus, cells that are

apoptotic and have compromised cellular membranes allow PI to diffuse in, resulting in a nuclear fluorescence that can be detected.

**2. Materials and Methods**

i. Cell Isolation and Sample Treatment

Please refer to chapter two for protocols for cell isolation and experimental conditions.

ii. Apoptosis Assay

In some experiments, cells from the same time points were analyzed for apoptosis with PI (Molecular Probes, Carlsbad, CA) staining. Cells prepared as described in the previous experiments and exposed to the same conditions were analyzed. Cell subset antibody staining was performed as previously described, along with addition of 5 μg/mL of PI. In this case, antibody and PI staining incubations were performed in the dark at room temperature for 30 minutes. This assay was performed at the 36 and 72 hour time points, post-TCR stimulation, in parallel to the proliferation assays described in chapter 2. To detect cells undergoing stages of apoptosis, only cells that were in the live resting lymphocyte and actively dividing lymphoblast gate were considered. Thus, cells in the lymphocyte/lymphoblast gate which were also PI positive were considered to be apoptotic cells. The frequency of apoptotic cells of the sample treated with media alone was compared to the other treatment samples. A ratio of less than

100% indicated a decrease in apoptosis whereas numbers higher than 100% indicated an increase in apoptosis.

iii. Data Analysis

After analyzing the raw data for homogeneity of variance with the Bartlett test and normality with a Q-Q line plot, deviations were detected that proved the raw data unusable. To correct for these departures from normality and variance all data were normalized as follow:

%Apoptotic Improvement = (frequency of apoptotic cells in the treated sample/frequency of apoptotic cells in the untreated sample)* 100

Transformed data were subjected to normality and variance tests, through Q-Q line plot and Bartlett tests, respectively. No significant departures were noted or the residuals of the outliers did not impact the outcome of the factors. Data were then analyzed with one-way ANOVA. If data sets showed significant variance ($p < 0.05$), further analysis between groups was performed using the Tukey Honestly Significant Difference (HSD) test. A *P* value of less than 0.05 was considered significant. Pearson correlation was also performed between apoptosis versus frequency of L-selectin positive cells. All data analysis was performed using R 2.15.2 (R Foundation for Statistical Computing, Vienna, Austria).

**3. Results**

i. $CD4^+$ T cell apoptosis at 36 hours post-TCR stimulation.

To ascertain if anti-apoptotic activity can also contribute to the increase in TCR-induced proliferation described in Chapter 2, subset apoptotic effects were

analyzed. In the $CD4^+$ T cell subset at 36 hours, no detectable differences between samples were detected regardless of tissue origin. In the spleen, $CD4^+$ T cells that were also PI positive (apoptotic cells, upper right hand quadrants, Figures 22 A-D), show results that are relatively similar to each other with 6.16% (negative), 6.59% (SLC), 6.2% (SLC+LAM1-116) and 6.8% (SLC+LAM1-101). This was also the case with $CD4^+$ T cells from the PLN with apoptotic cell frequencies of 4.83% (negative), 5.25% (SLC), 5.28% (SLC+LAM1-116) and 5.73% (SLC+LAM1-101) (Figures 22 E-H). Transforming the data relative to control, similar to the approach taken for proliferation in chapter 2 also showed the same result. In this regard, % Apoptotic Improvement<100%, indicates a lower rate of apoptosis relative to control. No variances were found between treatment groups in the spleen (n=4, $P$=0.511) or PLN (n=4, $P$=0.275). Interestingly, looking at the summary data (Figure 23), a trend of increased apoptosis for all treatment groups, with the LAM1-116 mAb-treated sample displaying the highest level, was observed.

ii. $CD4^+$ T cell apoptosis at 72 hours post-TCR stimulation

The data from the apoptotic analysis of $CD4^+$ T cells at 72 hours post-stimulation showed a distinct departure from the 36 hour time point. Looking at a representative spleen dot plot, one can see the LAM1-116 mAb-treated sample displaying the lowest frequency of $CD4^+$ apoptotic cells at 6.5% (Figure 24). This is in comparison to the control- (9.75%), SLC- (9.73%) and SLC+LAM1-101 mAb (9.21%) -treated cells (Figures 24, A-B and D). This was similar to the results from PLN $CD4^+$ T cell samples at the same time point, which displayed an

apoptotic frequency of 15.99% for the SLC+LAM1-116 mAb treatment compared to 20.97% (negative), 17.2% (SLC) and 18.81% (SLC+LAM1-101) (Figures 24 E-H). The transformed summary data are shown in Figure 25. The LAM1-116 mAb-treated $CD4^+$ splenic sample showed a mean % apoptotic improvement±SEM of 73.44±7.30, compared to 87.89±4.56 (SLC) and 84.62±4.40 (SLC+LAM1-101) (Figure 25). The variance between groups was significant at *P*=0.007 (n=4), with *post hoc* Tukey HSD tests showing significant difference between the LAM1-116 mAb- and SLC-treated samples (n=4, *P*=0.01) or the SLC+LAM1-101 mAb-treated sample (n=4, *P*=0.02). In the PLN, the values were similarly decreased in the LAM1-116 mAb-treated sample (77.10±5.31) compared to the SLC-treated sample (89.11±5.02) and the SLC+LAM1-101 mAb treated sample (88.01±3.68). The variance between groups was similarly significant at *P*=0.01 (n=4) and the Tukey HSD tests between the LAM1-116 mAb-treated sample compared to the SLC treatment (n=4, *P*=0.01) and SLC+LAM1-101 mAb treatment (n=4, *P*=0.02) both showed significance (Figure 25). These data indicate that activation through L-selectin exerts an anti-apoptotic effect in $CD4^+$ T cells that is discernible at 72 hours post-TCR stimulation.

iii. $CD8^+$ T cell apoptosis at 36 hours post-TCR stimulation

Similar to the results for $CD4^+$ T cells, $CD8^+$ T cell apoptosis was unaffected by L-selectin activation at the 36 hour post-TCR stimulation time point. The representative dot plot for this experiment shows splenic $CD8^+$ T cell apoptotic frequencies with minor variations at 8.95% (negative), 9.43% (SLC),

8.9% (SLC+LAM1-116) and 9.92% (SLC+LAM1-101) (Figure 26 A-D). The mean % Apoptotic Improvement±SEM (n=5) for this experiment confirms this lack of effect with SLC=112±2.77%, SLC+LAM1-116=134±9.35% and SLC+LAM1-101=116±4.13% (Figure 27). The variance for the spleen and PLN were P=0.276 and P=0.24, respectively (n=5 for both tissue). The representative PLN values shown in the dot plots are: 3.37% (negative), 9.21% (SLC), 3.26% (SLC+LAM1-116) and 3.57% (SLC+LAM1-101) (Figure 26 E-H). Summary transformed data demonstrate the same results (Figure 27). Therefore, a modest increase in apoptosis was observed for all SLC-treated cells with the LAM1-116 mAb-treated sample exhibiting the highest response, albeit statistically insignificant.

iv. $CD8^+$ T cell apoptosis at 72 hour post-TCR stimulation

Representative $CD8^+$ T cell dot plots at 72 hour post-stimulation showed a general decrease in apoptosis with the LAM1-116 mAb-treated sample showing the biggest decrease (Figure 28). These results were surprising given that the opposite effect was found at the 36 hour time point, post-TCR stimulation. Specifically, splenic $CD8^+$ T cells treated with SLC+LAM1-116 mAb showed 5.8% apoptosis, compared to 6.84% (negative), 7.63% (SLC) and 7.97% (SLC+LAM1-101) (Figure 28A-D). The same relative decrease in apoptosis was also observed in the representative PLN samples with 28.97% (negative), 24.75% (SLC), 19.59% (SLC+LAM1-116) and 25.83% (SLC+LAM1-101) (Figures 28 E-H). Variances between transformed samples in the spleen were significant at n=4, $P$=0.004 (SLC=68.86±2.4%, SLC+LAM1-116=53±3.31% and SLC+LAM1-101=71.5±3.06%) and in the PLN at n=4, $P=2.15\times10^{-6}$ (SLC=93±0.55%,

SLC+LAM1-116=84±0.74% and SLC+LAM1-101=92.69±0.27%) (Figure 29). These results show that activation through L-selectin results in an anti-apoptotic effect in $CD8^+$ T cells that is detectable at 72 hours post-TCR stimulation.

v. Correlation between L-selectin and apoptosis levels

Utilizing Pearson's *r*, we then subjected all apoptotic values compared to all frequencies of L-selectin positive cells regardless of tissue origin and cell subset to a correlation test, coupled with a correlogram (Figure 30). The frequency of L-selectin positive cells was not correlated to the 72 hour rates of apoptosis ($r$=0.11, $P$=0.47) but interestingly in the 36 hour rates of apoptosis there was a significant negative correlation ($r$=-0.40, $P$=0.0045). Interestingly, the 36 hour time point is when the rates of apoptosis were all increased across all treatments, with the LAM1-116 mAb treatment eliciting the greatest rate of apoptosis.

**4. Discussion**

Unlike the proliferation results described in chapter 2, the apoptosis results are much less straightforward. At the 72 hour time point, all samples treated with the LAM1-116 mAb showed a significant decrease in apoptosis, compared to all other samples (Figure 25 and 29). Interestingly, the lowest level of apoptosis observed was in the $CD8^+$ splenic T cell subset, contrary to our tissue origin prediction. We predicted the apoptotic effect would be more pronounced in the PLN, due to the higher frequency of L-selectin expressing cells in this tissue. It should be noted that T cells do not constitute the bulk of the

lymphocyte population in the spleen; rather B cells are the dominant lymphocytes in this tissue.

Analyzing our correlation data also shows no significant relationship between frequency of L-selectin positive cells and apoptotic rate at the 72 hour time point (Figure 30). However, a negative correlation between L-selectin frequency and apoptosis was detected at the 36 hour time point (Figure 30). This is in direct opposition to the summary data (Figure 23, 25, 27 and 29). Therefore, it is highly unlikely that there is any direct relationship between L-selectin frequency and apoptosis based on the present data. However, there may be a mechanistic reason behind these findings as discussed below.

At the 36 hour time point, our findings directly contradict our expectations. Specifically, LAM1-116 mAb treatment tended to induce higher levels of apoptosis in all samples regardless of tissue origin (Figures 23 and 27). It must be noted that initial TCR stimulation induced by cross linking CD3 can increase levels of apoptosis in a phenomenon described as activity induced cell death (AICD or ACD, 127-129). It should be noted that CD3 mediates initial activation of T cells and thus exerts its influence at early time points, similar to the 36 hours post-stimulation apoptosis analysis undertaken in this study. Thus, we can assume that the latter stages of cell proliferation are no longer mediated by CD3 or its effects are no longer dominant. Despite CD3 activation explaining initial increases in apoptosis, what explains the decline in apoptosis observed in the 72 hour post-stimulation samples? In light of the mechanism proposed in Chapter 2, the temporal basis of the initial increase in apoptosis followed by a decrease can

be explained. As discussed in Chapter 2, a possible mechanism for L-selectin signaling is through the Ras signaling pathway. We propose that Ras is recruited via a prototypical Grb2/SOS recruitment to the inner cell membrane, which in turn was mediated by 14-3-3 binding to the phosphoserine residues in the L-selectin tail. 14-3-3 has been shown to sequester pro-apoptotic factors in the cytoplasm through protein-protein interactions. The primary apoptotic factors sequestered by 14-3-3 includes but is not limited to: BCL-2/XL Associated Death promoter (130), BCL-2 associated x protein (131) and Forkhead box 01 transcription factor (FOXO, 132). If we consider the disruption of 14-3-3 interaction with pro-apoptotic genes, we can certainly see a possible increase in apoptosis when 14-3-3 protein leaves its pro-apoptotic partner and interacts with the phosphorylated L-selectin tail. This is reflected in the 36 hour apoptotic rates in the presence of L-selectin activation. However, what accounts for the 72 hour time point decrease in apoptosis? Again the L-selectin tail can point us in the right direction.

During L-selectin signaling one of the first molecules that is released from its interaction with the cytoplasmic tail is CaM. CaM has been shown to be an anti-apoptotic signal. CaM can counteract apoptosis by several mechanisms including but not limited to CaM dependent protein kinase 4 (133-134), CaM dependent kinase 2 (135-136) and via Protein Kinase B (137-138). At the 36 hours post-TCR stimulation time point, it is possible that the apoptotic factors released from sequestration by the 14-3-3 protein could overcome the anti-apoptotic effects of CaM. However, by the 72 hour post-TCR stimulation time point, it is possible that 14-3-3 together with CaM can exert an anti-apoptotic

effect that is detectable. This effect may be partly due to the proteolytic degradation of the L-selectin tail at the later time points. These temporal effects of 14-3-3 and CaM could explain the differences in the apoptotic rates observed at the 36 and 72 hours post-TCR stimulation time points. This complexity could also explain the lack or paradox of correlation between L-selectin activation and apoptosis at both time points. However, further biochemical analysis involving 14-3-3 and CaM must be undertaken to support the proposed mechanism outlined above.

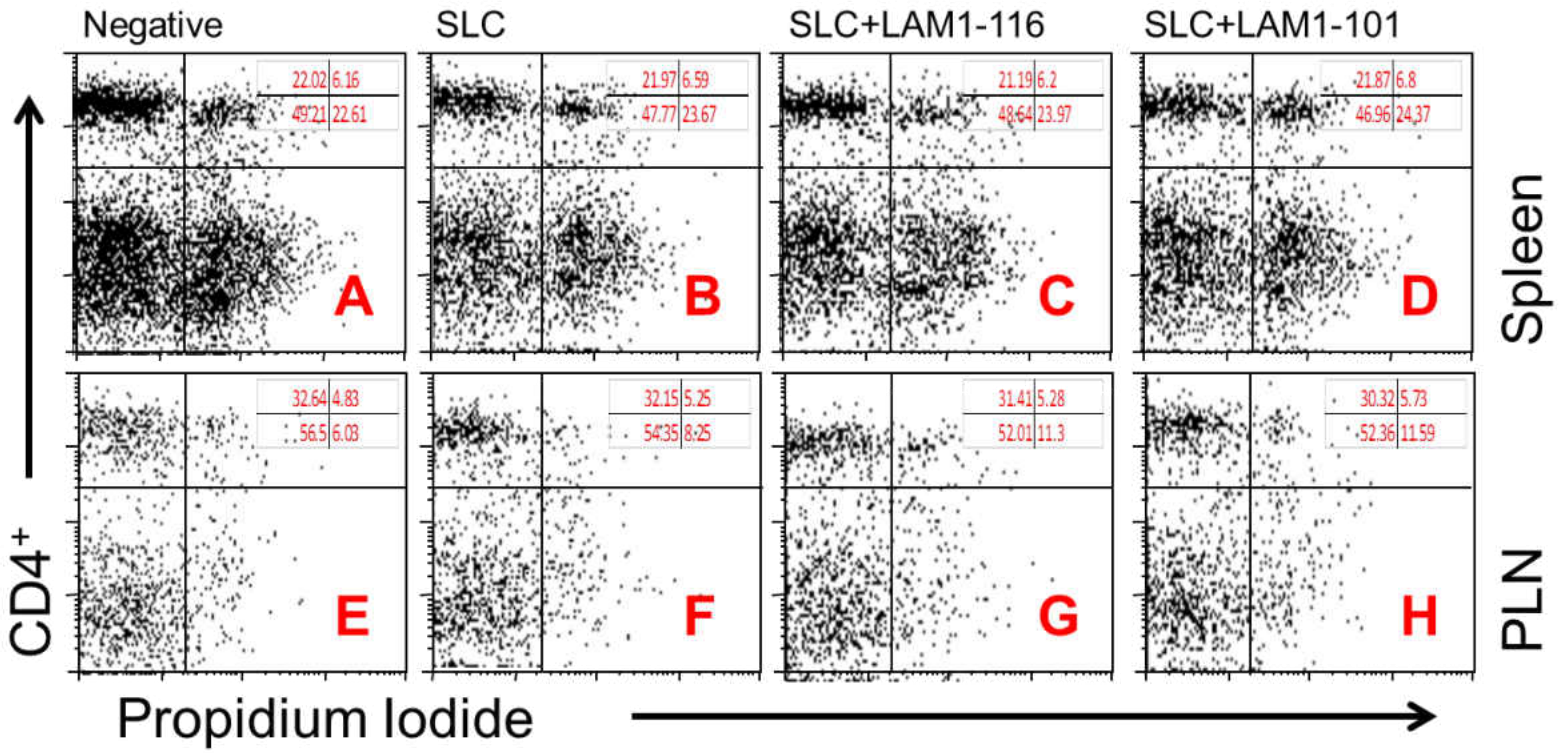


**Figure 22**. Representative dot plots of apoptotic $CD4^+$ T cells at 36 hours post-TCR stimulation. Cells were isolated from spleen ( A-D) and PLN (E-H), and stained with 0.25 μM of CFSE. Some samples were treated with 10 μg/mL of the L-selectin activating mAb, LAM1-116, before transmigration in the presence of 500 ng/mL of SLC (SLC+LAM1-116, C and G). Other samples were transmigrated to the same concentration of SLC with no mAb treatment (SLC, Figures B and F) or treated with 10 μg/mL of a control mAb, LAM1-101 (SLC+LAM1-101, D and H). Cells that transmigrated to media alone without mAb treatment are considered negative (A and E). All 4 treatment subsets were subsequently induced to proliferate in the presence of anti-CD3 and anti-CD28 mAbs in a 96 well plate (both mAb at 2μg, with $5x10^4$ cells per well). Subsequently, cells were collected after 36 hours, and the subset (y axis) analyzed for apoptosis (Propidium Iodide positive cells, x axis). Numbers in red indicate cell percentages per quadrant. Results are representative of 4 independent experiments per tissue.

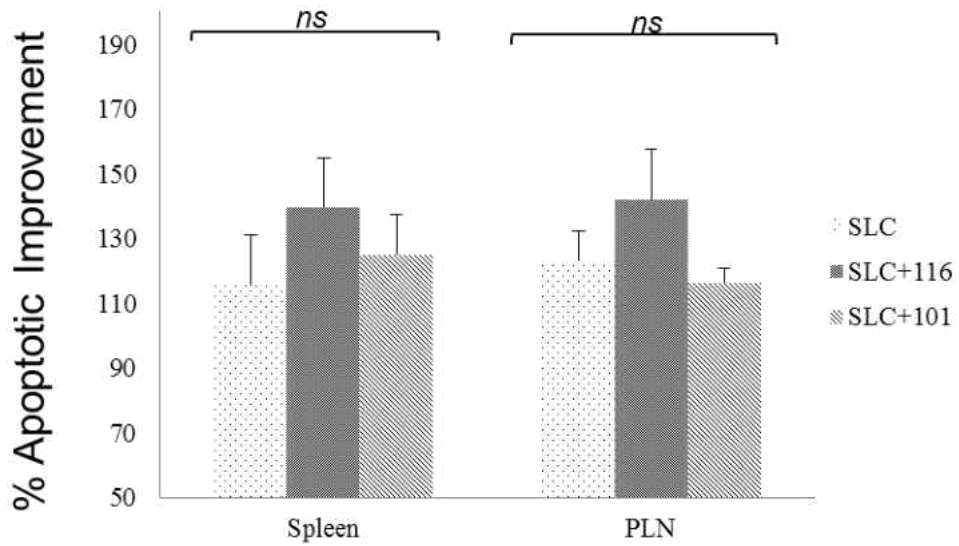


**Figure 23**. Summary data of $CD4^+$ T cell apoptosis at 36 hours post-TCR stimulation. Results are from experiments shown in Figure 22. All numbers (with SEM bars) are in comparison to a proliferated and CFSE stained control sample exposed to media alone (Treatment/Control*100). Group variances are not statistically significant, with *P* values of 0.511 and 0.275 for spleen (n=4) and PLN (n=4), respectively. Statistical analysis was performed using R version 2.15.2. *ns* indicates not significant.

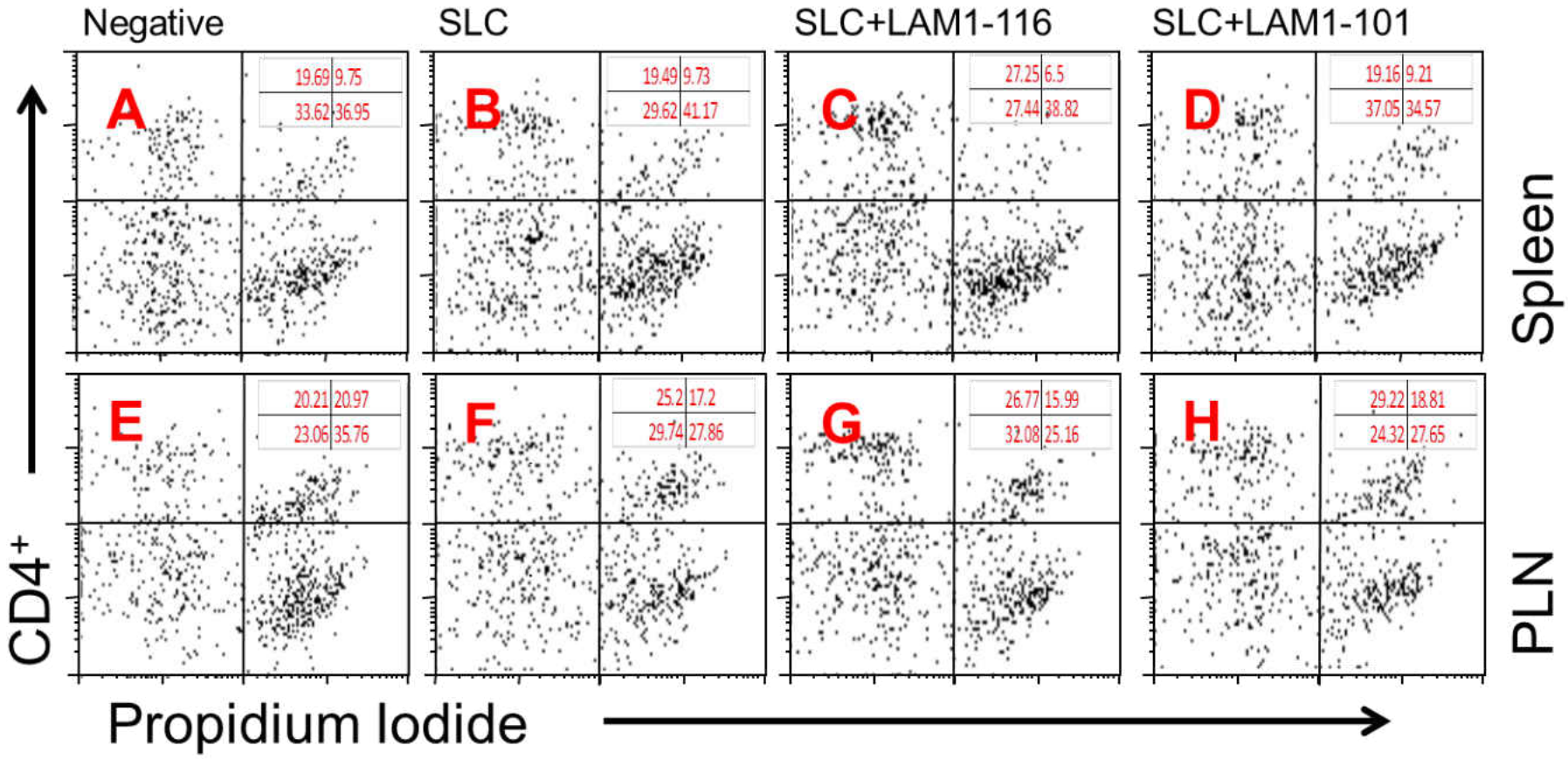


**Figure 24**. Representative dot plots of apoptotic $CD4^+$ T cells at 72 hours post-TCR stimulation. Samples were treated as described in Figure 22 and analyzed 72 hours post-TCR stimulation. Numbers in red indicate cell percentages per quadrant. Results are representative of 4 independent experiments per tissue.

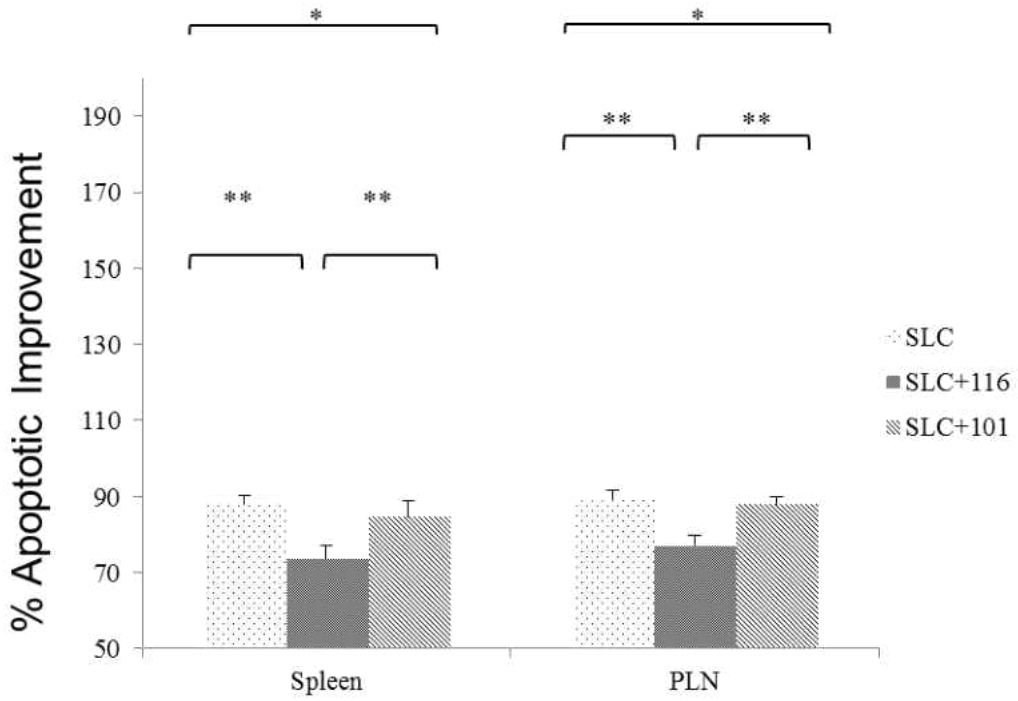


**Figure 25**. Summary data of CD4+ T cell apoptosis at 72 hours post-TCR stimulation. Results are from experiments shown in Figure 24. All numbers (with SEM bars) are in comparison to a proliferated and CFSE stained control sample exposed to media alone (Treatment/Control*100). In both the spleen and PLN, variances (one-way ANOVA) between treatments was significant, n=4, *P*=0.007; n=4, *P*=0.01; respectively. In the spleen, *post hoc* Tukey HSD tests showed significant difference between the LAM1-116 treated sample compared to the sample treated with SLC alone, n=4, *P*=0.01, or the sample treated with SLC along with the control mAb, LAM1-101, n=4, *P*=0.02. In the PLN, the differences between groups were significant in both cases: n=4, *P*=0.01; n=4, *P*=0.02; respectively. Statistical analysis was performed using R version 2.15.2. * indicates $_P$Anova<0.05. ** indicates $_P$Tukey HSD<0.05.

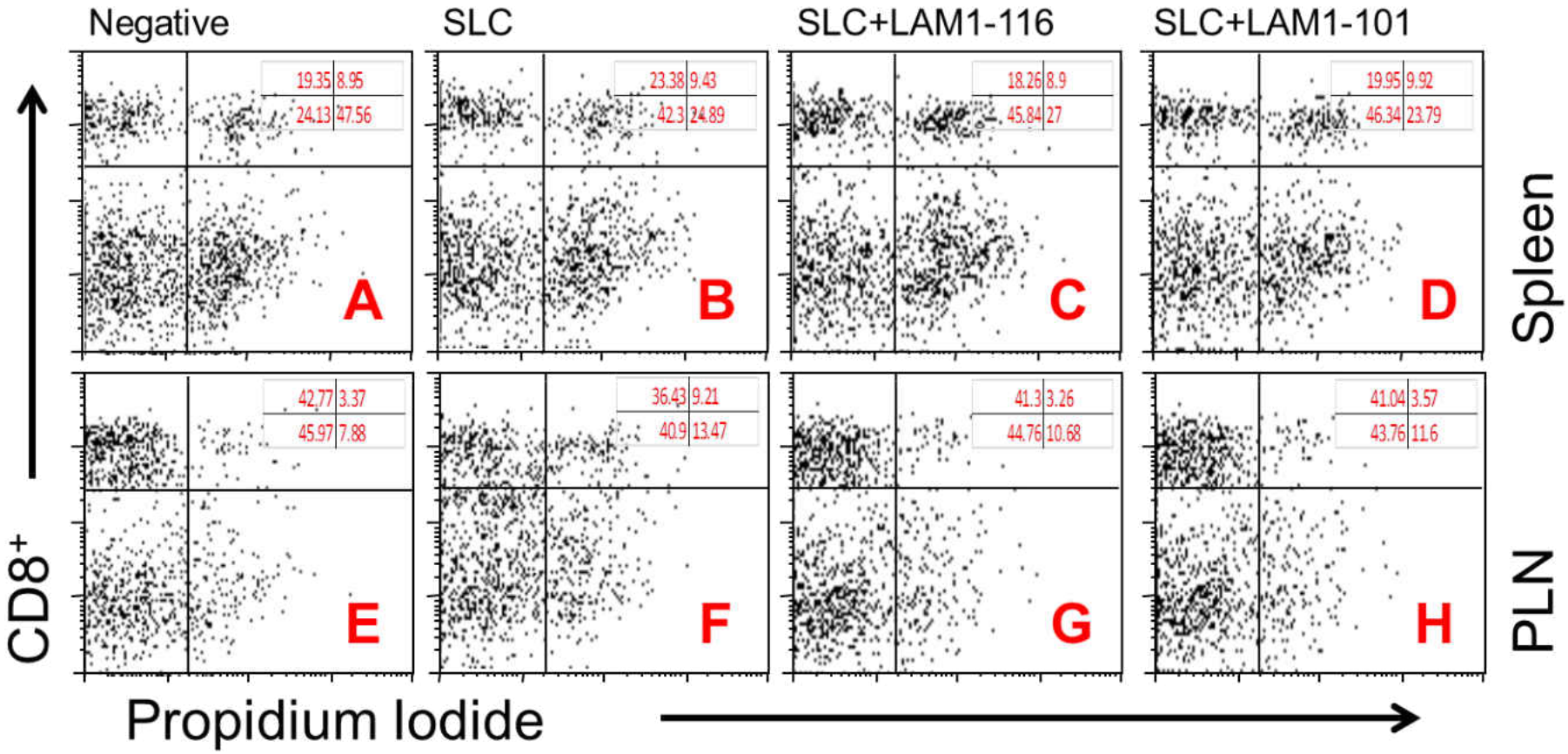


**Figure 26.** Representative dot plots of $CD8^+$ T cell apoptosis at 36 hours post-TCR stimulation. Cells were treated as described in Figure 22. Numbers in red indicate cell percentages per quadrant. Results are representative of 5 independent experiments per tissue.

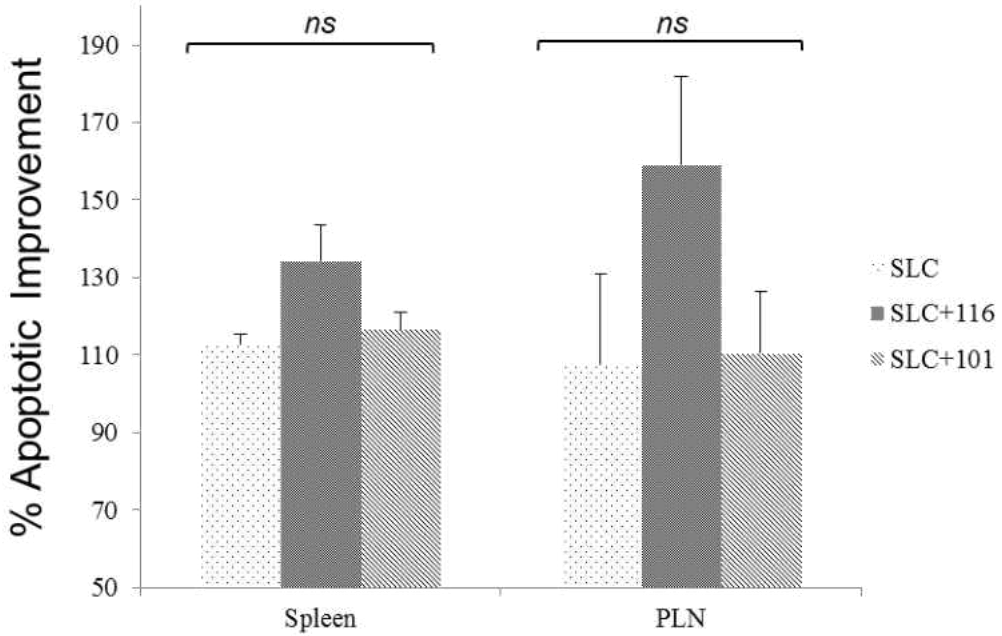


**Figure 27**. Summary data of CD8$^+$ T cell apoptosis at 36 hours post-TCR stimulation. All samples were treated as described in Figure 22. All numbers (with SEM bars) are in comparison to a proliferated and CFSE stained control sample exposed to media alone (Treatment/Control*100). Group variances were not statistically significant, with *P* values of 0.276 and 0.24 for spleen (n=5) and PLN (n=5), respectively. Statistical analysis was performed using R version 2.15.2. *ns* indicates not significant.

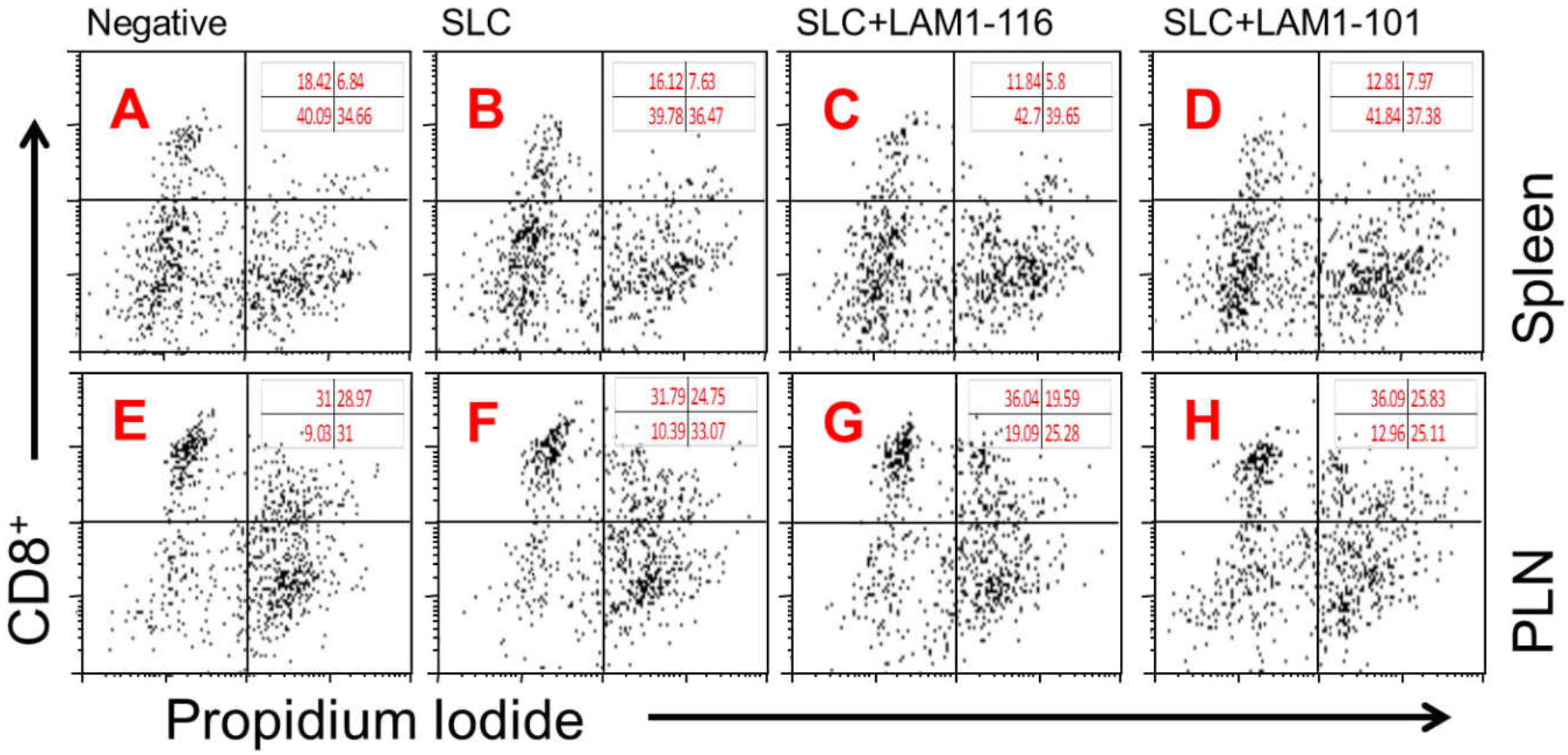


**Figure 28.** Representative dot plots of apoptotic $CD8^+$ T cells at 72 hours post-TCR stimulation. Samples were treated as described in Figure 22 and analyzed for apoptosis 72 hours post-TCR stimulation. Numbers in red indicate cell percentages per quadrant. Results are representative of 4 independent experiments per tissue.

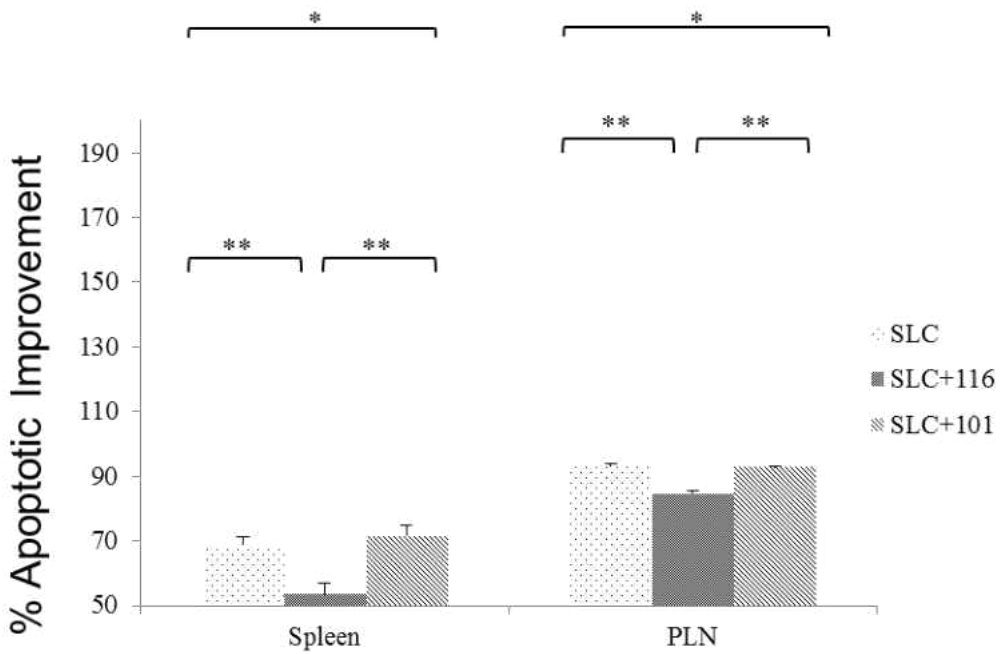


**Figure 29**. Summary data of $CD8^+$ T cell apoptosis at 72 hours post-TCR stimulation. Results are from experiments shown in Figure 28. All numbers (with SEM bars) are in comparison to a proliferated and CFSE stained control sample exposed to media alone (Treatment/Control*100). In both the spleen and PLN, variances (one-way ANOVA) between treatments was significant, n=4, $P$=0.004; n=4, $P$=$2.15 \times 10^{-6}$; respectively. In the spleen, *post hoc* Tukey HSD tests showed significant difference between the LAM1-116 treated sample compared to the sample treated with SLC alone, n=4, $P$=0.01, or the sample treated with SLC along with the control mAb, LAM1-101, n=4, $P$=0.005. In the PLN, the differences between groups were significant in both case : n=4, $P$=$5.5 \times 10^{-6}$; n=4, $P$=$9.3 \times 10^{-6}$; respectively. Statistical analysis was performed using R version 2.15.2. * indicates ${}_P$Anova<0.05. ** indicates ${}_P$Tukey HSD<0.05.

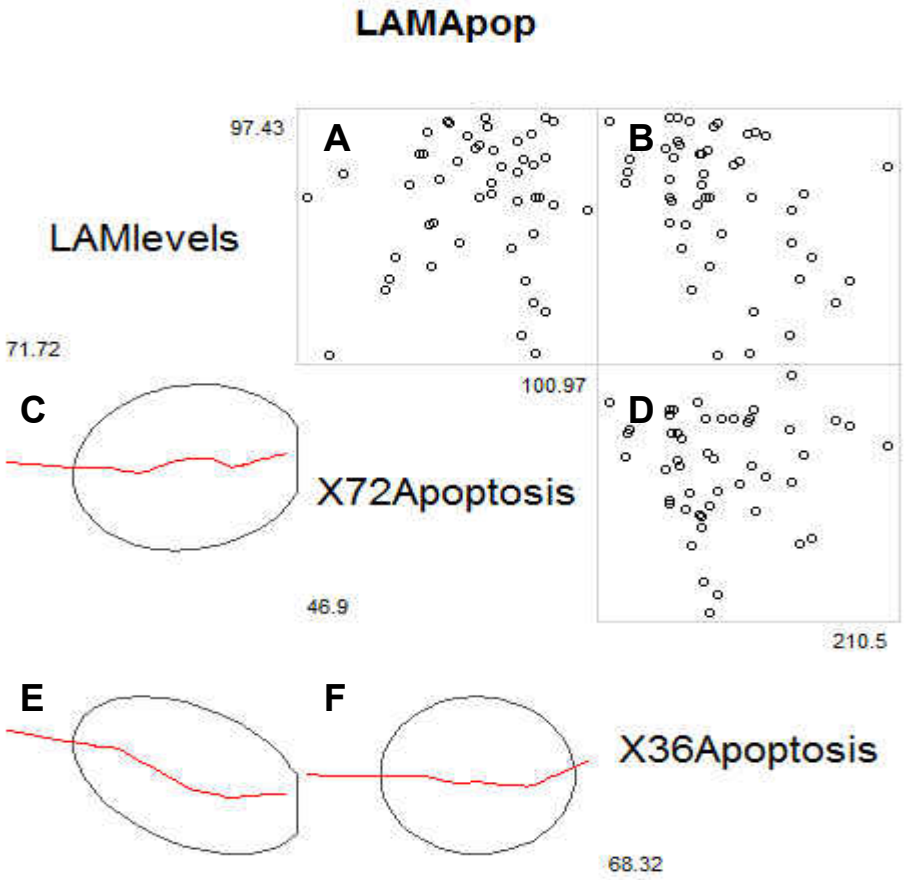


**Figure 30.** Correlogram of L-selectin positive cell frequency versus 36 and 72 hour apoptosis. Data is from experiments shown in Figures 22-29. The apoptotic frequency ( x axis) from both $CD4^+$ and $CD8^+$ T cells were correlated to frequency of L-$selectin^+$ cells (LAMlevels, y axis) in all cells from all tissues. Dot plots (A, B and D) and their corresponding best fit line (C, E and F) are shown. Pearson's correlation is significantly negative between L-$selectin^+$ cell frequency (LAMlevels, y axis) and decreases in apoptosis (x axis) with n=50, $r$=-0.40, $P$=0.0045,at 36 hours (Figures B and E). All other correlations were not significant. Statistical analysis was performed using R version 2.15.2.

## Chapter 4: Conclusions

The current studies show that L-selectin engagement in conjunction with the presence of a transmigration signal via CCR7, enhances subsequent TCR-induced proliferation and protects activated T cells from late apoptosis. As alluded to in the discussions of the previous chapters, we propose a model that involves the 14-3-3 adaptor protein. Although speculative in nature, 14-3-3 binding can explain the temporal differences observed in proliferation enhancements and apoptotic protection. It is known that the cytoplasmic tail of L-selectin contains one (for mice) or two (for humans) serine residues that are phosphorylated by PKC isoforms (84). It is also known that these potential phosphoresidues are protected by CaM and ERM binding during homeostatic conditions (101). It must be noted that CaM and 14-3-3 proteins are both helical in structure, CaM with 7 helices and 14-3-3 with 9 (139-140). We propose that the phosphoserine residues can attract 14-3-3 binding. This binding can bridge Grb2/SOS and Ras association. SOS could then exchange the bound nucleotide of Ras from GDP to GTP, resulting in an activated Ras molecule (113). This activated Ras molecule could now induce kinase cascades resulting in an increase in signaling pathways including: the Raf/MEK/ERK (Extracellular Signal-Regulated Kinases) pathway, the MEKK/SEK/JNK (Jun N-terminal Kinases) pathway, a PI3K (Phosphatidylinositol 3-Kinase)/Akt/NF-KappaB (Nuclear Factor-Kappa B) pathway, in addition to others (141-142). The ultimate purpose of this signaling collective is to drive T cell activation and proliferation. However, 14-3-3 binding to the phosphorylated L-selectin cytoplasmic domain is not without a cost. 14-3-3 is known to bind and sequester apoptotic factors in the

cytoplasm (143); it is likely then that the cost of an increase in proliferation is also a concomitant increase in apoptosis which we detected at 36 hours post-TCR stimulation. At the 36 hour time point it is likely that there are two conflicting signals in terms of apoptosis, the 14-3-3 release of its pro-apoptotic partners and the release of the CaM from the L-selectin tail, an anti-apoptotic molecule. It is possible then that at the early time points, the apoptotic signal is greater than the anti-apoptotic signal. However, once the L-selectin tail has been proteolytically digested, 14-3-3 returns to the cytoplasm and sequesters the pro-apoptotic factors again. Furthermore, with CaM no longer able to interact with the L-selectin tail, this molecule can add to the anti-apoptotic environment at 72 hours post-TCR stimulation. Figure 31 illustrates the model outlined above.

L-selectin's primary role has always been the homeostatic recirculation of naïve T cells. However, studies have also shown its ability to serve as a signaling molecule, improving the immunogenic ability of leukocytes as well as enhancing adhesion steps downstream from its own. The 17 amino acid cytoplasmic domain may be an incidental signaling molecule. Through its phosphorylated form, it likely serves as a signaling scaffold for multiple pathways, in a temporal and spatial fashion. The usefulness and importance of such signaling ability may be lost in the *in vitro* context of this study. Specifically, we need to be aware that the signaling context of this study is in receptor saturated conditions (i.e., antibody ligation), conditions that may not be applicable *in vivo*. However, in less than saturated conditions, where a minimal repertoire of receptors are engaged, a scaffolding function may be important, especially in focal adhesions and the

immunological synapse. Further studies, especially *in vivo* are required, before such functions may be directly attributable to L-selectin.

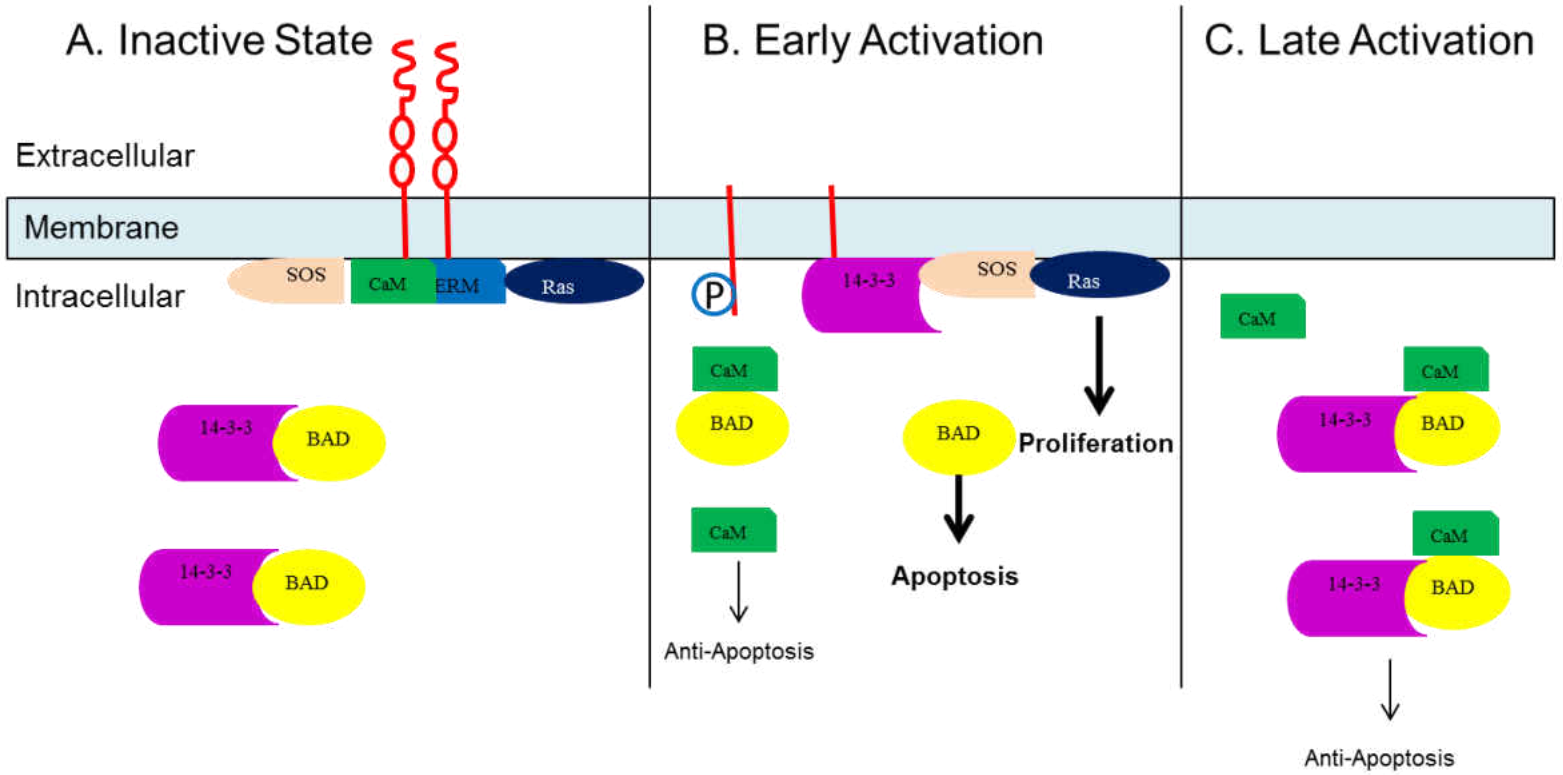


**Figure 31.** Proposed mechanism of L-selectin contribution to proliferation and apoptotic protection. In A, L-selectin is dimerized by CaM and ERM interaction. 14-3-3 sequesters BAD from the mitochondria and SOS and Ras are not associated with each. In B, L-selectin's interaction with Cam and ERM is disrupted by ligand binding, the cytoplasmic tail is phosphorylated which recruits 14-3-3. 14-3-3 can now mediate SOS-Ras interaction which activates Ras resulting in higher levels of proliferation. However, BAD is now free to translocate to the mitochondria resulting in higher levels of apoptosis. In C, after the initial levels of L-selectin activation has plateaued and the tail is proteolytically digested, CaM can phosphorylate excess free BAD, resulting in 14-3-3 interaction, sequestering BAD again from the nucleus.

## References


1. Arbones, M.L., Ord, D.C., Ley, K., Radich, H., Maynard-Curry, C., Capon, D. J., Tedder, T. F., *Lymphocyte homing and leukocyte rolling and migration are impaired in L-selectin-deficient mice.* Immunity, 1994. **1**: p. 247-260.
2. Tedder, T.F., Steeber, D. A., Chen, A., Engel, P., *The selectins: vascular adhesion molecules.* FASEB J., 1995. **9**: p. 866-873.
3. Kunkel, E.J., Ramos, C. L., Steeber, D. A., Muller, W., Wagner, N., Tedder, T. F., *The roles of L-selectin, $\beta$7 integrins and P-selectin in leukocyte rolling and adhesion in high endothelial venules of Peyer's patches.* J. Immunol., 1998. **161**: p. 2449-2456.
4. Tang, M.L.K., Hale, L. P., Steeber, D.A., Tedder, T. F., *L-selectin is involved in lymphocyte migration to sites of inflammation in the skin: delayed rejection of allografts in L-selectin-deficient mice.* J. Immunol., 1997. **158**: p. 5191-5199.
5. Baekkevold, Yamanaka, T., Palframan, R. T., Carlsen, H. S., Reinholt, F. P., Von Andrian, U. H., Brandtzaeg, P., Haraldsen, G., *The CCR7 ligand elc (CCL19) is transcytosed in high endothelial venules and mediates T cell recruitment.* J. Exp. Med., 2001. **193**(9): p. 1105-1112.
6. Subramanian, H.,Grailer, J. J., Ohlrich, K. C., Rymaszewski, A. L., Loppnow, J. J., Kodera, M., Conway, R. M., Steeber, D. A., *Signaling through L-selectin mediates enhanced chemotaxis of lymphocyte subsets to secondary lymphoid tissue chemokine.* J. Immunol., 2012. **188**(7): p. 3223-3236.
7. Subramanian, H. (2008). *Role of L-selectin-mediated signaling in SLC-induced lymphocyte migration.* (Order No. 3342781, The University of Wisconsin - Milwaukee). *ProQuest Dissertations and Theses,* , 249.
8. Simon, S.I., Burns, A. R., Taylor, A. D., Gopalan, P. K., Lynam, E. B., Sklar, L. A., Smith, C. W., *L-selectin (CD62L) cross-linking signals neutrophil adhesive functions via the Mac-1 (CD11b/CD18) $\beta_2$-integrin.* J. Immunol., 1995. **155**: p. 1502-1514.
9. Hwang, S.T., Singer, M. S., Giblin, P. A., Yednock, T. A., Bacon, K. B., Simon, S. I., Rosen, S. D., *GlyCAM-1, a physiologic ligand for L-selectin, activates ß2 integrins on naive peripheral lymphocytes.* J. Exp. Med., 1996. **184**: p. 1343-1348.
10. Steeber, D.A., Engel, P., Miller, A. S., Sheetz, M. P., Tedder, T. F., *Ligation of L-selectin through conserved regions within the lectin domain activates signal transduction pathways and integrin function in human, mouse, and rat leukocytes.* J. Immunol., 1997. **159**: p. 952-963.
11. Waddell, T.K., Fialkow, L., Chan, C. K., Kishimoto, T. K., Downey, G. P., *Potentiation of the oxidative burst of human neutrophils. A signaling role for L-selectin.* J. Biol. Chem., 1994. **269**: p. 18485-18491.
12. Miller, J.F., *Immunological function of the thymus.* Lancet, 1961. **2**(7205): p. 748-749.

13. Doherty, P.C. and R.M. Zinkernagel, *Enhanced immunological surveillance in mice heterozygous at the H-2 gene complex.* Nature, 1975. **256**(5512): p. 50-52.
14. Mosmann, T.R. and R.L. Coffman, *TH1 and TH2 cells: different patterns of lymphokine secretion lead to different functional properties.* Annu. Rev. Immunol., 1989. **7**: p. 145-173.
15. Boniface, J.J., Rabinowitz, J. D., Wulfing, C., Hampl, J., Reich, Z., Altman, J. D., Kantor, R. M., Beeson, C., McConnell, H. M., Davis, M. M., *Initiation of signal transduction through the T cell receptor requires the multivalent engagement of peptide/MHC ligands [corrected].* Immunity, 1998. **9**(4): p. 459-466.
16. Saparov, A., Wagner, F. H., Zheng, R., Oliver, J. R., Maeda, H., Hockett, R. D., Weaver, C. T., *Interleukin-2 expression by a subpopulation of primary T cells is linked to enhanced memory/effector function.* Immunity, 1999. **11**(3): p. 271-280.
17. Krummel, M.F. and J.P. Allison, *CD28 and CTLA-4 have opposing effects on the response of T cells to stimulation.* J. Exp. Med., 1995. **182**(2): p. 459-465.
18. Sloan-Lancaster, J., B.D. Evavold, and P.M. Allen, *Induction of T-cell anergy by altered T-cell-receptor ligand on live antigen-presenting cells.* Nature, 1993. **363**(6425): p. 156-159.
19. Schwartz, R.H., *T cell anergy.* Annu. Rev. Immunol., 2003. **21**: p. 305-34.
20. Gillis, S., Ferm, M. M., Ou, W., Smith, K. A., *T cell growth factor: parameters of production and a quantitative microassay for activity.* J. Immunol., 1978. **120**(6): p. 2027-2032.
21. Heinzel, F.P., Sadick, M. D., Mutha, S. S., Locksley, R. M., *Production of interferon gamma, interleukin 2, interleukin 4, and interleukin 10 by CD4+ lymphocytes in vivo during healing and progressive murine leishmaniasis.* Proc. Natl. Acad. Sci. U. S. A., 1991. **88**(16): p. 7011-7015.
22. Shi, L., Kam, C. M., Powers, J. C., Aebersold, R., Greenberg, A. H., *Purification of three cytotoxic lymphocyte granule serine proteases that induce apoptosis through distinct substrate and target-cell interactions.* J. Exp. Med., 1992. **176**: p. 1521-1529.
23. Kortum, R.L., A.K. Rouquette-Jazdanian, and L.E. Samelson, *Ras and extracellular signal-regulated kinase signaling in thymocytes and T cells.* Trends Immunol., 2013. **34**(6): p. 259-268.
24. Braiman, A., Barda-Saad, M., Sommers, C. L., Samelson, L. E., *Recruitment and activation of PLC[gamma]1 in T cells: a new insight into old domains.* EMBO J., 2006. **25**(4): p. 774-784.
25. Guan, E., Wang, J., Laborda, J., Norcross, M., Baeurle, P. A., Hoffman, T., *T cell leukemia-associated human Notch/translocation-associated Notch homologue has I kappa B-like activity and physically interacts with nuclear factor-kappa B proteins in T cells.* J. Exp. Med., 1996. **183**(5): p. 2025-2032.
26. Fehervari, Z. and S. Sakaguchi, *CD4+ Tregs and immune control.* J. Clin. Invest., 2004. **114**(9): p. 1209-1217.

27. Klebanoff, C.A., L. Gattinoni, and N.P. Restifo, *CD8+ T-cell memory in tumor immunology and immunotherapy.* Immunol. Rev., 2006. **211**: p. 214-224.
28. Bargatze, R.F., M.A. Jutila, and E.C. Butcher, *Distinct roles of L-selectin and integrins $\alpha 4\beta 7$ and LFA-1 in lymphocyte homing to Peyer's patch-HEV in situ: the multistep hypothesis confirmed and refined.* Immunity, 1995. **3**: p. 99-108.
29. Proudfoot, A.E.I., Handel, T. M., Johnson, Z., Lau, E. K., Liwang, P., Clark-Lewis, I., Borlat, F., Wells, T. N. C., Kosco-Vilbois, M. H., *Glycosaminoglycan binding and oligomerization are essential for the in vivo activity of certain chemokines.* Proc. Natl. Acad. Sci. U. S. A., 2003. **100**(4): p. 1885-1890.
30. Peled, A., Amnon, Kollet, O., Ponomaryov, T., Petit, I., Franitza, S., Grabovsky, V., Slav, M. M., Nagler, A., Lider, O., Alon, R., Zipori, D., Lapidot, T., *The chemokine SDF-1 activates the integrins LFA-1, VLA-4, and VLA-5 on immature human CD34+ cells: role in transendothelial/stromal migration and engraftment of NOD/SCID mice.* Blood, 2000. **95**(11): p. 3289-3296.
31. Schulz, B., Pruessmeyer, J., Maretzky, T., Ludwig, A., Blobel, C. P., Saftig, P., Reiss, K., *ADAM10 Regulates Endothelial Permeability and T-Cell Transmigration by Proteolysis of Vascular Endothelial Cadherin.* Circulation Research, 2008. **102**(10): p. 1192-1201.
32. Steeber, D., Subramanian, H. Grailer, J. J., Conway, R. M., Storey, T. J., *L-selectin-mediated leukocyte adhesion and migration*, in *Adhesion Molecules: Function and Inhibition*, K. Ley, Editor. 2007, Birkhäuser Basel. p. 27-70.
33. Tang, M.L.K., Steeber, D. A., Zhang, X-Q., Tedder, T. F., *Intrinsic differences in L-selectin expression levels affect T and B lymphocyte subset-specific recirculation pathways.* J. Immunol., 1998. **160**: p. 5113-5121.
34. Picker, L.J., *Regulation of tissue-selective T-lymphocyte homing receptors during the virgin to memory/effector cell transition in human secondary lymphoid tissues.* Am. Rev. Respir. Dis., 1993. **148**: p. S47-54.
35. Peschon, J.J., Slack, J. L., Reddy, P., Stocking, K. L., Sunnarborg, S. W., Lee, D. C., Russell, W. E., Castner, B. J., Johnson, R. S., Fitzner, J. N., Boyce, R. W., Nelson, N., Kozlosky, C. J., Wolfson, M. F., Rauch, C. T., Cerritti, D. P., Paxton, R. J., March, C. J., Black R. A., *An essential role for ectodomain shedding in mammalian development.* Science, 1998. **282**: p. 1281-1284.
36. Tu, L., Poe, J. C., Kadono, T., Venturi, G. M., Bullard, D. C., Tedder, T. F., Steeber, D. A., *A functional role for circulating mouse L-selectin in regulating leukocyte/endothelial cell interactions in vivo.* J. Immunol., 2002. **169**: p. 2034-2043.
37. Walcheck, B., Moore, K. L., McEver, R. P., Kishimoto, T. K., *Neutrophil-neutrophil interactions under hydrodynamic shear stress involve L-selectin*

*and PSGL-1. A mechanism that amplifies initial leukocyte accumulation on P-selectin in vitro.* J. Clin. Invest., 1996. **98**: p. 1081-1087.

38. Foxall, C., Watson, S. R., Dowbenko, D., Fennie, C., Lasky, L. A., Kiso, M., Hasegawa, A., Asa, D., Brandley, B. K., *The three members of the selectin receptor family recognize a common carbohydrate epitope, the sialyl lewis$^x$ oligosaccharide.* J. Cell Biol., 1992. **117**: p. 895-902.
39. Ivetic, A., Deka, J., Ridley, A., Ager, A., *The cytoplasmic tail of L-selectin interacts with members of the Ezrin-Radixin-Moesin (ERM) family of proteins: cell activation-dependent binding of Moesin but not Ezrin.* J. Biol. Chem., 2002. **277**: p. 2321-2329.
40. Waddell, T.K., Fialkow, L., Chan, C. K., Kishimoto, T. K., Downey, G. P., *Signaling functions of L-selectin. Enhancement of tyrosine phosphorylation and activation of MAP kinase.* J. Biol. Chem., 1995. **270**: p. 15403-15411.
41. Laudanna, C., Constantin, G., Baron, P., Scarpini, E., Scarlato, G., Cabrini, G., Dechecchi, C., Rossi, F., Cassatella, M. A., Berton, G., *Sulfatides trigger increase of cytosolic free calcium and enhanced expression of tumor necrosis factor-$\alpha$ and interleukin-8 mRNA in human neutrophils. Evidence for a role of L-selectin as a signaling molecule.* J. Biol. Chem., 1994. **269**: p. 4021-4026.
42. Zlotnik, A. and O. Yoshie, *Chemokines: a new classification system and their role in immunity.* Immunity, 2000. **12**(2): p. 121-127.
43. Cyster, J.G., *Chemokines and Cell Migration in Secondary Lymphoid Organs.* Science, 1999. **286**(5447): p. 2098-2102.
44. Forster, R., A.C. Davalos-Misslitz, and A. Rot, *CCR7 and its ligands: balancing immunity and tolerance.* Nat. Rev. Immunol., 2008. **8**(5): p. 362-371.
45. Willimann, K., Legler, D. F., Loetscher, M., Roos, R. S., Delgado, M. B., Clark-Lewis, I., Baggiolini, M., Moser, B., *The chemokine SLC is expressed in T cell areas of lymph nodes and mucosal lymphoid tissues and attracts activited T cells via CCR7.* Eur. J. Immunol., 1998. **28**: p. 2025-2034.
46. Yoshida, R., Nagira, M., Kitaura, M., Imagawa, N., Imai, T., Yoshie, O.,*Secondary lymphoid-tissue chemokine is a functional ligand for the CC chemokine receptor CCR7.* J. Biol. Chem., 1998. **273**: p. 7118-7122.
47. Hamel, D.J., Sielaff, I., Proudfoot, A. E., Handel, T. M., *Chapter 4. Interactions of chemokines with glycosaminoglycans.* Methods Enzymol, 2009. **461**: p. 71-102.
48. Stein, J.V., *CCR7-mediated physiological lymphocyte homing involves activation of a tyrosine kinase pathway.* Blood, 2003. **101**(1): p. 38-44.
49. Vicente-Manzanares, M. and F. Sanchez-Madrid, *Role of the cytoskeleton during leukocyte responses.* Nat. Rev. Immunol., 2004. **4**(2): p. 110-122.
50. Vicari, A.P., Figueroa, D. J., Hedrick, J. A., Foster, J. S., Singh, K. P., Menon, S., Copeland, N. G., Gilbert, D. J., Jenkins, N. A., Bacon, K. B., Zlotnik, A. *TECK: a novel CC chemokine specifically expressed by thymic*

*dendritic cells and potentially involved in T cell development.* Immunity, 1997. **7**(2): p. 291-301.
51. Ara, T., Itoi, M., Kawabata, K., Egawa, T., Tokoyoda, K., Sugiyama, T., Fujii, N., Amagai, T., Nagasawa, T., *A role of CXC chemokine ligand 12/stromal cell-derived factor-1/pre-B cell growth stimulating factor and its receptor CXCR4 in fetal and adult T cell development in vivo.* J. Immunol., 2003. **170**(9): p. 4649-4655.
52. Misslitz, A., Pabst, O., Hintzen, G., Ohl, L., Kremmer, E., Petrie, H. T., Forster, R., *Thymic T cell development and progenitor localization depend on CCR7.* J. Exp. Med., 2004. **200**(4): p. 481-491.
53. Taub, D.D., Sayers T. J., Carter, C. R., Ortaldo, J. R., *Alpha and beta chemokines induce NK cell migration and enhance NK-mediated cytolysis.* J. Immunol., 1995. **155**(8): p. 3877-3888.
54. Lenaz, G., *Lipid fluidity and membrane protein dynamics.* Biosci. Rep., 1987. **7**(11): p. 823-837.
55. Zola, H., Swart, B., Banham, A., Barry, S., Beare, A., Bensussan, A., Boumsell, L., D. Buckley, C., Buhring, H. J., Clark, G., Engel, P., Fox, D., Jin, B. Q., Macardle, P. J., Malavasi, F., Mason, D., Stockinger, H., Yang, X., *CD molecules 2006--human cell differentiation molecules.* J. Immunol. Methods, 2007. **319**(1-2): p. 1-5.
56. Cyster, J.G., *Chemokines, sphingosine-1-phosphate, and cell migration in secondary lymphoid organs.* Annu. Rev. Immunol., 2005. **23**: p. 127-159.
57. Newton, A.C., *Protein Kinase C: Structural and Spatial Regulation by Phosphorylation, Cofactors, and Macromolecular Interactions.* Chem. Rev., 2001. **101**(8): p. 2353-2364.
58. Gulli, M.P. and M. Peter, *Temporal and spatial regulation of Rho-type guanine-nucleotide exchange factors: the yeast perspective.* Genes Dev., 2001. **15**(4): p. 365-379.
59. Schaeuble, K., Hauser, M. A., Singer, E., Groettrup, M., Legler, D. F., *Cross-talk between TCR and CCR7 signaling sets a temporal threshold for enhanced T lymphocyte migration.* J. Immunol., 2011. **187**(11): p. 5645-5652.
60. Gollmer, K., Asperti-Boursin, F., Tanaka, Y., Okkenhaug, K., Vanhaesebroeck, B., Peterson, J. R., Fukui, Y., Donnadieu, E., Stein, J. V., *CCL21 mediates CD4+ T-cell costimulation via a DOCK2/Rac-dependent pathway.* Blood, 2009. **114**(3): p. 580-588.
61. Ding, Z., Isekutz, T. B., Downey, G. P., Waddell, T. K., *L-selectin enhances functional expression of surface CXCR4 in lymphocytes: implication for cellular activation during adhesion and migration.* Blood, 2003. **101**: p. 4245-4252.
62. Juliano, R.L., *Signal transduction by cell adhesion receptors and the cytoskeleton: functions of integrins, cadherins, selectins, and immunoglobulin-superfamily members.* Annu. Rev. Pharmacol. Toxicol., 2002. **42**: p. 283-323.

63. Barkhausen, T., C. Krettek, and M.v. Griensven, *L-selectin: Adhesion, signalling and its importance in pathologic posttraumatic endotoxemia and non-septic inflammation.* Exp. Tox. Path., 2005. **57**(1): p. 39-52.
64. Blankenberg, S., S. Barbaux, and L. Tiret, *Adhesion molecules and atherosclerosis.* Atherosclerosis, 2003. **170**(2): p. 191-203.
65. Amsen, D., Blander, J. M., Lee, G. R., Tanigaki, K., Honjo, T., Flavell, R. A., *Instruction of distinct CD4 T helper cell fates by different notch ligands on antigen-presenting cells.* Cell, 2004. **117**(4): p. 515-526.
66. Jung, S., Unutmatz, D., Wong, P., Sano, G., De los Santos, K., Sparwasser, T., Wu, S., Vuthoori, S., Ko, K., Zavala, F., Pamer, E. G., Littman, D. R., Lang, R. A., *In Vivo Depletion of CD11c+ Dendritic Cells Abrogates Priming of CD8+ T Cells by Exogenous Cell-Associated Antigens.* Immunity, 2002. **17**(2): p. 211-220.
67. Kasaian, M.T., Whitters, M. J., Carter, L. L., Lowe, L. D., Jussif, J. F., Deng, B., Johnson, K. A., Witek, J. S., Senices, M., Konz, R. F., Wurster, A. L., Donaldson, D. D., Collins, M., Young, D. A., Grusby, M. J., *IL-21 limits NK cell responses and promotes antigen-specific T cell activation: a mediator of the transition from innate to adaptive immunity.* Immunity, 2002. **16**(4): p. 559-569.
68. Graeler, M. and E.J. Goetzl, *Activation-regulated expression and chemotactic function of sphingosine 1-phosphate receptors in mouse splenic T cells.* FASEB J., 2002. **16**(14): p. 1874-1878.
69. Kruetzmann, S. and M.M.W. Rosado, H. Germing, U. Tournilhac, O. Peter, H.H. Berner, R. Peters, A. Boehm,T. Plebani, A. Quinti, I. Carsetti, R., *Human immunoglobulin M memory B cells controlling Streptococcus pneumoniae infections are generated in the spleen.* J. Exp. Med., 2003. **197**((7)): p. 939-945.
70. Gunn, M.D., Tangemann, K., Tam, C., Cyster, J. G., Rosen, S. D., Williams, L. T., *A chemokine expressed in lymphoid high endothelial venules promotes the adhesion and chemotaxis of naive T lymphocytes.* Proc. Natl. Acad. Sci. U. S. A., 1998. **95**: p. 258-263.
71. Tangemann, K., Gunn, M. D., Giblin, P., Rosen, S. D., *A high endothelial cell-derived chemokine induces rapid efficient, and subset-selective arrest of rolling T lymphocytes on a reconstituted endothelial substrate.* J. Immunol., 1998. **161**: p. 6330-6337.
72. Ley, K., *Integration of inflammatory signals by rolling neutrophils.* Imm. Rev., 2002. **186**(1): p. 8-18.
73. Haribabu, B., Steeber, D. A., Ali, H., Richardson, R. M., Snyderman, R., Tedder, T. F., *Chemoattractant receptor-induced phosphorylation of L-selectin.* J. Biol. Chem., 1997. **272**: p. 13961-13965.
74. Weyermann, J., D. Lochmann, and A. Zimmer, *A practical note on the use of cytotoxicity assays.* Int. J. Pharm., 2005. **288**(2): p. 369-376.
75. Murray, J., Zhang, B., Taylor, S. W., Oglesbee, D., Fahy, E., Marusich, M. F., Ghosh, S. S., Capaldi, R. A., *The Subunit Composition of the Human NADH Dehydrogenase Obtained by Rapid One-step Immunopurification.* J. Biol. Chem., 2003. **278**(16): p. 13619-13622.

76. Chen, Y.-R., Chen, C-L., Zhang, L., Green-Church, K. B., Zweier, J. L., *Superoxide Generation from Mitochondrial NADH Dehydrogenase Induces Self-inactivation with Specific Protein Radical Formation.* J. Biol. Chem., 2005. **280**(45): p. 37339-37348.
77. Seo, B.B., Marella, M., Yagi, T., Matsuno-Yagi, A., *The single subunit NADH dehydrogenase reduces generation of reactive oxygen species from complex I.* FEBS Lett., 2006. **580**(26): p. 6105-6108.
78. Seluanov, A., Hine, C., Azpurua, J., Feigenson, M., Bozzella, M., Mao, Z., Catania, K. C., Gorbunova, V., *Hypersensitivity to contact inhibition provides a clue to cancer resistance of naked mole-rat.* Proc. Natl. Acad. Sci. U. S. A., 2009. **106**(46): p. 19352-19357.
79. Kim, J.-Y., et al., *BH3-only Protein Noxa Is a Mediator of Hypoxic Cell Death Induced by Hypoxia-inducible Factor 1α.* J. Exp Med., 2004. **199**(1): p. 113-124.
80. Weston, S.A. and C.R. Parish, *New fluorescent dyes for lymphocyte migration studies: Analysis by flow cytometry and fluorescence microscopy.* J. Immunol. Methods, 1990. **133**(1): p. 87-97.
81. Venken, K., Thewissen, M., Hellings, N., Somers, V., Hensen, K., Rummens, J. L., Stinissen, P., *A CFSE based assay for measuring CD4+CD25+ regulatory T cell mediated suppression of auto-antigen specific and polyclonal T cell responses.* J. Immunol. Methods, 2007. **322**(1-2): p. 1-11.
82. Hawkins, E.D., Hommel, M., Turner, M. L., Battye, F. L., Markham, J. F., Hodgkin, P. D., *Measuring lymphocyte proliferation, survival and differentiation using CFSE time-series data.* Nat. Protoc., 2007. **2**(9): p. 2057-2067.
83. Parish, C.R., Glidden, M. H., Quah, B. J., Warren, H. S., *Use of the intracellular fluorescent dye CFSE to monitor lymphocyte migration and proliferation.* Curr. Protoc. Immunol., 2009. **Chapter 4**: p. Unit4.9.
84. Kilian, K., Dernedde, J., Mueller, E-C., Bahr, I., Tauber, R., *The interaction of protein kinase C isozymes $\alpha$, $\iota$, $\theta$ with the cytoplasmic domain of L-selectin is modulated by phosphorylation of the receptor.* J. Biol. Chem., 2004. **279**: p. 34472-34480.
85. Martinez, M., Joofraud, M., Giraud, S., Baisse, B., Bernimoulin, M. P., Schapira, M., Spertini, O., *Regulation of PSGL-1 Interactions with L-selectin, P-selectin, and E-selectin: Role of Human Fucosyltransferase-IV and -VII.* J. Biol. Chem., 2005. **280**(7): p. 5378-5390.
86. Toetsch, S., Olwell, P., Prina-Mello, A., Volkov, Y., *The evolution of chemotaxis assays from static models to physiologically relevant platforms.* Integr. Biol. (Camb), 2009. **1**(2): p. 170-181.
87. Weber, K.S., Klickstein, L. B., Weber, P. C., Weber, C., *Chemokine-induced monocyte transmigration requires cdc42-mediated cytoskeletal changes.* Eur. J. Immunol., 1998. **28**(7): p. 2245-2251.
88. Li, L., C. Yee, and J.A. Beavo, *CD3- and CD28-Dependent Induction of PDE7 Required for T Cell Activation.* Science, 1999. **283**(5403): p. 848-851.

89. Lenschow, D.J., T.L. Walunas, and J.A. Bluestone, *CD28/B7 system of T cell costimulation.* Annual Review of Immunology, 1996. **14**(1): p. 233-258.
90. Tseng, S.-Y. and M.L. Dustin, *T-cell activation: a multidimensional signaling network.* Curr. Op. Cell Biol. , 2002. **14**(5): p. 575-580.
91. Magness, S.T., Jijon, H., Van Houten Fisher, N., Sharpless, N. E., Brenner, D. A., Jobin, C., *In Vivo Pattern of Lipopolysaccharide and Anti-CD3-Induced NF-κB Activation Using a Novel Gene-Targeted Enhanced GFP Reporter Gene Mouse.* J. Immunol., 2004. **173**(3): p. 1561-1570.
92. Sperling, A.I. and J.A. Bluestone, *The Complexities of T-Cell Co-stimulation: CD28 and Beyond.* Immunol. Rev., 1996. **153**(1): p. 155-182.
93. Kruisbeek, A.M., E. Shevach, and A.M. Thornton, *Proliferative Assays for T Cell Function*, in *Curr. Protoc. Immunol*., 2001, John Wiley & Sons, Inc.
94. Pereira, J.P., L.M. Kelly, and J.G. Cyster, *Finding the right niche: B-cell migration in the early phases of T-dependent antibody responses.* Int. Immunol., 2010. **22**(6): p. 413-419.
95. Chao, C.C., R. Jensen, and M.O. Dailey, *Mechanisms of L-selectin regulation by activated T cells.* J. Immunol., 1997. **159**(4): p. 1686-1694.
96. Klebanoff, C.A., Gattinoni, L., Torabi-Parizi, P., Kerstann, K., Cardones, A. R., Finkelstein, S. E., Palmer, D. C., Antony, P. A., Hwang, S. T., Rosenberg, S. A., Waldmann, T. A., Restifo, N. P., *Central memory self/tumor-reactive CD8+ T cells confer superior antitumor immunity compared with effector memory T cells.* Proc. Natl. Acad. Sci. U. S. A., 2005. **102**(27): p. 9571-9576.
97. Caligiuri, M.A., *Human natural killer cells.* Blood, 2008. **112**(3): p. 461-469.
98. De Maria, A., Bozzano, F., Cantoni, C., Moretta, L., *Revisiting human natural killer cell subset function revealed cytolytic CD56(dim)CD16+ NK cells as rapid producers of abundant IFN-gamma on activation.* Proc. Natl. Acad. Sci. U S A, 2011. **108**(2): p. 728-732.
99. Steinman, R.M. and Z.A. Cohn, *Identification of a novel cell type in peripheral lymphoid organs of mice: II Functional Properties in vitro*. J. Exp. Med., 1974. **139**(2): p. 380-397.
100. Kahn, J., Walcheck, B., Migaki, G. I., Jutila, M. A., Kishimoto, T. K., *Calmodulin regulates L-selectin adhesion molecule expression and function through a protease-dependent mechanism.* Cell, 1998. **92**: p. 809-818.
101. Killock, D.J., Parsons, M., Zarrouk, M., Ameer-Beg, S. M., Ridley, A. J., Haskard, D. O., Zvelebil, M., Ivetic, A., *In Vitro and in Vivo Characterization of Molecular Interactions between Calmodulin, Ezrin/Radixin/Moesin, and L-selectin.* J. Biol. Chem., 2009. **284**(13): p. 8833-8845.
102. Gifford, J.L., H. Ishida, and H.J. Vogel, *Structural insights into calmodulin-regulated L-selectin ectodomain shedding.* J. Biol. Chem., 2012. **287**(32): p. 26513-26527.
103. Walcheck, B., Jahn, J., Fisher, J. M., Wang, B. B., Fisk, R. S., Payan, D. G., Feehan, C., Betageri, R., Darlak, K., Spatola, A. F., Kishimoto, T. K.,

*Neutrophil rolling altered by inhibition of L-selectin shedding in vitro.* Nature, 1996. **380**: p. 720-723.
104. Hafezi-Moghadam, A. and K. Ley, *Relevance of L-selectin shedding for leukocyte rolling in vivo.* J. Exp. Med., 1999. **189**: p. 939-947.
105. Brenner, B., Gulbins, E., Schlottmann, K., Koppenhoefer, U., Busch, G. L., Walzog, B., Steinhausen, M., Coggeshall, K. M., Linderkamp, O., Lang, F., *L-selectin activates the Ras pathway via the tyrosine kinase p56$^{lck}$.* Proc. Natl. Acad. Sci. USA, 1996. **93**: p. 15376-15381.
106. Tzivion, G. and J. Avruch, *14-3-3 proteins: active cofactors in cellular regulation by serine/threonine phosphorylation.* J. Biol. Chem., 2002. **277**(5): p. 3061-3064.
107. Singh, L.P., Y. Jiang, and D.W. Cheng, *Proteomic identification of 14-3-3zeta as an adapter for IGF-1 and Akt/GSK-3beta signaling and survival of renal mesangial cells.* Int. J. Biol. Sci., 2007. **3**(1): p. 27-39.
108. Craparo, A., R. Freund, and T.A. Gustafson, *14-3-3 (epsilon) interacts with the insulin-like growth factor I receptor and insulin receptor substrate I in a phosphoserine-dependent manner.* J. Biol. Chem., 1997. **272**(17): p. 11663-11669.
109. Tzivion, G., Z. Luo, and J. Avruch, *A dimeric 14-3-3 protein is an essential cofactor for Raf kinase activity.* Nature, 1998. **394**(6688): p. 88-92.
110. Panchamoorthy, G., Fukazawa, T., Stolz, L., Payne, G., Reedquist, K., Shoelson, S., Songyang, Z., Cantley, L., Walsh, C., Band, H., *Physical and functional interactions between SH2 and SH3 domains of the Src family protein tyrosine kinase p59fyn.* Mol. Cell. Biol., 1994. **14**(9): p. 6372-6385.
111. Thomas, J.W., Ellis, B, Boerner, R. J., Knight, W. B., White, G. C., Schaller, M. D., *SH2- and SH3-mediated Interactions between Focal Adhesion Kinase and Src.* J. Biol. Chem., 1998. **273**(1): p. 577-583.
112. Chardin, P., Cussac, D., Maignan, S., Ducruix, A., *The Grb2 adaptor.* FEBS Lett., 1995. **369**(1): p. 47-51.
113. Chardin, P., Camonis, J. H., Gale, N. W., van Aelst, L., Schlessinger, J., Wigler, M. H., Bar-Sagi, D., *Human Sos1: a guanine nucleotide exchange factor for Ras that binds to GRB2.* Science, 1993. **260**(5112): p. 1338-1343.
114. Li, N., Batzer, A., Daly, R., Yajnik, V., Skolnik, E., Chardin, P., Bar-Sagi, D., Margolis, B., Schlessinger, J., *Guanine-nucleotide-releasing factor hSos1 binds to Grb2 and links receptor tyrosine kinases to Ras signalling.* Nature, 1993. **363**(6424): p. 85-88.
115. Egan, S.E., Giddings, B. W., Brooks, M. W., Buday, L., Sizeland, A. M., Weinberg, R. A., *Association of Sos Ras exchange protein with Grb2 is implicated in tyrosine kinase signal transduction and transformation.* Nature, 1993. **363**(6424): p. 45-51.
116. Valencia, A., Chardin, P., Wittinghofer, A., Sander, C., *The ras protein family: evolutionary tree and role of conserved amino acids.* Biochemistry, 1991. **30**(19): p. 4637-4648.

117. Brenner, B., Weinmann, S., Grassme, H., Lang, F., Linderkamp, O., Gulbins, E., *L-selectin activates JNK via src-like tyrosine kinases and the small G-protein Rac.* Immunology, 1997. **92**: p. 214-219.
118. Smolen, J.E., Petersen, T. K., Koch, C., O'Keefe, S. J., Hanlon, W. A., Seo, S., Pearson, D., Fossett, m. C., Simon, S. I., *L-Selectin Signaling of Neutrophil Adhesion and Degranulation Involves p38 Mitogen-activated Protein Kinase.* J. Biol. Chem., 2000. **275**(21): p. 15876-15884.
119. Sitrin, R.G., Pan, P. M., Blackwood, R. A., Huang, J., Petty, H. R., *Cutting Edge: Evidence for a Signaling Partnership Between Urokinase Receptors (CD87) and L-Selectin (CD62L) in Human Polymorphonuclear Neutrophils.* J. Immunol., 2001. **166**(8): p. 4822-4825.
120. Xu, T., Chen L., Shang, X., Cui, L., Luo, J., Chen, C., Ba. X., Zeng, X., *Critical role of Lck in L-selectin signaling induced by sulfatides engagement.* J. Leuk. Biol., 2008. **84**(4): p. 1192-1201.
121. Xu, L.-H., Yang, X., Bradham, C. A., Brenner, D. A., Baldwin, A. S., Craven, R. J., Cance, W. G., *The Focal Adhesion Kinase Suppresses Transformation-associated, Anchorage-independent Apoptosis in Human Breast Cancer Cells:Involvement of death receptor-related signaling pathways.*J. Biol. Chem., 2000. **275**(39): p. 30597-30604.
122. Hanaoka, K., Fujita, N., Lee, -H., Seimiya, H., Naito, M., Tsuruo, T., *Involvement of CD45 in Adhesion and Suppression of Apoptosis of Mouse Malignant T-Lymphoma Cells.* Cancer Res., 1995. **55**(10): p. 2186-2190.
123. Kirshner, J., Chen, C-J., Liu, P., Huang, J., Shively, J. E., *CEACAM1-4S, a cell–cell adhesion molecule, mediates apoptosis and reverts mammary carcinoma cells to a normal morphogenic phenotype in a 3D culture.* Proc. Natl. Acad. Sci. U. S. A., 2003. **100**(2): p. 521-526.
124. Daigeler, A., Chromik, A. M., Geisler, A., Bulut, D., Hilgert, C., Krieg, A., Klein-Hitpass, L., Lehnhardt, M., Uhl, W., Mittelkotter, U., *Synergistic apoptotic effects of taurolidine and TRAIL on squamous carcinoma cells of the esophagus.* Int. J. Oncol., 2008. **32**(6): p. 1205-1220.
125. Watson, R.W., Rotstein, O. D., Nathens, A. B., Parodo, J., Marshall, J. C., *Neutrophil apoptosis is modulated by endothelial transmigration and adhesion molecule engagement.* The Journal of Immunology, 1997. **158**(2): p. 945-953.
126. Matsuba, K.T., Van Eeden, S. F., Bicknell, S. G., Walker, B. A., Hayashi, S., Hogg, J. C., *Apoptosis in circulating PMN: increased susceptibility in L-selectin-deficient PMN.* Am. J. Phys. - Heart and Circulatory Physiology, 1997. **272**(6): p. H2852-H2858.
127. Oyaizu, N., Than, S., McCloskey, T. W., Pahwa, S., *Requirement of P56lck in T-Cell Receptor CD3-Mediated Apoptosis and Fas-Ligand Induction Jurkat Cells.* Biochem. Biophys. Res. Comm., 1995. **213**(3): p. 994-1001.
128. Groux, H., Monte, D., Plouvier, B., Capron, A., Ameisen, J-C., *CD3-mediated apoptosis of human medullary thymocytes and activated peripheral T cells: Respective roles of interleukin-1, interleukin-2,*

*interferon-γ and accessory cells.* Eur. J. Immunol., 1993. **23**(7): p. 1623-1629.
129. Hoshi, S., Furutani-Selki, M., Seto, M., Tada, T., Asano, Y., *Prevention of TCR-mediated apoptosis by the elevation ofcAMP.* Int. Immunol., 1994. **6**(7): p. 1081-1090.
130. Yang, E., Zha, J., Jockel, J., Boise, L. H., Thompson, C. B., Korsmeyer, S. J., *Bad, a heterodimeric partner for Bcl-$x_L$ and Bcl-2, displaces Bax and promotes cell death.* Cell, 1995. **80**: p. 285-291.
131. Samuel, T., Weber, H. O., Rauch, P., Verdoodt, B., Eppel, J-T., McShea, A., Hermeking, H., Funk, J-O. *The G2/M Regulator 14-3-3ς Prevents Apoptosis through Sequestration of Bax.* J. Biol. Chem., 2001. **276**(48): p. 45201-45206.
132. Brunet, A., Bonni, A., Zigmond, M. J., Lin, M. Z., Juo, P., Hu, L. S., Anderson, M. J., Arden, K. C., Blenis, J., Greenberg, M. E., *Akt promotes cell survival by phosphorylating and inhibiting a Forkhead transcription factor.* Cell, 1999. **96**(6): p. 857-868.
133. See, V., Boutillier, A-L., Bito, H., Loeffler, J-P., *Calcium/calmodulin-dependent protein kinase type IV (CaMKIV) inhibits apoptosis induced by potassium deprivation in cerebellar granule neurons.* FASEB J., 2001. **15**(1): p. 134-144.
134. Soon Bae, J., Kyoo Jang, M., Hong, S-H., An, W-G., Choi, Y-H., Kim, H-D., Cheong, J-H., *Phosphorylation of NF-κB by calmodulin-dependent kinase IV activates anti-apoptotic gene expression.* Biochem. Biophys. Res. Comm., 2003. **305**(4): p. 1094-1098.
135. Lin, M.Y., Zal, T., Chen, I. L., Gascoigne, N. R., Hedrick, S. M., *A pivotal role for the multifunctional calcium/calmodulin-dependent protein kinase II in T cells: from activation to unresponsiveness.* J. Immunol., 2005. **174**(9): p. 5583-5592.
136. Lee, B.-H. and E. Ruoslahti, *α5β1 integrin stimulates Bcl-2 expression and cell survival through Akt, focal adhesion kinase, and Ca2+/calmodulin-dependent protein kinase IV.* J. Biol. Chem., 2005. **95**(6): p. 1214-1223.
137. Yano, S., H. Tokumitsu, and T.R. Soderling, *Calcium promotes cell survival through CaM-K kinase activation of the protein-kinase-B pathway.* Nature, 1998. **396**(6711): p. 584-587.
138. Deb, T.B., C.M. Coticchia, and R.B. Dickson, *Calmodulin-mediated Activation of Akt Regulates Survival of c-Myc-overexpressing Mouse Mammary Carcinoma Cells.* J. Biol. Chem., 2004. **279**(37): p. 38903-38911.
139. Babu, Y.S., C.E. Bugg, and W.J. Cook, *Structure of calmodulin refined at 2.2 Å resolution.* J. Mol. Biol., 1988. **204**(1): p. 191-204.
140. Xiao, B., Smerdon, S. J., Jones, D. H., Dodson, G. G., Soneji, Y., Aitken, A., Gamblin, S. J., *Structure of a 14-3-3 protein and implications for coordination of multiple signalling pathways.* Nature, 1995. **376**(6536): p. 188-191.
141. Fitzgerald, K.A., Bowie, A. G., Skeffington, B. S., O'Neill, L. A., *Ras, protein kinase C zeta, and I kappa B kinases 1 and 2 are downstream*

*effectors of CD44 during the activation of NF-kappa B by hyaluronic acid fragments in T-24 carcinoma cells.* J. Immunol., 2000. **164**(4): p. 2053-2063.

142. Chang, F., Steelman, L. S., Shelton, J. G., Lee, J. T., Navolanic, P. M., Blalock, W. L., Franklin, R., McCubrey, J. A., *Regulation of cell cycle progression and apoptosis by the Ras/Raf/MEK/ERK pathway (Review).* Int. J. Oncol., 2003. **22**(3): p. 469-480.
143. Zha, J., Harada, H., Yang, E., Jockel, J., Korsmeyer, S. J., *Serine phosphorylation of death agonist BAD in response to survival factor results in binding to 14-3-3 not BCL-$X_L$.* Cell, 1996. **87**: p. 619-628.